THE

LONDON, EDINBURGH, AND DUBLIN

PHILOSOPHICAL MAGAZINE

AND

JOURNAL OF SCIENCE.

[SEVENTH SERIES.]

SUPPLEMENT, APRIL 1937.

LXV. *The Ignition of Gaseous Mixtures by Hot Particles.* *By* ROBERT S. SILVER, *B.Sc., M.A., formerly Houldsworth Research Student, Glasgow University* *.

1. HISTORICAL INTRODUCTION.

THE problem of the ignition of gaseous mixtures by hot particles has a special significance in connexion with the ignition of fire-damp in coal-mining operations. It is well known that explosive mixtures of fire-damp and air can be ignited when shots are fired to release coal masses. As a result of experience, empirical regulations have been drawn up as to types of explosive, method of detonation, etc., which may be permitted in shot-firing. These generally do not go beyond the laying down of limits to the nature and size of charge, of provision for stemming, of size and character of bore-hole, and of methods of detonation. It is clear that the fundamental aims of such regulations were

(*a*) to control the size of flame emitted ;

(*b*) to control the pressure wave.

The probability that the flame and the pressure wave were not the only causes of ignition of the surrounding

* Communicated by Prof. E. Taylor Jones.

explosive atmosphere received confirmation from a series of experiments described by Dr. E. Beyling at the International Conference on Safety in Mines held at Buxton in 1931 [1]. He concluded that the probable cause when neither of these could be suspect was hot particles of undecomposed explosive, or hot particles of cartridge-casing, stemming, etc.

The problem may be linked up with the history of attempts to investigate the ignition of fire-damp by frictional sparks. The general results of such investigations are summarized by Coward and Wheeler [2] in the section devoted to Frictional Sparks. The total of the evidence is inconclusive. Recently M. J. Burgess and R. V. Wheeler [3] have reported investigations on this problem. The general trend of their results is that frictional sparks will produce ignitions of methane, but with great difficulty. In the cases where they did obtain ignitions they draw attention to the heat produced by the contacting surfaces. From first principles, however, it is very probable that the size and temperature of a particle would be important factors determining its ability to cause ignition. These factors, and any possible correlation between them, should obviously be investigated. Furthermore, frictional sparks can certainly ignite some gaseous mixtures, as shown by Burgess and Wheeler with carbon bisulphide [3], while such ignitions form the principle of the usual form of cigarette lighter. A detailed investigation into the general characteristics of non-burning hot particles in their power of igniting gaseous mixtures is certainly required, and for this the present work may serve as a beginning.

Ignition of Methane

Before proceeding with the account of the experimental work, we give a summary review of the ignition characteristics of methane, in so far as these are relevant to the particle problem. Mixtures of from 5 to 15 per cent. methane in air are explosive. A very important feature is the time-lag of its ignition. H. B. Dixon has investigated this effect very thoroughly, and his work is fully reviewed by Bone and Townend [4]. He found that, for all the gases with which he worked, there were time-lags of ignition at certain temperatures, the amount of

the lag depending on the temperature. *E. g.*, for carbon bisulphide he found :—

Ignition temp. ..	156°	151°	145°	138°	130°	124°	120°
Lag in seconds ..	0·5	1·0	2·0	3·0	5·0	7·0	10·0

All the results are of this type, the higher the temperature, the smaller the lag. Methane proved to have very high ignition temperatures. Dixon found :—

Observed ignition point	740°	728°	710°	694°	657°
Lag in seconds	0·6	1·0	2·0	3·0	10·0

The relative proportions of combustible gas to air are unspecified. Naylor and Wheeler [5], for a mixture of 6·5 per cent. in air, found a lag of nearly 11 secs. for a source of 700° C. They found that the lag was reduced to about 1/100th of a second for a temperature of 1175° C. These experiments were performed by admitting the gas mixture into a vessel whose quartz surface was kept at the observed temperature. It was carried out for a number of mixtures, and it was found that for a given temperature the mixtures containing smaller concentrations of methane were the more easily ignitable. The relevance of the results is obvious. A hot particle travelling through a gas mixture is not in contact with any portion of the gas for any appreciable time. If it is to cause ignition it is probable that it will have to be at a temperature such that Naylor and Wheeler's results indicate a very small time-lag.

Now ignition by heated metal bars and by hot wires approaches to the particle case in that, because of convection currents, the gas does not remain for more than a brief period of time at the temperature attained by contact with the metal. Again, then, one would expect the lowest temperature at which a metal bar would inflame methane-air mixtures to be one for which the time-lag was short. Some results on metal bars are given by Coward and Wheeler [6]. No mixture of methane was ignited by a nickel bar until the bar was above 1025° C.

A straight line is shown when igniting temperature of the nickel bar is plotted against percentage of methane, the temperature rising for increasing concentration. The experiment was performed for various metals and steels, which give graphs similar to that of nickel. The curve for platinum was abnormal in that it rose to a peak at over 1400° C. for 9 per cent. and then fell away, but at all its points it was much higher than the others. Coward and Wheeler, on the basis of work done by Coward and Guest [7], suggest that this is probably due to the high catalytic activity of platinum. The conclusion from the experiments is that no bar of heated metal is capable of igniting methane unless its temperature is at least near 1000° C., almost white-heat.

While ignition by heated wires might be taken as a further approach to the particle case, the work of Shepherd and Wheeler [8] shows that the problem is complicated by the current fusing the wire. No sufficiently confirmed relevant matter appears in this type of ignition.

Lastly, reference may be made to the work of J. W. McDavid in the Nobel Research Laboratories at Ardeer [9]. He aimed at eliminating the lag as far as possible, the express object of his experiments being to determine the minimum temperature to which a given gaseous mixture must be heated, by the *sudden* application of a heated body, so as to cause its instantaneous ignition. The heated body was a small electrically heated wire—he compared results with Eureka alloy and platinum—wound on a small silica tube in which was a thermo-junction to measure the temperature. This was applied to a bubble of the gas formed in glycerine. He concluded definitely that "pure methane when mixed with air does not ignite below 1000° C.," *i. e.*, for the short time-lag given by this method. For a coal-gas air mixture he found an ignition temperature of 878° C., and states that, within the limits of explosive mixtures, the variation of percentage of air in the mixture does not cause great variation in the temperature observed for ignition. As regards his aim of obtaining an instantaneous ignition, it seems probable that the method of the present work will give a closer approximation, for in this case the hot body is a particle in rapid motion through the gas mixture, whereas his heated wire was merely placed against the bubble.

2. Experimental Method.

The following general mode of attack was adopted :—

(*a*) To introduce heated *spherical* particles of different sizes into gas mixtures.

(*b*) To use non-combustible spheres, for a direct thermal ignition effect.

In the first form of apparatus the method tried was to drop the particle vertically into an explosion chamber, the particle being electrically heated by a resistance wound round a tube. It was eventually abandoned for the following reasons :—

(*a*) Difficulty in temperature measurement. The sphere had to be loose in order to fall, and so a thermocouple could not be connected to it.

(*b*) The convection up the tube caused very inefficient heating of the particle.

(*c*) The greatest difficulty was to devise a trap-door, platform, and a diaphragm arrangement to allow the sphere to fall and to open the explosion chamber at the correct time. Any platform used has to remain mechanically efficient while at the same temperature as the particle.

In the apparatus eventually adopted the particle was heated in a horizontal tube. Thus the first of the above difficulties was overcome by using an optical pyrometer, while the second ceased to exist. After several trials an arrangement was devised which would admit the particle to the gas mixture. The main features of the apparatus are apparent from fig. 1, which represents a vertical section.

The explosion chamber on the left was formed from a brass cylinder, of diameter 8·2 cm. At one end this was closed by a brass plate in which a hole 6 mm. in diameter was made. To the other end a brass ring was soldered, R in fig. 1, forming a rim for the tube. A sheet of commercial cellophane was held between two rubber rings placed on the rim, and a brass cover-ring C of the same dimensions as the rim screwed down, thus effectively closing this end. Outside the hole in the other end a slide S was constructed. In the slide was a slit Sl 6 mm. broad and 2·3 cm. long. This, sliding past the hole, served to open the chamber to admit the sphere. The gas inlet and outlet, each of which

had a stop-cock, were on opposite sides of the cylindrical wall of the chamber, in which was also a small window. A brass strip was soldered into the chamber to form a

Fig. 1.

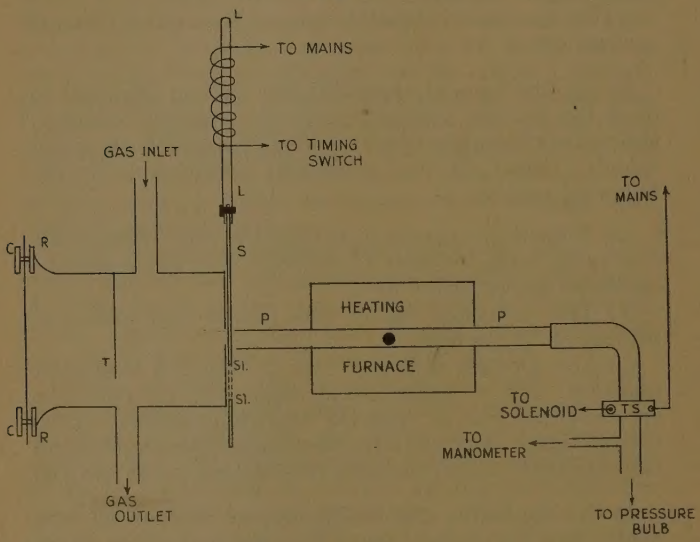

Fig. 2.

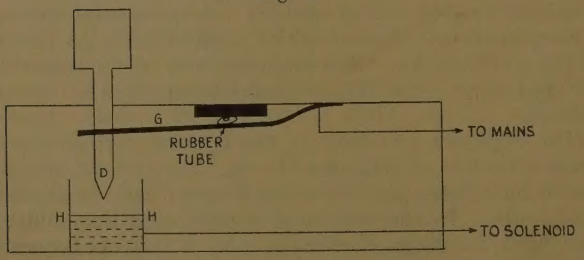

target T which the sphere would strike, in order to prevent it shooting through the cellophane. The slide was attached to the soft iron rod L slipped into the hollow core of a solenoid.

The particle was heated by a coil of either nickel chrome alloy or platinum wire wound round a silica or porcelain

tube P, which was set in alignment with the hole in the chamber. The shooting apparatus consisted of a hand-pressure bulb B connected through the timing switch TS to the end of the heating tube and to a manometer. The timing switch is shown in detail in fig. 2. The brass strip G there acts as a spring which constricts the rubber tubing leading from the pressure bulb to the heating tube. In fig. 2 this constriction is shown in section. The cup H contains mercury into which the dipper D may be pushed, closing the solenoid circuit. This also releases the pressure by depressing G so that the particle is shot along while the slide travels up. Adjustment for correct timing may be made by altering the mercury level or by the amount of friction between the iron rod and the solenoid core, and so the particle may be made to arrive at the end of the tube just as the hole is open. The winding on the tube P was covered first by a layer of fireclay and then by a winding of asbestos string.

The method of taking observations consisted in the following procedure. The gas mixture was made up over water in a gasholder and allowed to stand to ensure a thoroughly diffused mixture, and the rubber tube from the gasholder was connected to the gas inlet. The sphere was placed in the quartz tube and the heating current switched on, at a value which would give a higher temperature than the one being investigated. A previously standardized optical pyrometer was set to measure the temperature by looking along the heating tube from the end distant from the explosion chamber, the leading tube from the pressure bulb being at this stage not affixed to the end. When the temperature of the ball had become higher than was required, the current was cut down, and the rheostats in the heating circuit adjusted until the temperature reached and remained steady at the required value. This done, the leading tube from the pressure bulb and timing switch was connected to the end of the heating tube, ready to blow out the particle. The gas mixture was then turned on to run through the explosion chamber, the outlet leading to a burner set with its mouth to a flame, so as to burn up the issuing gas. The mixture was allowed to run through for a time sufficient to expel the original air and ensure the required concentration in the chamber. This could be judged by the appearance of the jet issuing at the burner. The

gas outlet and inlet were closed, the former first, to avoid the risk of air re-entering. This left the mixture in the chamber with a pressure slightly greater than atmospheric, causing a bulge in the cellophane cover. The outlet stop-cock was then rapidly opened and shut, to release this pressure, and then the release key depressed. If the particle did not enter, the timing arrangement was adjusted and the experiment repeated. When it went in, if an ignition occurred, the cellophane sheet was shattered by the explosion. In the adjustment of the pressure bulb it was always set to the same pressure, measured on an open manometer, for any one particle, so that an approximately constant velocity of firing might be obtained. The effect of varying velocity has not been investigated in the present work, although in view of the time-lag discussed in Section 1 it may be of importance. The speeds used were of the order of 4 metres per second, but may vary between 2 and 5 metres per second.

Note on Measurement of Temperature.

The scale-readings on the pyrometer are correctly calibrated only for black-body conditions. As shown in fig. 1, the heating coil was surrounded with clay and asbestos wrapping. Since the coils were usually from 5 to 6 cm. in axial length, there was a fairly uniformly heated portion of tube on each side of the sphere. Moreover, the particle was always at least 10 cm. from the end of the tube. The radiation entering the pyrometer is thus contained in a very small solid angle. For this reason and since radiation from the ball is reflected from the walls of the tube, the conditions under which the temperature is being measured approach black-body conditions. This is important, since for platinum Waidner and Burgess [10] have shown that a correction, varying from 70° at an apparent temperature of 800° to over 200° at an apparent temperature of 1500°, has to be added to the apparent temperature as read by the pyrometer if it is only direct radiation from the platinum that is being observed. The conditions in our case, while not exactly black-body conditions, are much closer approximations to them than to those of direct observation. The temperatures given in the tables of results are thus the direct scale readings of the pyrometer.

3. Results.

The first attempts were made with methane air mixtures, but were abandoned because of the high temperatures required. The heating coils used burnt out before an igniting temperature was attained. For a 10 per cent. methane mixture the sphere of diameter 4 mm. was heated to 1200° without causing ignition. Coal-gas air mixtures were therefore resorted to, to attempt with them a preliminary investigation of the general characteristics of ignition by hot particles. This done, it will be fairly safe to say that the failures to ignite methane were due to insufficient heating of the particles, and not to the fact that the source was a particle.

In the statement of results the particles will be referred to by numbers, the sizes of which are given in Table I. The diameters were measured with a travelling microscope, and, the particles not being accurately spherical, mean values, obtained for different sections, are given. Table I. gives the observations, + for ignition and − for non-ignition, found with the platinum spheres for a mixture of 10 per cent. coal-gas in air. The temperatures are given in centigrade. It will be seen that for some spheres more observations required to be taken than for others, in order to be sure of the minimum ignition point. The ignition points observed were for ignition immediately on the entrance of the sphere. On a few occasions, with the larger spheres, ignition occurred after striking the target and falling to the bottom of the chamber. This effect was erratic, and was counted as a non-ignition, for the purpose of determining the minimum *instantaneous* igniting point. It did not occur at all with the smaller spheres.

Note on the Cooling of Particles.

The rate of cooling of the spheres in moving from the heated portion of the quartz tube to the gas mixture will vary with the diameter. It is possible then that some of the difference in the ignition temperatures shown in Table I. may be due to this factor. To ascertain whether the different rates of cooling were influencing the observations to a great extent, experiments were repeated for particles 6 and 2, shooting them from various distances from the explosion chamber. If the cooling is sufficiently

TABLE I.—Platinum Spheres. 10 per cent. Coal-gas.

Particle No.	1		2		3		4		5		6		7	
Diameter in cm.	·109		·151		·197		·303		·349		·398		·500	
	Temp.	Obs.	Temp.	Obs.	Temp.	Obs.	Temp.	Obs.	Temp.	Obs.	Temp.	Obs.	Temp.	Obs.
	1250	+	990	−	1080	+	945	+	920	+	905	+	940	+
	1240	+	1005	−	1025	+	915	−	895	−	875	−	905	+
	1200	+	1025	−	985	−	955	+	915	+	890	+	890	+
	1160	+	1050	+	1040	+	940	+	905	−	885	+	875	+
	1090	−	1065	+	1025	+	925	+	920	+	880	+	855	+
	1130	−	1045	+	1005	−	915	+	915	+	880	−	845	−
	1140	−	1040	+	1025	+	900	−	905	+	875	+	870	+
	1050	−	1040	+	1010	+	915	+	900	−	880	+	865	+
	1100	−	1020	−	1000	−	905	−	890	+	865	−	840	−
	1120	−	1025	−	1015	+	915	+	895	+	885	+	840	−
	1270	+	1030	−	1010	−	910	−	890	+	870	−	850	−
	1230	+	..	..	1025	+	..	..	885	−	..	..	860	+
	1200	+	..	..	1000	−	..	..	895	−	..	..	850	−
	1160	+	..	..	1010	+	..	..	900	+	..	..	855	+
	1130	−	..	..	..	..	..	..	890	+				
	1140	−	..	..	..	..	..	..	885	−				
	1170	+	..	..	..	..	..	..	890	−				
	1160	+	..	..	..	..	..	..	895	+				
	1150	+												
	1145	+												
	1140	+												
	1130	−												
	1150	+												
Ignition point	1140		1040		1015		915		890		875		855	

rapid to be an important factor in our observed ignition temperatures, it should be shown by a variation of observed ignition points with distance moved by the particle, which variation would increase for smaller spheres. The results for nos. 6 and 2 are given in Table II., and show practically no variation with distance moved, the apparatus not being accurate to 5° in 1000°. It can therefore be taken that each particle enters the explosion chamber approximately at the temperature observed.

TABLE II.

Ignitions from Different Distances.

	Platinum sphere No. 2.		Platinum sphere No. 6.	
	Distance 26 cm.	Distance 11 cm.	Distance 24 cm.	Distance 10 cm.
Ignition point ..	1040	1035	880	875

Experiments with Quartz Spheres.

The above results show clearly the importance of size of a particle in determining its igniting power. It was now decided to investigate the effect of different material,

TABLE III

Quartz Spheres. · 10 per cent. Coal-gas.

Particle No.	1	2	3	4	5
Diameter in cm.	0·23	0·275	0·36	0·41	0·5
Ignition point	960	920	905	870	850

and quartz spheres covering the same range of sizes were obtained. The experiments were performed in the same manner, with the results given in Table III.

In fig. 3 the minimum ignition points are plotted against the diameters. The circles are the points given for the platinum spheres and the curve is drawn with reference to them. The crosses are the points found for the quartz spheres. They lie practically on the same curve as the

platinum, so that for at least quartz and platinum, in spite of the large difference in character of these substances, the difference in material has no appreciable effect.

Experiments with Pentane.

The results of the coal-gas experiments are at the present stage mainly of qualitative value.

The curve appears at first to be asymptotic for increasing diameters, and, if it is so, it is of interest to have a similar curve for a purer substance whose ignition temperature

Fig. 3.

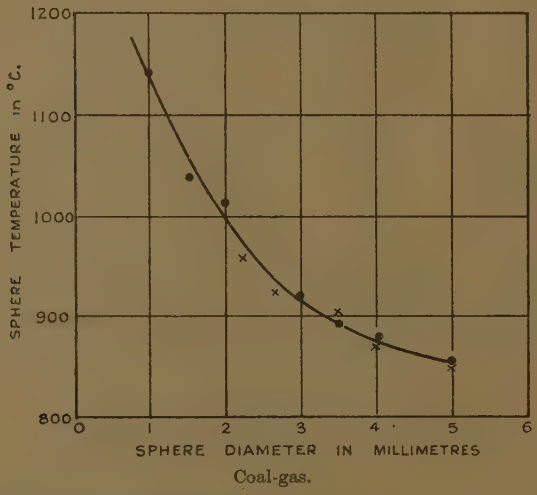

Coal-gas.

by the usual methods is well known, and we may see how it compares with our results. Accordingly methane was tried again, using platinum-wound heating coils. Even with these ignitions could only be obtained with larger spheres, and the hope of obtaining a set of results for methane comparable with those for coal-gas had to be abandoned. We may state, however, that for an 8 per cent. methane in air mixture the ignition point for a platinum sphere 6·5 mm. in diameter appeared to be about 1200° C.

Pentane was chosen in place of methane, and a set of experiments carried out upon it with the platinum spheres.

The first mixture investigated was 3 per cent. pentane air, and the results obtained are given in Table IV. Here again a pronounced variation of minimum ignition point with size is apparent.

TABLE IV.

Platinum Spheres. 3 per cent. Pentane.

Particle No.	1	3	4	6	7	8
Diameter in cm.	0·109	0·197	0·303	0·398	0·500	0·550
Ignition point	1370	1240	1155	1065	1040	1005

Further experiments were again made with quartz spheres, the results of these being given in Table V.

For pentane we find, as for coal-gas, that within the limits of accuracy of the method the igniting points of quartz spheres are not appreciably different from those for platinum spheres of the same diameter. This is shown in fig. 4, where minimum ignition point is plotted against diameter. The curve shows the results for platinum, the crosses representing those for quartz. It is seen that the results for platinum and quartz agree.

TABLE V.

Quartz Spheres. 3 per cent. Pentane.

Particle No.	1	3	4	5
Diameter in cm.	0·23	0·360	0·41	0·5
Ignition point	1220	1100	1060	1040

Once more size seems to be the main factor in determining the temperature at which a sphere can ignite a given explosive mixture.

Meanwhile, the problem had been considered from the theoretical standpoint, which is dealt with fully in the appropriate section. The formula there derived was tested for the coal-gas and pentane results in the manner discussed. The agreement for pentane was striking, so it was decided to repeat the experiments for another

gas. Butane and hydrogen were considered, hydrogen being desired, since a value for the activation energy of the hydrogen-oxygen reaction was available in the literature, and butane desirable as another member of the paraffins. Hydrogen was eventually adopted, being more easily obtainable.

Fig. 4.

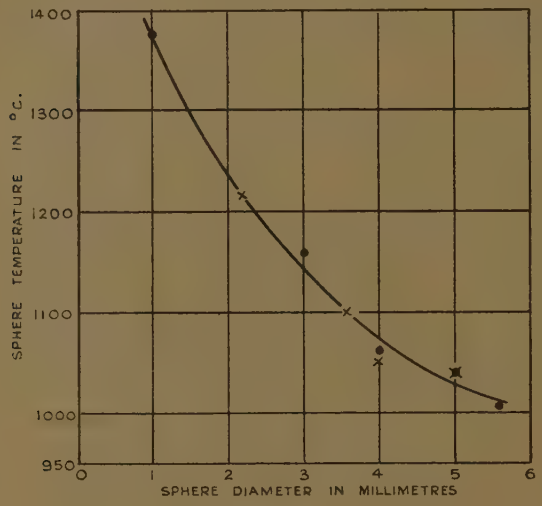

Pentane.

Experiments with Hydrogen.

The above results for pentane show that the minimum temperatures at which the spheres will ignite the mixture are much higher than the usual "ignition temperature" of the mixture as determined by adiabatic compression or concentric tube methods. Thus the curve has only a small gradient at about 1000° C. when the sphere diameter is $5\frac{1}{2}$ mm., while the ignition temperature for a 3 per cent. mixture is about 515° C. [11]. It was therefore decided to perform a similar set of experiments, using hydrogen-air mixtures instead, to see whether this feature of a minimum igniting temperature which is higher than the ignition temperature of the mixture still obtained, and, if so, if it appeared to the same extent.

The hydrogen was obtained in a cylinder from the British Oxygen Co. The mixture investigated was 20 per cent. hydrogen in air. The results for platinum spheres are in Table VI. and for the quartz spheres in Table VII.

TABLE VI.

Platinum Spheres. 20 per cent. Hydrogen.

Particle No.	3	3 *a*	4	7	8
Diameter in cm.	0·197	0·240	0·303	0·500	0·550
Ignition point	930	880	840	810	795° C.

TABLE VII.

Quartz Spheres. 20 per cent. Hydrogen.

Particle No.	1 *a*	2 *a*	3	4	5
Diameter in cm.	0·170	0·257	0·360	0·410	0·500
Ignition point	930	845	825	810	800

Fig. 5.

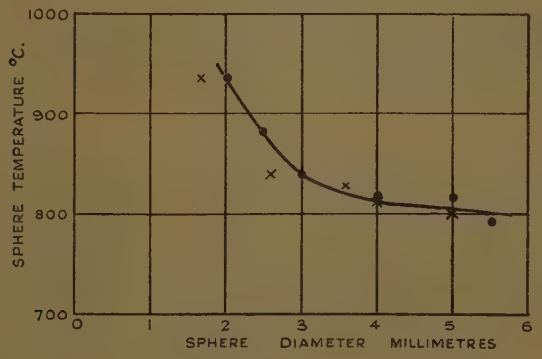

Hydrogen.

When the igniting points in the hydrogen experiments are plotted against diameter of sphere, as in fig. 5, it is seen that the quartz temperatures do not coincide so closely with the platinum temperatures for the same

diameter, as was the case with coal-gas and with pentane. The difference is now noticeable, but is still not very great, and is prominent only for the smaller spheres.

Now the ignition temperature of a 20 per cent. hydrogen-air mixture is about 590° C. [12]. Again the spheres in the range of size used require to be at a higher temperature than the ignition temperature of the mixture. The excess required, however, is not so great proportionally for hydrogen as it is for pentane.

4. Theoretical.

In the following attempt to discuss theoretically the ignition of gaseous mixtures by heated spheres it has been found necessary to assume very ideal conditions. To begin with, we deal only with a stationary sphere, and the first problem presented is that of the temperature distribution produced in the gas round the sphere, neglecting convection movements. It was originally hoped that the approximation derived in a previous paper [13], for the case of a non-burning gas, might be developed by superimposing the effect of combustion. This hope had to be abandoned. It will not be out of place, however, to give the derivation of the simplest differential equation for the heat-flow in the burning gas, although we have been unable to obtain a solution.

For a non-burning uniform medium the Fourier equation for spherically symmetrical temperature distribution is

$$\frac{\partial^2\theta}{\partial r^2}+\frac{2}{r}\frac{\partial\theta}{\partial r}=\frac{1}{k}\frac{\partial\theta}{\partial t}, \quad . \quad . \quad . \quad . \quad . \quad (1)$$

where k is the thermometric conductivity, whose variation with temperature is here neglected. But in the case of a combustible gas mixture, when we consider the heat-content of the thin shell between radii r and $r+dr$ we must allow for combustion proceeding at a velocity appropriate to the temperature θ in the shell. If V_θ is the fraction of unit volume of mixture which would react per second, and if Q is the amount of heat produced by the burning of unit volume of the mixture, heat is produced by combustion in the shell at rate $4\pi r^2 V_\theta Q\,dr$. The Fourier equation is therefore replaced by

$$K\left(\frac{\partial^2\theta}{\partial r^2}+\frac{2}{r}\frac{\partial\theta}{\partial r}\right)+V_\theta Q=C\frac{\partial\theta}{\partial t}$$

or
$$\frac{\partial^2\theta}{\partial r^2}+\frac{2}{r}\frac{\partial\theta}{\partial r}=\frac{1}{k}\frac{\partial\theta}{\partial t}-\frac{V_\theta Q}{K} \quad . \quad . \quad . \quad . \quad (2)$$

Chemical kinetics show that V_θ depends on the concentration of the reacting substances in a manner determined by the molecular order of the reaction, and on temperature approximately in the exponential fashion indicated by the Arrhenius equation for the velocity constant m of the reaction, i. e., $m=Ce^{\frac{-A}{R\theta}}$, where C and A are constants, A being the energy of activation of the reaction, and θ is the *absolute* temperature. If we neglect the variation with concentration, which we may do for our purpose since we are concerned only with initial stages in the ignition, we obtain the simplest form of the differential equation as

$$\frac{\partial^2\theta}{\partial r^2}+\frac{2}{r}\frac{\partial\theta}{\partial r}=\frac{1}{k}\frac{\partial\theta}{\partial t}-\alpha e^{\frac{-\beta}{\theta}} \quad . \quad . \quad . \quad . \quad (3)$$

where α and β are constants.

Since we have failed to find a solution of equation (3), we turn to the following convenient treatment. It is in general undoubtedly inexact, since by leaving out the differential equation we are considering only a shell at the surface of the sphere, and ignoring the effect of the heat passing out from it on the outer regions. But it may be the best possible theoretical attack on the problem, since questions of adsorption and accommodation coefficient effects might in any case vitiate the application of the exact solution of equation (3).

Let us assume

(*a*) that the layer of gas immediately in contact with the surface is raised instantaneously to the sphere surface temperature T_p;

(*b*) that the rate of loss of heat per unit area of the sphere surface is proportional to the difference between its temperature T_p and the initial temperature T_0 (room temperature) of the gas, *i. e.*, is $p(T_p-T_0)$, where p is a constant;

(*c*) that this gradient is uniform throughout the thin shell of gas instantaneously heated round the surface.

If these assumptions are permitted, we are picturing a distribution of temperature of the form of fig. 6.

Now we assume that extinction of initial combustion is caused by too rapid loss of heat into the unburnt portions of the gas mixture. Then, considering the shell dr round the sphere surface, heat will flow into it by conduction at rate $4\pi a^2 p(T_p - T_0)$, while heat is also lost by conduction away from the outer surface at rate $4\pi(a+dr)^2 p(T_p - T_0)$. Hence, if we neglect the square of dr, we have a net loss from the shell at rate $8\pi a p(T_p - T_0)dr$. Meanwhile heat has begun to be produced by combustion, and, since in the initial stages, neglecting variation in concentration of the reacting gases, we can put the fraction of unit volume of mixture reacting per second as $V_\theta = \alpha k_\theta$, where α is the concentration factor and k_θ the velocity

Fig. 6.

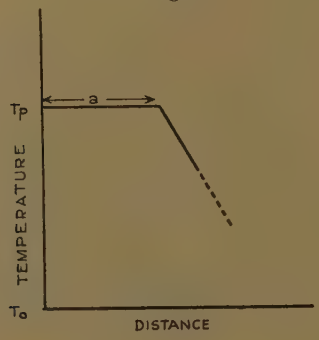

constant. Assuming the Arrhenius equation, we have $k_\theta = Ce^{\frac{-A}{R\theta}}$, where θ is the *absolute* temperature. Hence the initial rate of heat production in the shell is

$$4\pi a^2 dr \,.\, V_{T_p} Q = 4\pi a^2 dr \,.\, Q\beta e^{\frac{-A}{RT_p}},$$

where β includes the concentration factor and the C of the Arrhenius equation.

Now it may be assumed that if this initial rate of heat production is greater than the above rate of heat loss by conduction, the temperature of the shell will rise, heating outer portions, and so combustion will spread throughout the gas mixture. If it is less, the shell will cool and we may consider extinction to take place. The first case

will give explosion, the second will not. When the two are equal, the equality should define a limiting temperature for explosion, and this equality should be satisfied by the minimum temperature at which the sphere of radius a will ignite the gas mixture. On equating them we find, the temperatures being on the absolute scale,

$$8\pi ap(T_p - T_0)\,dr = 4\pi a^2\,dr\,.\,Q\beta e^{\frac{-A}{RT_p}}, \quad . \quad . \quad (4)$$

$$\therefore \quad \frac{2p}{a}(T_p - T_0) = \beta Q e^{\frac{-A}{RT_p}},$$

$$\therefore \quad \log\frac{2p(T_p - T_0)}{\beta Q a} = -\frac{A}{RT_p}$$

$$\therefore \quad \log\frac{(T_p - T_0)}{a} = \log\frac{\beta Q}{2p} - \frac{A}{RT_p}; \quad . \quad . \quad . \quad (5)$$

or we may express a in terms of T_p as follows:

$$a = \frac{2p}{\beta Q}(T_p - T_0)e^{\frac{A}{RT_p}} \quad . \quad . \quad . \quad . \quad (6)$$

The theory thus leads to a relationship between sphere radius and sphere temperature which is satisfied when explosion only just takes place. Hence T_p in equation (6) is the minimum temperature at which a sphere of radius a will ignite a certain gas mixture. The gas mixture in question is characterized by the constant βQ, while the material of the sphere must be characterized by the constant p, since it defines the heat exchange between the surface and the gas. It is thus at present out of the question to test the validity of this expression by direct calculation and comparison with the foregoing experimental results, since the constant p is unknown, and in most cases so also are A and β, which are derived from the kinetic equation of the reaction. Moreover, it is improbable that β and A as they occur here will be the same as for a homogeneous reaction. The values applicable in equations (5) and (6) will be those for a heterogeneous reaction taking place on the surface. The only type of test to which we can subject the theory is to see if it predicts certain qualitative results which agree well with the experiments.

In the first place we see from equation (5) that if A and β are constant, $\log\frac{T_p - T_0}{a}$ plotted against $\frac{1}{T_p}$ abs.

should give a straight line, whose gradient would be A/R. In fig. 7 are plotted the values obtained from the experimental results, taking T_p as the minimum igniting points obtained for the respective spheres, and room temperature as 18° C. We have plotted $\log_{10}\frac{(T_p-T_0)}{a}$ against $\frac{10,000}{\text{abs. } T_p}$.

It is seen that the pentane results lie very closely to a straight line, but the coal-gas and hydrogen results are not so convincing. In connexion with this, however, it

Fig. 7.

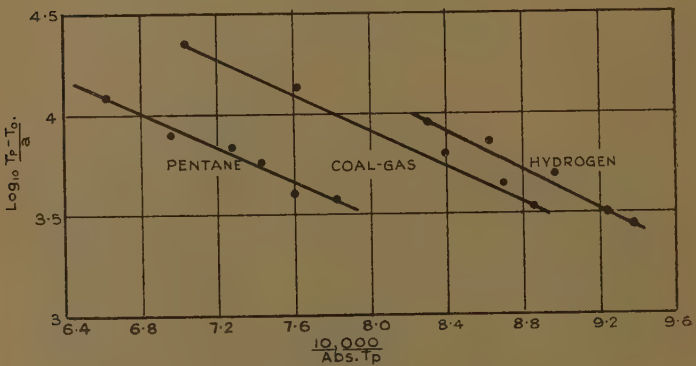

Platinum spheres. Pentane, coal-gas, and hydrogen.

must be remarked that Garner and Willavoys, in a paper on the lower limit of ignition of hydrogen-oxygen mixtures, have shown that the activation energy in the hydrogen-oxygen reaction may not be constant [14]. They found it varying from 15,000 to 7,000 calories per mol. Naturally this would affect the coal-gas also, although to a less extent.

The most striking feature, however, is the near equality of the slopes of the three lines. If the suffixes 1, 2, 3 designate pentane, coal-gas, and hydrogen respectively, calculation of the slope of the lines drawn gives

$$\frac{A_1}{R}=10,470,$$

$$\frac{A_2}{R} = 10{,}790,$$

$$\frac{A_3}{R} = 11{,}510.$$

Now since R is 1·96 cals. per mol., this would indicate the following activation energies for the three reactions concerned :—

	Cals. per mol.
Pentane-oxygen	= 20,520
Coal-gas-oxygen (probably average of components)	= 21,150
Hydrogen-oxygen	= 22,560

all of which are certainly of the order of activation energies.

With the second of these we have no values for comparison, but a value of the pentane oxidation may be obtained from the experiments of Pidgeon and Egerton [15]. They give 50,000 cals./gm.mol., which does not approach the value A_2. For the hydrogen-oxygen reaction we may refer to the paper of Garner and Willavoys mentioned above. Their values of the activation energy, even at the upper end, do not approach A_3.

We conclude, as was suggested above, that the value of A in the equations (5) and (6) must be an apparent heat of activation of a heterogeneous reaction rather than the true activation energy required in a homogeneous combination. Its difference from the latter will depend in general upon the adsorption relations existing between the material of the sphere and the different gases in the mixtures. If this is so, the similarity of the quartz and platinum igniting points in the cases of pentane and coal-gas is probably a fortuitous result, due to equivalence of the adsorption phenomena in these cases, while a slight difference begins to make itself effective with hydrogen. Another choice of substance might show wider differences in igniting points.

5. Discussion in Terms of Chain Theory.

The theory which has been developed is a " thermal " theory. No statement concerning the mechanism of the reaction has been made, beyond assuming the Arrhenius

equation as characteristic of the reaction velocity, and modifying this with reference to adsorption. This type of picture, which is essentially molecular, is abandoned when propagation out from the surface is considered and the macroscopic phenomenon of thermal conduction is utilized. Since it is now more or less agreed that gaseous oxidations all proceed with a chain mechanism, *cf.* Semenoff [16], it is of interest to see how chain theory may be applied to ignition by hot spheres, and how it may serve to connect up the two portions of the above theory.

The rôle of the hot sphere, from the chain-theory standpoint, must be to create initial active centres. While in principle the self-acceleration of a chain reaction with branching chain to a purely chain explosion is independent of the number of initial centres, Semenoff [17] shows that this simplicity is modified by the mutual action of the chains. If f is the probability of branching of the chains and g the probability of their rupture, the equation for the stationary state of the reaction is

$$n_0+(f-g)n=0, \quad . \quad . \quad . \quad . \quad . \quad . \quad (7)$$

n_0 being the number of active centres generated uniformly per unit volume per unit time by thermal motion or other agency outside the chain production, and n the total number of active centres per unit volume at the instant. Semenoff discusses a number of cases of mutual action of the chains. In particular, when the branching is dependent on the mutual action, but the rupture is not. we may put $f=f_0 n$. This is the most favourable set of circumstances for explosion. Equation (7) now becomes

$$n_0+f_0 n^2-gn=0. \quad . \quad . \quad . \quad . \quad . \quad (8)$$

If $4n_0 f_0 \geqslant g^2$ the stationary reaction is thus impossible, since n becomes imaginary. The reaction is now self-accelerated to explosion, the condition involving n_0 the number of active centres generated per unit time, so that the elementary simplicity is no longer tenable.

In the expression $4n_0 f_0 \geqslant g^2$, both sides are functions of the temperature and pressure. since f_0 and g are both dependent on these quantities, and since, moreover, n_0 is of the form $Ae^{-\frac{E}{RT}}$. In applying this discussion to the present work we know that the condition $4n_0 f_0 \geqslant g^2$ was not fulfilled with the gas mixtures at room temperature and at atmospheric pressure, since they did not explode.

The introduction of a hot sphere can alter the quantities n_0, f_0, and g only by raising the gas temperature. These quantities must therefore vary from shell to shell, according to the temperature distribution. We are thus brought back to a thermal conductivity problem : n_0, f_0, and g are varying radially, and the condition that for explosion to take place $4n_0f_0 \geqslant g^2$ must be satisfied in shell after shell will lead to a similar heat-balance condition, since it simply defines the temperature which must be maintained.

Secondly, if we can assume that the mutual action of the chains is negligible, the self-acceleration to a purely chain explosion is independent of the number of initial centres, but can only take place between an upper and a lower pressure limit. These limits depend on the temperature. Hinshelwood and Gibson [18] have shown for oxygen and hydrogen that the upper limit rises with temperature, and give it as 700 mm. for 576° C., while Sagulin, Kowalsky, and Semenoff [19] show that the addition of nitrogen lowers it. The mixtures of combustible gas with air in the above experiments, being under atmospheric pressure at about 18° C., were therefore well above any threshold for purely chain explosion of this kind to take place by a kind of trigger action of the hot ball. Even if they had not been, the variation of igniting point with size of sphere shows definitely that a purely chain explosion independent of the number of initial centres created is not occurring. Hence even if the effect of mutual action of the reaction chains in the gases used is negligible, we are still working in a region where the reaction is stationary. Explosion must therefore involve acceleration of local reaction to a state where rate of heat production is greater than rate of heat loss.

The above theory attempts to define that state on the simplest possible assumptions.

Summary.

(1) The need for investigation of the ignition of gaseous mixtures by hot particles is seen to arise in the literature of fire-damp explosions in coal mines.

(2) The literature on ignition of methane is summarized in so far as relevant to the problem of particle ignition.

(3) An experimental method for finding the minimum

temperature at which a hot sphere will cause ignition of a gaseous mixture of known composition is described.

(4) Results for platinum and quartz spheres with coal-gas-air and pentane-air mixtures show no appreciable difference in igniting point with the different sphere substance, although variation with size of sphere is marked.

(5) Results for platinum and quartz spheres with hydrogen-air mixtures show slight difference in igniting point with the different sphere substance.

(6) In every case the minimum igniting point varies greatly with size, diminishing with increase in sphere diameter, although less rapidly as the size increases. But in every case, even with the largest spheres used, the minimum igniting point was still very much above the known " ignition temperature " of the mixture.

(7) The possibility of theoretical treatment of the problem is discussed and an approximate form of theory suggested on the assumption that extinction is due to cooling by conduction to the unburnt parts of the gas. The theory only describes this process qualitatively and derives a formula which cannot be verified by direct calculation, as the constants involved in it refer to the finer phenomena underlying the gross processes actually described, and are not at present available in arithmetical values. But it can be compared in at least one respect with the results of the experiments described in the previous portions of the paper, and is therein found to agree qualitatively, and to give values of one of the unknown constants which are of the order required.

(8) The theory, which is a " thermal " one, is now discussed with reference to the chain character of the molecular reactions. It is shown that the experiments were conducted in a region where the reaction was stationary, even allowing for the effect of mutual action of chains upon the probability of branching. The necessity for the heat-transfer conditions being such as to allow of self-heating therefore remains.

The experiments were carried out in the Research Laboratories of the Natural Philosophy Department of Glasgow University, and I wish to express my appreciation of the help and encouragement which I received from Professor E. Taylor Jones.

References.

(1) Safety in Mines Research Board Paper No. 74. E. Beyling, p. 57.
(2) S.M.R.B. Paper No. 53. Section on Frictional Sparks.
(3) S.M.R.B. Paper No. 54. Burgess and Wheeler.
(4) Bone and Townend, ' Flame and Combustion in Gases,' 1927 ed. pp. 66–71.
(5) S.M.R.B. Paper No. 9. Naylor and Wheeler.
(6) S.M.R.B. Paper No. 53. Section on Ignition by Heated Metal Bars.
(7) Coward and Guest, Journ. Amer. Chem. Soc. xlix. p. 2479 (1927).
(8) S.M.R.B. Paper No. 36. Shepherd and Wheeler.
(9) J. W. McDavid, Trans. Chem. Soc. cxi. pp. 1003–1015 (1917).
(10) Waidner and Burgess, American Bull. Bur. Stds. i. p. 243.
(11) Bone and Townend, ' Flame and Combustion in Gases,' 1927 ed. Appendix I, p. 482.
(12) Bone and Townend, *loc. cit.* p. 478.
(13) R. S. Silver, Phil. Mag. xxii. no. 147, p. 466 (Sept. 1936).
(14) W. E. Garner and H. J. Willavoys, Trans. Far. Soc. xxxi. (1) p. 809 (1935).
(15) Pidgeon and Egerton, J. Chem. Soc. 1932, p. 661.
(16) Semenoff, ' Chemical Kinetics and Chain Reactions,' p. 462. Oxford, 1935.
(17) Semenoff, *loc. cit.* p. 74 *et seg.* '
(18) Hinshelwood and Gibson, Proc. Roy. Soc. A, cxix. p. 591 (1928).
(19) Sagulin, Kowalsky, and Semenoff, *Z. Phys. Chem.* 6 B, p. 307 (1930).

I.C.I. (Explosives) Research Division,
Stevenston, Ayrshire.
September 1936.

LXVI. *On the Production of Auroral and Night-Sky Light.* *By* S. Chapman *.

1. In recent years our knowledge of the auroral and the night-sky light has been greatly advanced †, particularly as regards the identification of the bands and lines in their spectra. Much of this knowledge, especially for the night-sky light, is set forth in a recent admirable summary by Déjardin ‡; it proceeds from two sources, namely, from long and difficult photographic

* Communicated by the Author.

† On the observational side, by Vegard and his collaborators (for the aurora), and by Rayleigh, Slipher, Cabannes, Dufay and Sommer (for the night sky); through laboratory studies by McLennan, Vegard, Kaplan, and others; and, more generally, by spectroscopists such as Schumann, Runge, Lyman, Birge, Hopfield, and, of course, through the theoretical work of those who have constructed a satisfactory theory of atomic and molecular spectra.

‡ G. Déjardin, Rev. Mod. Phys. viii. (1936).

studies of the spectra of the two kinds of light—both very faint—and from laboratory and theoretical studies of spectra in general, and especially, of course, of the atmospheric gases. Though details remain to be settled, the main facts are now clear. The auroral and night-sky spectra contain both lines and bands; the lines, which are of great prominence, are almost exclusively those of neutral atomic oxygen; the bands are mainly those of molecular nitrogen, both neutral and ionized, though in the infra-red the night-sky light probably includes bands due also to water-vapour and molecular oxygen. Lastly, in the night sky, "the greater part of the other radiations are very near the most intense comet nucleus lines (of unknown origin) and several AI (neutral argon) lines. The presence of lines of nitrogen atoms or of helium should be considered very doubtful" (Déjardin, *loc. cit.* p. 12).

2. Both the auroral and night-sky spectra show the oxygen lines prominently, but they differ greatly in the nature of their nitrogen-band components. As regards these nitrogen bands in the night-sky light, Déjardin writes (*loc. cit.* p. 12): "the Vegard-Kaplan bands (6·1) volts) are the most intense, then come the bands of the first and second positive systems (7·4 and 11·0 volts); lastly, the negative bands (19·6 volts) have a much reduced intensity. *The order of intensities is exactly reversed in the auroral spectrum.*" Hence Déjardin concludes that the essential difference between the two spectra consists especially in the *degree of excitation*. This probably expresses the view of all those who have seriously considered how auroræ and the night-sky light are produced.

3. It is generally agreed, with good reason, that auroræ are due to the entry into the earth's atmosphere of rapidly moving charged particles that are guided preferentially towards the polar regions by the action, over at least part of their path, of the earth's magnetic field. There is much difference of opinion, however, as to the processes that produce the night-sky light. Déjardin gives great prominence to a theory by Dauvillier that attributes all the phenomena of the high atmosphere to high-speed electronic emission from the sun, acting either directly, or indirectly. It is not my intention

here to examine this theory, but rather to set forth the merits of an alternative view.

A Theory of the Night-Sky Light.

4. Firstly, I maintain the hypothesis that in the upper atmosphere, above some level not yet determined, but probably not far from 100 km. height, the main constituents are molecular nitrogen and atomic oxygen, nearly (but not quite) all the oxygen being dissociated by absorption of sunlight. This hypothesis regarding the oxygen, proposed in 1930, arose out of a theoretical discussion (1929) of atmospheric ozone *. The observed ozone data underlying this theory have since been somewhat modified—in particular, the inferred mean height of the ozone has been lowered from about 50 to about 25 km.; but this change only strengthens the arguments for a high degree of oxygen-dissociation in the upper atmosphere, and for the belief that ozone is practically absent, and plays no significant part, at levels above about 100 km.

5. Secondly, I consider it probable that the energy represented by the light of the night sky is originally derived from sunlight, and is stored up during the day mainly in the form of dissociation (including ionization as a special case); though possibly some of the infra-red nocturnal light is derived from thermal energy stored up during the daytime. Much of the energy of the ultraviolet sunlight absorbed is doubtless first transformed into energy of excitation, but energy can be stored up in this form only for a very brief period, and little can survive after the sun's rays have been cut off in the earth's shadow.

6. The dissociation energy of individual pairs of ions and electrons exceeds that of oxygen atom-pairs derived from oxygen molecules, by a factor of 2 or 3; but the number of oxygen molecules dissociated into neutral atoms probably exceeds the number of ions by a far larger factor, so that (as was proposed in 1931) † the most likely source of the energy of the night-sky light is the dissociation energy of oxygen. The two

* Phil. Mag. x. p. 369 (1930); Mem. Roy. Meteor. Soc. iii. p. 103 (1930); Gerlands, *Beitr. z. Geophys.* xxiv. p. 66 (1929).

† Proc. Roy. Soc. A, cxxxii. p. 353 (1931).

atoms into which oxygen molecules are dissociated by day may both be in the lowest state (^3P) or one may be in this state and the other in the ^1D excited state. But very soon after sunset (*i. e.*, within about 100 seconds, which is the mean life-time for the metastable ^1D state) all the ^1D atoms then existing will have reverted to the lowest state, so that the energy derived from the re-formation of oxygen molecules from such atoms will be 5·1 electron volts. This, then, is the energy of the main source of excitation of the night-sky light, though processes yielding higher amounts of energy will also go on to a minor degree—as, for example, by the reunion of ions and electrons, yielding 12 volts or more.

7. The recombination of oxygen atoms to form molecules requires the participation of a third particle M *, to permit the fulfilment of the conditions of conservation of energy and momentum. The energy of dissociation yielded up on recombination may go partly into kinetic energy of the oxygen molecule and of the particle M, and partly into excitation of M. The particle M will, in general, be either a nitrogen molecule or an oxygen atom, the former being more probable, since nitrogen is more abundant than oxygen.

8. The nitrogen molecules will mostly be in their lowest state, and the first excited state above this requires an energy of 6·2 volts, which is more than can be provided for the excitation of N_2 by two oxygen atoms in their lowest state (^3P). Hence excitation of N_2 is unlikely to take place in such triple collisions. When, however, the particle M is a third oxygen atom (^3P), the dissociation energy (5·1 volts) can raise this atom (*i. e.*, any one of the three taking part in the triple encounter) to the ^1S state, requiring 4·2 volts, the balance of energy taking the kinetic form, or exciting the O_2 molecule to vibration or rotation. By descent to the ^1D state the ^1S oxygen atom can emit the green auroral light (λ 5577) leaving a ^1D oxygen atom (and an oxygen molecule) as the residual result of the whole process.

Every quantum of radiation λ5577 thus implies the

* Unless one of the O atoms is a negative ion—a case considered by Martyn and Pulley, Proc. Roy. Soc. A, cliv. p. 455 (1936); I think, however, that such cases are probably infrequent compared to recombinations of neutral atoms.

existence after emission of a ^{1}D oxygen atom. These must, therefore, be formed in considerable numbers throughout the night.

9. Some of them will emit their energy of excitation (1·96 volts) by radiating the red auroral light (λ 6300 or λ 6363), which, like λ 5577, is prominent in the spectrum of the night sky. If all of them did this, the number of quanta of such light should equal the number of quanta λ 5577. But some of the ^{1}D atoms will collide with normal oxygen atoms (^{3}P) in the presence of a third particle M, and recombine to form an oxygen molecule, yielding up energy of amount 5·1+1·96 or 7·1 volts. This is now sufficient to excite the third particle even if this is a nitrogen molecule. The result may be to raise the nitrogen molecule to the $A\Sigma^3g$ state, requiring 6·2 volts, or in cases where the kinetic energy of triple impact can contribute a small amount (about 0·3 volts) to the excitation energy, the $B^3\Pi$ excited state (7·4 volts) may be formed. By this means a steady supply of such excited nitrogen molecules is ensured throughout the night, those in the $A^3\Sigma g$ state being far more common than those in the $B^3\Pi$ state. The latter will emit light of the first positive nitrogen bands (which are present in the night-sky light, though they contribute far less light than the oxygen lines), being thereby transformed to the $A^3\Sigma g$ state. Thus all the nitrogen molecules excited by the recombination of a ^{1}D with a ^{3}P oxygen atom come, directly or indirectly, into the $A^3\Sigma g$ state.

[Actual observation shows that the integrated intensity of the red lines of oxygen in the night-sky spectrum is less than the intensity of the green line. This gives definite indication that an important fraction of the ^{1}D atoms of oxygen resulting from the emission of quanta of wave-length λ 5377 do get rid of their energy of excitation by processes not directly radiative.

It may also be remarked that recently it has been found, independently by Erophin and by Cabannes and Garrique, that the red emission lines in the "evening flash" or twilight sky is more intense than in the "morning flash" or dawn sky, at corresponding angles of the sun below the horizon. This points points to the presence of more ^{1}D atoms in the evening than in the morning sky, as § 6 would imply.]

10. Though the $A^3\Sigma g$ state is metastable, the pressures existing in the upper atmosphere are so low that many of the N_2 molecules in this state will have time, before making a collision, to radiate away the energy of excitation; in so doing, they emit light of the Vegard-Kaplan bands, which are now recognized to be an important part of the night-sky spectrum.

Those, however, that collide before radiating may impart their excitation energy to the particle encountered: if this be another nitrogen molecule, in the lowest state, no significant change would result: but in collisions with (normal) oxygen atoms, excitation of these to the ^1S state (4·2 volts) might occur, yielding another quantum of green light λ 5577, and thereafter another ^1D oxygen atom. The latter can form the beginning of another recombination process leading to the excitation of a nitrogen molecule.

11. Thus it is seen how the dissociative energy of oxygen can lead to the excitation of the Vegard-Kaplan bands and (with less intensity) the first positive nitrogen bands: and also, in two ways (one without and one with the intervention of metastable nitrogen), to the emission of the green and the red oxygen lines. The importance of the rôle of metastable nitrogen in the production of the night-sky spectrum has been shown by Kaplan * in numerous experiments. Thus our hypothesis explains the *main* features of the night-sky spectrum. Weaker constituents are the second positive and the negative bands of nitrogen. These require more energy, 11·0 and 19·6 (or more) volts respectively, reckoning from the ground states; but the negative bands, emitted by excited nitrogen ions, can be produced by exciting normal nitrogen ions—which are doubtless numerous in the ionized layers—by adding energy to the extent of only 3 volts. These excitations may result from the recombination of ions and electrons (which must undoubtedly go on through the night), but perhaps more probably by the excitation of metastable N_2 molecules (in the $A^3\Sigma g$ state), or normal nitrogen ions, by the addition of energy to the amount 4·8 or 3 volts respectively, through oxygen-recombinations.

* Kaplan, Phys. Rev. xlix. p. 67 (1936) and earlier papers.

12. In addition to these oxygen lines and nitrogen bands thus explained, the night-sky spectrum contains other bands in the infra-red, whose explanation seems to offer no serious difficulty in the presence of processes which can supply 5·1 volts energy.

The Auroral Spectrum.

13. Next consider the auroral spectrum as distinct from the ordinary spectrum of the night sky.

This I attribute to strong excitation by impact, due to particles, whether ions or electrons, entering the atmosphere from outside, with high speed. These particles traverse an atmosphere mainly composed (§ 4) of nitrogen molecules and oxygen atoms, most of which are neutral and in their lowest state. We may expect that the impact of the incoming particles will highly excite some of these atmospheric particles, yet without ionizing them, while some will be just ionized, and others will be both ionized and excited. The merely ionized N_2 and O particles will not radiate except when they recombine with an electron, and then almost all the radiation emitted will be far in the invisible ultra-violet, because the electron transition probabilities for N_2 and O happen to be greatest for the lowest states. The excited particles, however, both neutral and ionized, will radiate. Much of their radiation, however, will be in the invisible ultraviolet; this applies to most of the radiation from the highly excited oxygen atoms, whether ionized or neutral; for example, many of the latter may be brought by impact into the ^1P state (14 volts), from which they will descend either to the ^1S state or to the ^1D state, emitting the unobservable lines $\lambda 1217$ or $\lambda 999$ respectively. Only after thus getting rid of most of the energy imparted by the impact will they be in a condition to radiate the observed green and red light $\lambda 5577$ and $\lambda 6363$, $\lambda 6300$.

14. As regards the nitrogen molecules, those that are excited and ionized will emit the visible negative bands; these may be expected to be comparable in prominence with the green and red oxygen light, as is usually the case. After thus radiating, normal nitrogen ions will remain, which will gradually recombine with electrons with little or no emission of visible radiation.

[Similarly, the excited nitrogen molecules in the upper states corresponding to the Hopfield Rydberg series will emit unobservable ultraviolet light. However, many of the excited neutral molecules will be in the states A, B, C, or D (6·2, 7·4, 11·0, or 12·8 volts), the higher of these being the more strongly populated. All these states are triplet molecular states. Direct transitions to the ground state of N_2, which is a singlet state, are strictly forbidden for the B, C, and D levels. Thus they are unable to get rid of their energy in a single step. The selection rule breaks down somewhat for the A state, and as a result the Vegard-Kaplan bands ($A^3\Sigma \rightarrow X'\Sigma$) are emitted.] Molecules in the C and D states will descend to the B state by emission of the second and fourth positive bands; the latter (fourth) bands are too far in the ultraviolet to be seen, but the second positive bands should be, as they are, quite prominent in the aurora. The fact that they are less intense than the negative band suggests that the impact-excitation produces far more high-energy excited ions (of energy 19–21 volts) than moderately excited neutral molecules, of energy only 11 volts (C state) or 13 volts (D state). Most of the latter probably descend to the B state, from which, with emission of the first positive bands (likewise faint relative to the the negative bands) they descend further to the metastable A state. On account of the longer life of this state, many of these neutral N_2 molecules, that have thus descended from relative affluence in energy to the "moderate means" of the A state, will complete their return to the lowest rungs on the energy-ladder, not by emission of the Vegard-Kaplan bands (though this will occur to some extent), but by exciting O atoms to the ^1S state, and thus increasing the emission of the green and red oxygen lines.

15. Another consequence of the impact of the external particles on the nitrogen molecules may be their dissociation into atoms; but, judging from absorption spectra, nitrogen is far more readily ionized than dissociated, so that, though impinging particles may not act in quite the same way as photons, dissociation is likely to be of minor importance; moreover, though the nitrogen atoms formed, if at the same time they are also excited, will radiate, they will do so only in the far

ultraviolet, so that they will not contribute to the observable spectrum of the aurora. In the night-sky spectrum any contribution by nitrogen atoms seems still less likely, on account of the low energy of the main excitation process (as here proposed). For this reason I doubt Sommer's identification of the line λ 5208 on Slipher's plates of the night-sky spectrum, as due to atomic nitrogen; I prefer to conclude, with Déjardin (p. 12) that "in the night-sky spectrum the presence of lines of atomic nitrogen (as also of helium) is to be considered very doubtful."

16. The passages within square brackets, in §§ 9 & 14, have been rewritten partly in accordance with suggestions by W. C. Price, who saw this paper in manuscript.

LXVII. *An Acoustic Impedance Bridge.*

By N. W. Robinson, *A.R.C.S., B.Sc., Ph.D.**

Abstract.

The development of an acoustical bridge for measuring acoustical impedances is described. The bridge consists of two similar tubes forming ratio arms, into which sound waves are propagated equally by a loud speaker. The tubes are terminated by a known reactance standard and the unknown impedance respectively. The acoustical pressures at points equidistant along the ratio arms are balanced by adjusting the standard reactance. The balance is indicated by a differential microphone which acts as an acoustical galvanometer.

Measurements were made on Helmholtz resonators and on orifices, and the results obtained verified those obtained by an independent single tube method.

THE mathematical analogy between the behaviour of sound waves, mechanical vibrations, and alternating current electricity, has led to the search for acoustical and mechanical structures which would behave in a manner similar to that of well-known electrical circuits. Of electrical circuits the bridge is one of the most valuable

* Communicated by Dr. E. G. Richardson, B.A.

and powerful methods of measuring the resistance of conductors to direct current, and also the impedance of electrical apparatus to alternating current. Prof. H. L. Callendar constructed an analogue of the Wheatstone bridge for measuring the viscosity of gases, while an acoustical analogue of the more general bridge has been proposed by Smythe and Flanders in America. No results have been published by them.

The investigation of the properties of a similar bridge forms the subject of this paper.

The apparatus proposed by Smythe and Flanders [1] consists of a loud speaker working into two similar tubes forming the ratio arms. At the distant ends of these tubes are narrow bore branch tubes which communicate with the acoustic galvanometer or differential microphone. This takes the form of a thin-metal diaphragm clamped between two hollow chambers and faced on each side by fixed metal plates. By a suitable amplifying arrangement, changes in an electrostatic field set up between the plates and the diaphragm, due to movements of the latter, may be heard in telephones. Equality of pressure at the ends of the ratio arms, like equality of potential in the alternating current bridge, produces no sound in the telephones. The remaining arms of the bridge consist of the unknown and known standard impedances.

Another form of bridge has been described by Schuster [2], [3]. Here the source of sound divides a tube into two parts (the ratio arms) ; between the ends of these is placed the galvanometer in the form of a stethoscope, and beyond are the known and unknown impedances.

Before describing the actual bridge constructed, it is desirable to consider the requirements of a standard variable impedance. The structure should have resistance and reactance components, which are separately variable, and each component should be calculable.

The resistance portion of the standard impedance proposed by Smythe and Flanders consists of a flat spiral of copper tape wound with a narrow gap between each turn. If the slots are sufficiently narrow, they form constrictions in which dissipative forces are predominant and the reactive components are negligible. Following the resistance element comes a tube whose length can be varied by a tightly fitting piston. The effect of the

tube is considered to be purely reactive and its impedance given by the relation

$$-i\rho.c/\mathrm{S}.\cot 2\pi l/\lambda, \quad . \quad . \quad . \quad . \quad . \quad (1)$$

where ρ is the density of air, c the velocity of sound, S the area of cross-section of the tube, l the length of the tube, and λ the wave-length of the tone used. The total impedance Z, therefore, consists of the resistance and reactance in series, or

$$\mathrm{Z}=\mathrm{R}-i\rho.c./\mathrm{S}.\cot 2\pi l/\lambda \quad . \quad . \quad . \quad . \quad (2)$$

The resistance can be altered by introducing resistances of different known values, just as in the Post Office Box.

Unlike the electrical analogue, the position of the resistance is very important, as can be seen by examination of the well-known relation for the impedance at any point P in a cylindrical tube, viz. :—

$$\mathrm{Z_P}=\frac{(i\cos 2\pi l/\lambda\,.\,\mathrm{Z}-\rho c/\mathrm{S}.\sin 2\pi l/\lambda)}{\left(-1/\frac{\rho c}{\mathrm{S}}.\sin 2\pi l/\lambda.\mathrm{Z}_x+i\cos 2\pi l/\lambda\right)}, \quad . \quad . \quad (3)$$

where Z denotes the impedance at point X distant l from P. If Z_x is a pure resistance R, the expression for $\mathrm{Z_P}$ consists of a resistive and reactive part, both of which depend upon the value of R. Similarly, if, beyond the resistance portion there is a second length of tube, Z_x becomes

$$\mathrm{R}-i\rho.c./\mathrm{S}\,.\cot 2\pi l_2/\lambda, \quad . \quad . \quad . \quad . \quad . \quad (4)$$

where l_2 is the length of stopped tube beyond the resistance. Again, the resistive and reactive components are very complicated and interdependent. A similar result is obtained if the resistance units are used in parallel with the reactance.

The Schuster standard impedance is composed of two tubes, one sliding in the other. The outer tube is stopped by a rigid disk, while the inner one is stopped by a disk of hair-felt, kept in place by zinc gauze. The lengths of the two tubes can be varied separately. The impedance of this structure is given by replacing R in (4) by Z_h, where the latter is the complex impedance of the hair-felt. When the modified expression is exerted in (3) it is evident that the resistive and reactive components of $\mathrm{Z_P}$ are again interdependent. In practice, Schuster

calibrated his known impedance for different lengths of l and l_2 by a separate electro-acoustical method.

The actual bridge constructed is illustrated in fig. 1 (*a*), which shows the general arrangement of the branch tubes and the way in which the differential microphone was connected. A moving coil loud speaker LS, fitted with a plane diaphragm, was attached at one end of a brass tube 7·62 cm. internal diameter. The other end

Fig. 1.

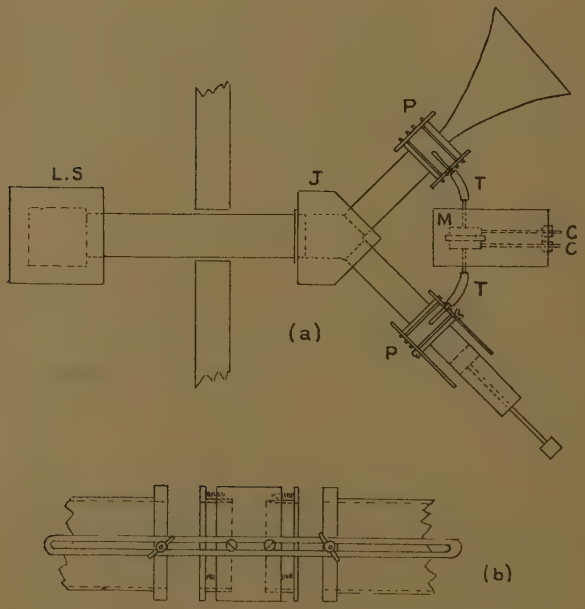

(*a*) Layout of apparatus. (*b*) Connecting pieces.

of the tube had a flange, which was screwed to the wooden junction J. The junction was made as symmetrical as possible and varnished so that it presented a similar polish to that of the brass tubes. The ratio arms were pushed into the junction piece. They were 5·08 cm. internal diameter, so that there was not more than 12 per cent. change in area at the junction to give rise to reflected waves in the loud speaker conduit. The

connecting pieces P, P between the ratio arms and the known and unknown impedances had to be such that the slot resistances could be inserted rapidly in the measuring arm and the unknown impedances rapidly attached at the unknown side. They are shown in detail in fig. 1 (*b*). The faces were capable of moving about 1·0 cm. parallel to the axis of the tube, but could be pressed back towards the main body of the connector against the tension of three spiral springs. A short length of copper tube, 0·32 cm. internal diameter, was passed to the centre through a hole in the wall of the connector to form the pressure tube leading to the differential microphone M. The openings of the pressure tubes T, T were, therefore, 1·27 cm. from the point of attachment of the unknown impedance on one side and from the measuring tube on the other. Lengths of slotted brass strip allowed the tubes and connectors to be clamped together, as illustrated in fig. 1 (*b*).

The first differential microphone constructed consisted of two telephone receiver cases with the magnets removed, clamped face to face with a single diaphragm between them. An ordinary carbon microphone button was attached to the diaphragm, and the output was amplified by a 4-valve amplifier. The cavities on each side of the diaphragm were made as symmetrical as possible by filling them to the same extent with plasticene. A copper tube, 0·32 cm. internal diameter, was screwed into each receiver case, and connexion was made to the pressure tubes by short lengths of rubber tubing. Owing to the difficulty of ensuring that the lengths of these conduits were exactly the same, and that equal pressures in the branch tubes resulted in equal pressures at the diaphragm, a second tube, about 0·95 cm. diameter, was screwed into one of the receiver cases. This tube was fitted with a piston, and by adjusting its position the impedance on one side of the diaphragm could be made to match that on the other. The adjustment was made by terminating the two branches by rigid disks at equal distances from the pressure tubes, then adjusting the movable piston in the microphone case until silence was obtained. Compensation was found difficult with this microphone, and although it was very sensitive, the carbon proved noisy, so that it was eventually discarded.

The second microphone also consisted of two receiver

cases sharing a single diaphragm, but the magnets were retained, and an adjusting tube was provided in each receiver case. With this arrangement, control was obtained over the impedances on both sides of the diaphragm. Moreover, by suitable adjustment, the sensitivity of the microphone could be varied. The microphone M was placed in a metal box with the compensating tubes and pistons C, C protruding through the ends, as shown in fig. 1. It was packed with cotton wool and mounted on rubber supports, so that it was insulated as far as possible from extraneous sounds. The loud speaker was also packed round with cotton wool in a metal box, and as a further precaution against sound reaching the observer's ears direct, it was placed on a support outside the room, and the conduit passed through the wall to the inside of the observation room.

The first experiments were confined to the measurement of reactances which admitted of theoretical treatment such as Helmholtz resonator. A resonator was made up of a brass disk, 0·635 cm. thick, with a hole 1·27 cm. diameter bored through the centre, and a length of 5·08 cm. diameter brass tube fitted with an adjustable piston. The orifice was clamped between the connecting piece and the extension tube.

The impedance of such a structure is given by

$$\frac{i\rho\omega}{K} - \frac{i\rho.c}{S}\cot\frac{2\pi l}{\lambda}, \quad . \quad . \quad . \quad . \quad . \quad (5)$$

where $\frac{i\rho\omega}{K}$ is the impedance of the orifice, K being the conductivity, ω=the pulsatance, and the second term is the impedance due to the length of stopped pipe. This is the general relation for a Helmhotz resonator of any dimensions, but when $\frac{2\pi l}{\lambda}$ is small it can be thrown into the more usual form

$$\frac{i\rho\omega}{K} - \frac{i\rho c}{S}\frac{\lambda}{2\pi l} = \frac{i\rho\omega}{K} - \frac{i\rho c^2}{\omega V}, \quad . \quad . \quad . \quad (6)$$

where V denotes the volume of the resonator. It is therefore possible to calculate the impedance of the resonator from its dimensions. Following Rayleigh, the conductivity was taken to be equal to the diameter

of the orifice and then corrected for finite thickness by means of the following relation :

$$\frac{1}{K} = \frac{1}{C} + \frac{L}{A}, \quad \ldots\ldots \quad (7)$$

where L=length of the orifice and A=area of the orifice, and C the conductivity of the same orifice in a thin sheet. This gave K=0·67. In order to make the bridge as symmetrical as possible, a tube of 1·27 cm. diameter, fitted with a piston, was chosen as the known variable reactance. The impedance of this tube was that of a closed tube viz. :

$$-\frac{i\rho c}{S_1}\cot\frac{2\pi l_1}{\lambda},$$

where S_1 was the area of cross-section.

There were found considerable differences between the theoretical values of the impedances given by

$$\frac{i\rho\omega}{K} - \frac{i\rho c}{S_2}\cot\frac{2\pi l_2}{\lambda}, \quad \ldots\ldots \quad (5)$$

and the measured values given by

$$-\frac{i\rho c}{S_1}\cot\frac{2\pi l_1}{\lambda},$$

when l_1 and l_2 were taken to be the geometrical lengths of the tubes without end correction. The values obtained are shown on fig. 2, which show the theoretical values in addition. In his treatment of Acoustic wave-filters, W. P. Mason [4] has advised that at the junction between tubes of unequal diameters the ordinary Rayleigh correction of 0·785×radius, *i. e.*, 0·5 cm. in this case, should be applied where the radius is that of the smaller tube. A correction of this order was used. The result is shown on fig. 2. It will be seen that this correction was much too large, and it seemed that some intermediate value would lead to better agreement between theoretical and measured results.

A second orifice was now used in place of the small one. It consisted of a hole, 1·27 cm. diameter, bored in a disk 0·32 cm. thick. From these dimensions the conductivity was calculated to be K=0·965, using the classical formula. The same measuring reactance tube was used as before. This time, however, it was found

that an end correction of $0{\cdot}785 \times r$ applied to the measuring tube was much too small to agree with the theoretical values of the impedance of the resonator. This is shown in fig. 3.

Owing to the difficulty of interpreting these results the Helmholtz resonator was replaced by a tube and piston similar to the measuring tube itself. The impedances of lengths of 5, 10, and 15 cm. of this tube

Fig. 2.

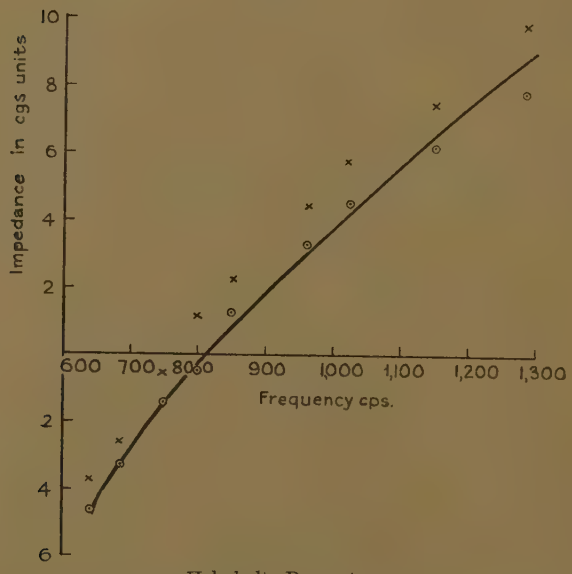

Helmholtz Resonator.

— Impedance calculated taking K = 0·67.
○ Impedance measured taking end correction = 0·32 cm.
× Impedance measured taking end correction = 0·5 cm.
Diameter of orifice 0·95 cm. Length of orifice = 0·32 cm.
Diameter of chamber 5·08 cm. Length of chamber = 1·5 cm.

were measured at various frequencies, and the results are shown on fig. 4. Comparing the measured and calculated results it is seen that good agreement was obtained. The apparatus was therefore functioning as a bridge, and the discrepancies obtained with the Helmholtz resonators could only be attributed to the

uncertainties of the value assigned to the conductivity of the orifice in the case of the resonator and the end correction in the case of the measuring tube. The latter uncertainty was removed by making the measuring tube the same diameter as the ratio arm. In addition, a set of orifices were used bored out of thinner disks. The diameters ranged from 1·0 to 4·0 cm., in steps of

Fig. 3.

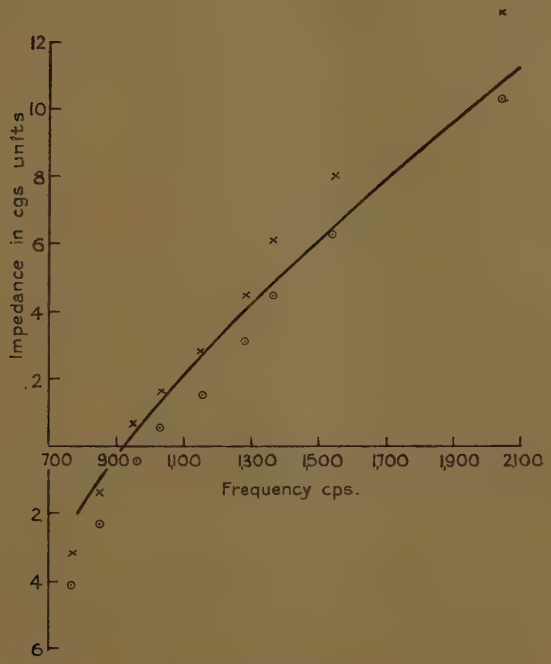

Helmholtz resonator.

— Impedance calculated taking K = 1·18.
C Impedance measured taking end correction 0·32 cm.
× Impedance measured taking end correction 0·50 cm.
Diameter of orifice 1·27 cm. Length of orifice 0·32 cm.
Diameter of chamber 5·08 cm. Length of chamber 2·0 cm.

0·5 cm., the thickness being 0·16 cm. These orifices were inserted in turn in the tube to form resonators with it, and the piston in the measuring tube adjusted

to balance the bridge. The conductivities of the orifices were calculated from the lengths of the reactance standard required for balance. In each case the measured conductivities were found to be greater than the Rayleigh values. Table I. shows the results.

Fig. 4.

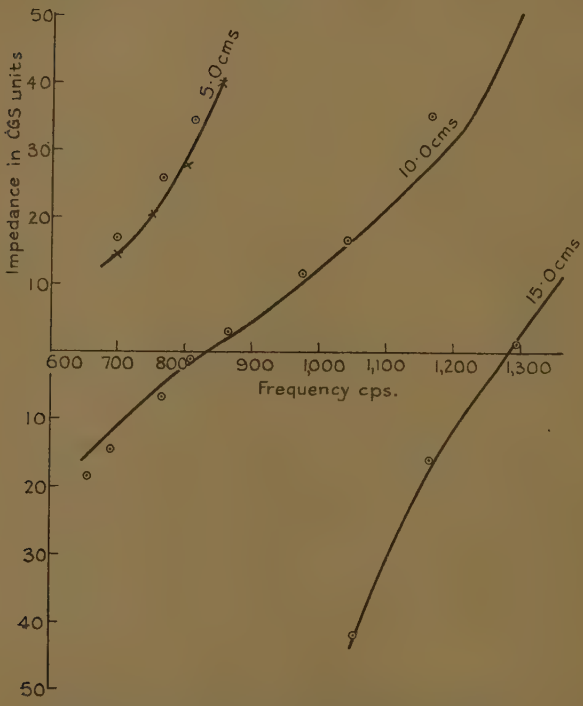

Impedance of lengths of stopped tube, $\frac{1}{2}$-inch diameter.

Curves show calculated impedance.
Points show measured impedance

The first two orifices were also used alone, *i. e.*, without the Helmholtz resonator chamber. The small diameter measuring tube was retained. The values of the conductivities obtained were 0·85 and 1·37 instead of the theoretical values of 0·67 and 0·965 respectively. The

geometrical lengths of the measuring tube were taken in each case. These figures show considerable differences.

An attempt was also made to eliminate the end correction for the smaller measuring tube by bending the ends of the pressure tubes at right angles in both branches of the bridge, so that the openings lay on the axis of the tubes and in the same plane as the junction between the measuring tube on the one side, and in the plane of the orifice in the other. This arrangement led to no better agreement between theoretical and practical results than before, but in this case the presence of the pressure tubes in the orifices would be a disturbing factor.

TABLE I.

Diameter of orifice.	Measured conductivity bridge 1.	Measured conductivity bridge 2.
cm.	cm.	cm.
3·0	7·43	8·8
2·5	5·44	5·5
2·0	3·45	3·5
1·5	2·02	1·9
1·0	0·94	0·90

Thickness of orifices 0·16 cm.

We may sum up the disturbances encountered in the bridge method of measuring acoustic reactances as follows :—

1. The effect at the junction between two tubes of different diameters.

2. The effect on the conductivity of an orifice due to its position in a tube.

3. The effect of the presence of the pressure tubes in the two branches.

There were indications from the results obtained by E. J. Irons[5] and A. E. Bate[6] that the conductivities of orifices placed as constrictions in a Kundt's tube were considerably greater than those for orifices in a plane sheet. In addition, G. W. Stewart[7], in his experiments on the transmission-ratio for sound waves, of a tube fitted with a Helmholtz resonator as a side branch, had to assume a conductivity for the orifice of about

50 per cent. greater than the theoretical value in order to make his measured transmission ratio agree with the calculated value.

Because of this uncertainty, and the difficulty of interpreting the bridge results, a second method[8] of measuring the reactances was devised. It was found advisable to restrict the investigation to the measurement of the conductivities of orifices, since the uncertainty as to the values to be inserted for these quantities nullified the usefulness of the bridge.

Briefly, the second method consisted in so adjusting the end impedances of a closed tube that the pressure at a fixed point was zero. One end was fitted with a quarter wave-length of stopped pipe and the other end, which consisted of a loud speaker and branch tube, was adjusted to give zero pressure at the point. The quarter wave-length of stopped tube was then replaced by the impedance to be measured attached to a variable length of tube. The impedance of the combination could now be made zero, and hence it was possible to calculate the unknown impedance by putting Z_p equal to zero in equation (3).

It was found that the conductivity of an orifice forming a constriction could be closely represented by the relation

$$C = \frac{0{\cdot}787d}{(1-d/D)^{1{\cdot}895}}, \quad \ldots\ldots \quad (9)$$

where d is the diameter of the orifice, D is the diameter of the tube, and C is the required conductivity in an infinitely thin sheet. C was obtained by reduction from the measured conductivity K by the relation

$$\frac{1}{K} = \frac{1}{C} + \frac{L}{A},$$

which was afterwards shown to be applicable to these orifices[9]. The conductivities of the orifices used in the Helmholtz resonators were calculated from equation (9) and found to be 1·18 for the 1·27 cm. diameter orifice, and 0·67 for the 0·95 cm. orifice, compared with 0·965 and 0·67 calculated previously from classical theory. The impedance of the resonator with the larger orifice was recalculated and shown on fig. 3. That of the resonator with the smaller orifice required no revision.

On recalculating the results obtained by the bridge

method for the same two orifices terminating the bridge tube, similarly improved agreement was obtained. Thus applying the end correction of 0·32 * to the measuring tube, the larger orifice gave 1·15 as the conductivity and the smaller 0·66. The conductivities of orifices terminating a tube were also measured by the single tube, and it was found that they could be represented by the equation

$$C = d(1+d/D)^{1\cdot19} \quad . \quad . \quad . \quad . \quad . \quad . \quad (10)$$

where C is the conductivity in a thin sheet and d and D the diameters of the orifice and tube respectively. Curve 3, fig. 4, also represents the results. From equation (10) the conductivities for these orifices were 1·07 and 0·65. These values show closer agreement with the above figures than with the classical values of 0·965 and 0·67.

Another factor which was found to have caused errors in the first bridge experiments was that introduced by having the openings of the pressure tubes leading to the microphone too near to the orifices. It was found possible [9] to map the equi-pressure surfaces near to orifices, and it was discovered that the wave fronts were disturbed at distances of 1·5 to even 2 cm. near the orifices. The disturbances were, in general, more pronounced near the centre of the tube. It is important, therefore, that the pressure tubes leading to the differential microphone should be not less than 2 cm. from the junction in each arm of the bridge. The impedance of this length, provided it is exactly the same in each arm, must not be included in the impedance of any structure attached at the junctions.

Since the pressure tubes were 1·27 cm. from the junctions when the measurements were made on the resonators, the error due to this factor would be small.

The discrepancy between the recalculated values and the measured values of the impedances could only arise through the effect at the junction between the 1·27 cm. measuring tube and the 5·08 cm. ratio arm. This effect was also investigated by the single tube method [9]. The junction was treated as an orifice and its conductivity measured. The results were found to be represented by

$$C = 2\cdot00/(1-d/D)^{1\cdot446}, \quad . \quad . \quad . \quad . \quad (11)$$

* See p. 678.

where d and D are the diameters of the small and large tubes respectively. From this equation the conductivity at the junction between the measuring tube and the ratio arm was 3·95, which corresponds to an "end correction" of 0·32 cm. instead of 0·5 cm. which was used. The measured impedances calculated with this new "end correction" gave much better agreement with the new calculated impedances shown in figs. 2 and 3.

The meaning of "end correction" becomes vague when dealing with two tubes having a common axis, and effectively in series, for each tube can be considered as an open tube, and hence each should require an end correction. But the value associated with the separate tubes would be very difficult to estimate. It seems preferable, therefore, to consider each junction in an acoustical apparatus as an orifice having an impedance

Fig. 5.

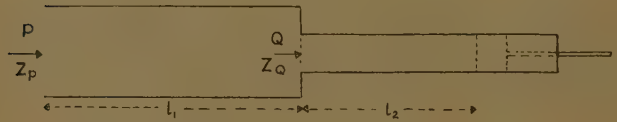

given by $\frac{i\rho\omega}{K}$, where K is a conductivity factor, and to make use of the geometrical lengths of the various tubes for calculating the impedance. Thus the impedance at point P in fig. 5, due to two lengths of tubes of different diameters, will be obtained by application of equation (3), viz. :

$$Z_P = \frac{i\cos\frac{2\pi l}{\lambda}\cdot Z_Q - \frac{\rho c}{S_1}\sin\frac{2\pi l_1}{\lambda}}{-\frac{1}{\frac{\rho c}{S_1}}\cdot\sin\frac{2\pi l_1}{\lambda}\cdot Z_Q + i\cos\frac{2\pi l_2}{\lambda}},$$

where Z_Q is

$$Z_Q = \frac{i\rho\omega}{K} - \frac{i\rho c}{S_2}\cdot\cot\frac{2\pi l_2}{\lambda}, \quad . \quad . \quad . \quad . \quad (12)$$

and l_1 and l_2 are the geometric lengths of the respective tubes, and K is the conductivity factor measured under

the same conditions. If, however, the idea of an end correction is retained, then Z_P would become

$$Z_P = \frac{i \cos\frac{2\pi}{\lambda}(l_1+\alpha_1)\, Z_Q - \frac{\rho c}{S_1}\sin\frac{2\pi}{\lambda}(l_1+\alpha_1)}{-\frac{1}{\frac{\rho c}{S_1}}\cdot\sin\frac{2\pi}{\lambda}(l_1+\alpha_1)\, Z_Q + i\cos\frac{2\pi}{\lambda}(l_1+\alpha_1)}, \quad . \quad (13)$$

and in this case Z_Q would be

$$-i\frac{\rho c}{S_2}\cot\frac{2\pi}{\lambda}(l_2+\alpha_2), \quad . \quad . \quad . \quad . \quad (14)$$

where α_1 and α_2 are the end corrections to be applied to l_1 and l_2 respectively. Since α_1 and α_2 cannot be determined separately, the former method of calculating the impedances must be adopted.

The difference between the old and the new methods may be appreciated by examining the two expressions for Z_Q. Equation (12) may be written as

$$Z_Q = \frac{i\rho c}{S_2}\left(k\alpha_2 - \frac{\cos kl_2}{\sin kl_2}\right),$$

putting

$$k = \frac{2\pi}{\lambda} = \frac{\omega}{c} \text{ and } \alpha_2 = \frac{S_2}{K}. \quad (10)$$

The end correction is usually very small, and if the wavelength is fairly large, then the above expression may be thrown into the form

$$Z_Q = \frac{i\rho c}{S_2}\left[\frac{\sin kl_2 \sin k\alpha_2 - \cos k\alpha_2 \cos kl_2}{\sin kl_2}\right],$$

assuming $\sin k\alpha_2 = k\alpha_2$ and $\cos k\alpha_2 = 1$.

Hence

$$Z_Q = -\frac{i\rho c}{S_2}\frac{\cot k(l_2+\alpha_2)}{\sin kl_2} \quad . \quad . \quad . \quad . \quad (15)$$

$$\doteqdot -\frac{i\rho c}{S_2}\cot k(l_2+\alpha_2). \quad . \quad . \quad . \quad . \quad (16)$$

Having shown that the original bridge could be used satisfactorily to measure reactances, it was thought

possible to simplify the structure to make it more compact. The new bridge consisted essentially of a single tube about 10 inches long, with a single telephone source as a branch at the centre. Two pressure tubes were placed on the axis of the tube symmetrical with the source and the ends of the tube. The ends of the pressure tubes were arranged to be 2·54 cm. from the ends of the main tube. The differential microphone previously used was attached to the two pressure tubes.

The two parts of the main tube on either side of the telephone source, leading to the pressure tubes, now constituted the ratio arms, and with the pressure tubes so far removed from the ends of tube there was no possibility of their being situated in a region of non-planar wave-fronts when the unknown impedances were attached.

The thin orifices were placed in turn at the end of one ratio arm, and a length of stopped pipe equal to $\lambda/4$ was placed behind. The impedance of the stopped pipe was, therefore, zero. The reactance arm was then adjusted to give silence in the telephones. From the length of the reactance arm the impedance of the orifice could be calculated. The conductances of the orifices obtained with the modified bridge are shown in Table I.

This type of bridge is much more compact than the original one, and it may be used with great facility at any fixed frequency. For measuring the impedance of a structure over an extended range of frequencies, however, the differential microphone must be adjusted to denote the correct balance at the particular frequency used. The process has been already described. It would be possible to make a permanent calibration of the plungers in the adjusting tubes attached to the microphone, by preliminary experiments, so that for future use, the plungers could be set at the calibration appropriate to the frequency.

The bridge has been shown to be a useful and an accurate method of measuring acoustical reactances, but it can only be of universal application if it measures acoustical resistances also. Some acoustical resistances of the slot type have been constructed, both for series and for parallel working, and experiments are being carried out with these in the bridge.

The results of this work will be published in a future paper.

Bibliography.

(1) Smythe and Flanders, U.S.A. Patent.
(2) Schuster, *Phys. Zeits.* xxxv. p. 408 (1934).
(3) Schuster, E.N.T., May 1936.
(4) Mason, Phys. Rev. xxxi. p. 283 (1928).
(5) Irons, Phil. Mag. v. p. 580 (1928).
(6) Irons, Phil. Mag. vii. p. 873 (1929).
(7) Stewart, Phys. Rev. xxvii. (1926).
(8) Robinson, Proc. Phys. Soc. xlvi. p. 772 (1934).
(9) Robinson, Ph.D. Thesis (University of London) (1936).
(10) Stewart and Lindsay, ' Acoustics ', p. 150 (1931).

LXVIII. *The Aerodynamic Characteristics of a Cylinder having a Heated Boundary Layer.*

By E. G. Richardson, *B.A., Ph.D., D.Sc.* (*Armstrong College, Newcastle-on-Tyne*) *.

Abstract.

Recent developments in the theory of the boundary layer in fluid motion indicate that it is the local Reynolds' number peculiar to a layer near the wall of an obstacle in a stream rather than that proper to the complete obstacle which determines the resistance shown by the obstacle to the motion of the fluid. This suggests that a cylinder having an " ultra-viscous " boundary layer may, under certain conditions, show a less resistance than that of a normal cylinder. Experiments to test this point are described, in which the " lubrication " of the boundary layer is attained through heating the cylinder, and hence the air in its close vicinity, and the gain discussed in the light of the temperature gradient in the boundary layer. The paper concludes with a note on the " dust-free space," examined in conjunction with these results.

THE idea, introduced by Osborne Reynolds, that a criterion of the type vd/ν (v=velocity, d=a linear dimension, ν=dynamical viscosity) determines the nature of a fluid motion, and incidentally the resistance to flow, has more recently been applied by Prandtl and others to the " boundary layer," viz., that layer of fluid adjacent to a solid boundary in which the gradient of velocity

* Communicated by the Author.

from zero to the stream value is accomplished. In accordance with these ideas change of the type of flow in the boundary layer, *e. g.*, from streamline to turbulent, will occur when the local Reynolds' number delimited by putting d equal to the depth of the layer, v and ν equal to the mean velocity and viscosity in it, reaches a certain value. Thus in rounding the curve of a bluff obstacle in the stream the Reynolds' number of the boundary layer tends to grow until *ablösung* or breakaway of the layer into discrete vortices in the wake occurs. At very high speeds a sudden change in the resistance coefficient is believed to indicate turbulence in the boundary layer throughout its path. For practical purposes it is usually sufficiently near the truth to set the velocity gradient as constant within the boundary layer, so that v may be put equal to half V, the general stream velocity. For a given value of V we should be able to lower the eddy-making resistance of an obstacle exposed to a stream either by a suitable reduction of d, the thickness of the layer, or by an increase of ν, the mean viscosity within the layer.

The former scheme, in its application to slots on aeroplane wings, is well known, and consists in giving the fluid a boost of momentum as it passes over the bluff forepart of an obstacle sufficient to carry it part at least of the way through the adverse pressure gradient which usually exists along the stern, delaying the widening of the boundary layer and consequent breakaway of fluid which would otherwise occur towards the rear stagnation point. Alternatively, and with the same effect, fluid may be sucked into the (hollow) body of the object near the stern by a suitable vacuum pump.

The other device which suggests itself as a means to raise the critical velocity of the boundary layer is to lubricate it, *i. e.*, to increase the mean value of ν within the layer. This seems to have been little explored at present. It is the object of this paper to describe some experiments with such an " ultraviscous " boundary layer.

Experiments in Water.

Nikitine * has described some preliminary experiments in which a stream of water ($\nu = \cdot 012$ c.g.s.) bathed an

* *C. R.* cxcvii. p. 896 (1933).

obstacle of which the boundary layer was an air-film ($\nu = \cdot 15$ c.g.s.). In fact the model was held in a water channel while a jet of air played on the bow, completely enveloping the model. A reduction of resistance was recorded and ascribed to the presence of the air-sheath. Difficulties were experienced in preventing the air from breaking up into bubbles at too weak injections, or exerting a force on the model at strong injections. These facts, together with the drastic discontinuity between air and water due to surface tension, preclude, in the opinion of the present writer, reliance being placed on this method of exploring the question of reducing resistance. One would expect the resistance measured by Nikitine to be the same as that in an extensive *air* medium, and unaffected by the presence of the water.

In connexion with an investigation on the resistance and mechanics of propulsion of fishes * the writer tried to measure the effect on the resistance of a wooden fish-form model of rubbing a light oil on its surface, to imitate the mucus with which the body of a living fish is covered. The resistance was computed from times of free fall of the model in a water-tower. While the resistance at low speeds seemed to be unchanged there was some indication that the breakdown of the Stokes type of viscous flow was deferred until higher speeds were reached by the greased model; but the method of estimating resistance was not sufficiently accurate to justify the tabulation of the data. Accordingly recourse was made to a heated cylinder, so that the required local increase of viscosity was produced by a rise of temperature in the boundary layer.

Experiments in Still Air.

It was found that the most convenient form of heated cylinder for these experiments was one made of refractory material—actually glazed vitreosil, made by the Thermal Syndicate. Hollow tubes of the material were wound internally with a spiral heating coil, the tubes having diameters ·65, 1·3, 2·6, and 15·6 cm. The change in the aerodynamic forces on the thin cylinders associated with the heating was expected to be small, so that not only had the heat supply to be large, involving the use

* J. Expt. Biol. xiii. p. 63 (1936).

of electric power up to 1 kilowatt, but the force balance had to be very sensitive. Considerable thought was given to the problem of designing such a balance to allow the leading in of large currents without variation due to deflexion of the balance, and finally the form shown in fig. 1 was adopted for all but the largest cylinder.

The cylinder AB rests on an aluminium frame rigidly attached to the balance-beam CD. The pivot of the beam is that formed by the junction of the two wires EF, GH, which may be given tension and torsion through the operation of the wing-nuts on the stanchions J, K. The inner ends F and G of these two wires are soldered

Fig. 1.

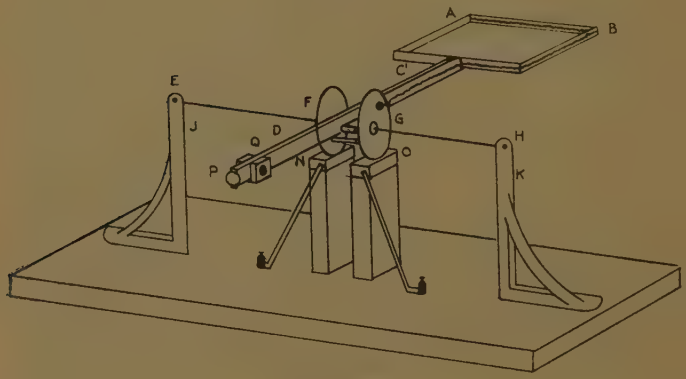

Force balance.

to the centres of two disks, which are in turn attached to the balance-beam through two ebonite distance pieces. The disks float in the mercury cups N, O, to which the current leads are taken. From the disks the current passes to the heating element through the balance-beam and back through an insulated wire laid alongside it. Deflexion of the balance by small forces is measured through the intervention of the mirror P and the usual lamp and scale. Larger forces are balanced by a resetting of counterpoises such as Q along the calibrated beam. In measuring very small forces (of the order of ·1 gm. wgt.) the instrument was used as a Threlfall balance, *i. e.*, the counterpoise was set in a little too far

for equilibrium and the suspension wires twisted until the beam returned to the horizontal, any change in the aerodynamic force being then indicated by the spot of light on the scale. Under these conditions the balance is very sensitive, in fact unstable, if the principle is applied too thoroughly. (The Threlfall Principle, though apparently new to aerodynamics, is used with effect on magnetometers, where the same desideratum—sensitivity, in spite of ponderousness—is met.)

Fig. 2.

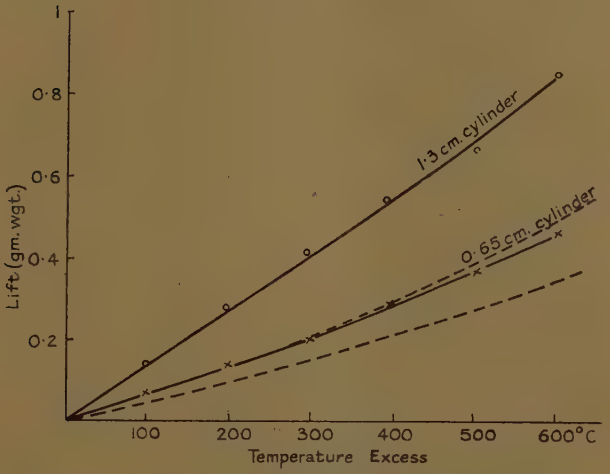

Lift on heated cylinders due to natural convection; total effect, continuous lines; less buoyancy, broken lines.

Firstly, to get measurements of the aerodynamic forces involved in *natural convection* the whole apparatus was shielded from draughts by side screens, and deflexions observed through a glass window. Fig. 2 shows the lift on the two smallest cylinders at various temperatures. A considerable proportion of the lift is due to change in buoyancy. When this is subtracted we are left with a lift (due to natural convection current) proportional to $\theta_0^{\frac{1}{4}}$ (θ_0 being the excess temperature of the cylinder (measured by a thermocouple) and to $r^{\frac{1}{3}}$, where r is the radius).

Experiments in a Wind Channel.

The cylinders were now introduced into a small vertical wind channel, so that the supporting frame and balance lay outside. The air was sucked through the channel downwards, while the natural convection current was, of course, upward. Figs. 3 and 4 show results for the ·65 and 1·3 cm. cylinders respectively, when cold and

Fig. 3.

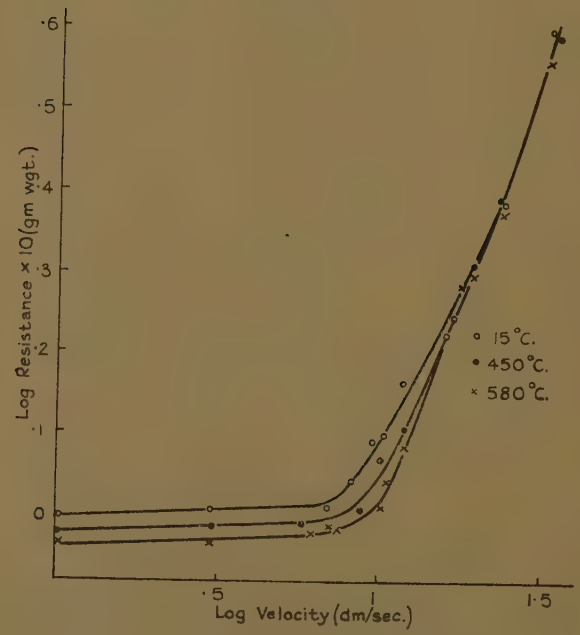

Resistance of 0·65 cm. cylinder (hot and cold).

when heated to two constant values of the temperature. The resistance of the hot cylinder at first appears negative owing to the natural convection current, but even when this has been neutralized by the contrary channel wind the slope of the resistance : velocity curve of the hot cylinder remains low for longer than that of the cold cylinder. At values of Vd exceeding 300, however, the

curves appear to concur, and the "improvement" is lost.

Before proceeding to discuss the effect in detail, it is desirable to have some knowledge of the extent of the temperature boundary layer associated with forced convection. Accordingly an iron-constantan thermocouple made by silver-soldering a pair of ·02 cm. wires

Fig. 4.

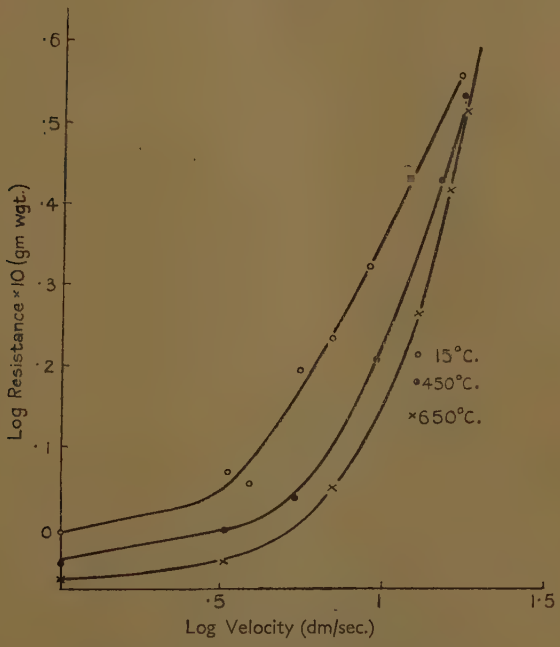

Resistance of 1·3 cm. cylinder (hot and cold).

together was set parallel to the axis of each cylinder in turn, and traversed on a micrometer screw in the space of a few mm. from the surface outward, (A) in the horizontal plane through the axis of the cylinder, (B) in a horizontal plane through the rear stagnation point. The results for the 1·3 cm. cylinder are exposed on fig. 5 (for the A position) and fig. 6 (B position). The channel

speed is noted on each curve, positive upward and negative downward.

The curves of fig. 5 fall steeply to a level of 60° to 80° C., whence they descend quite slowly as the separation from the cylinder increases; this stage of nearly constant temperature probably represents the effect of radiation on to the thermocouple. When the channel wind is opposed to the natural convection quite thick temperature

Fig. 5.

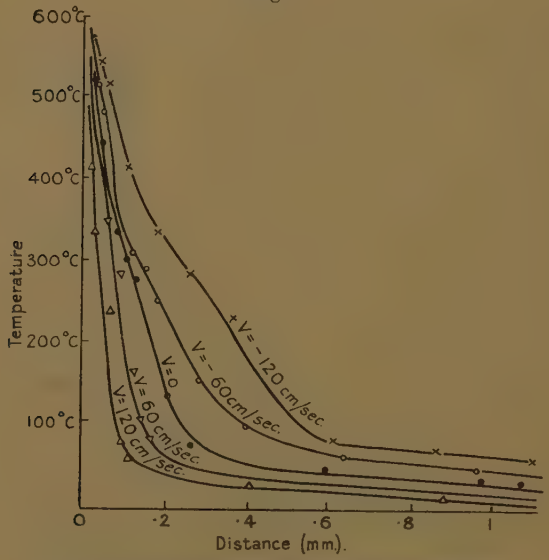

Temperature distribution in horizontal plane through axes of 1·3 cm. cylinder.

boundary layers are produced having a less regular fall. The curves of fig. 6 are reproduced to indicate the extent of the heat wake at various speeds in the neighbourhood of the critical.

It should be noted that Hartmann * has recently published measurements on the resistance of an electrically heated sphere at Reynolds' numbers between 100,000 and 170,000—the interesting region where the

* Franklin Inst. J. ccxviii. p. 593 (1934).

resistance coefficient of the cold obstacle, having remained constant since 100, begins to drop. Although the temperature rise used by Hartmann was small—up to 80° C.—a reduction of resistance was observed when the cylinder was heated, but a detailed analysis of the effect of heating the boundary layer was not possible, since the

Fig. 6.

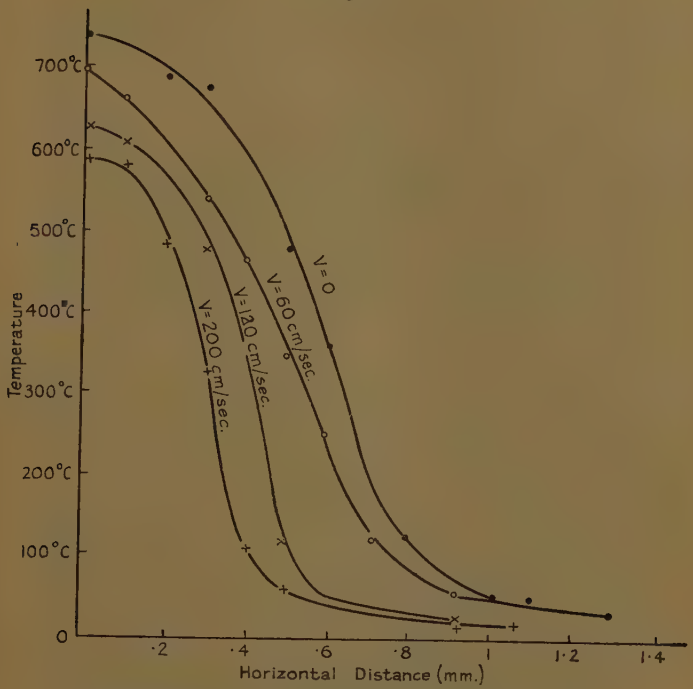

Temperature distribution in horizontal plane through rear stagnation point of 1·3 cm. cylinder.

temperature field near the sphere was not measured. The reason for the inclusion of the 15 cm. cylinder among those of the present experiments was to test this effect at Reynolds' numbers near 10^5. As this represented the limit which could be reached in the author's channel, this second critical region could not be further explored,

but the data given in the table below indicate that this fall in the drag coefficient is likewise delayed by heating the boundary layer. It is hoped to examine this region more thoroughly later.

Velocity	250	355	440	620	710	750
Drag (cold)	20	40	60	110	140	150
D/V^2	3·1	3·2	3·15	2·9	2·8	2·7
Drag (hot)	20	40	60	115	150	170
D/V^2	3·1	3·2	3·15	3·0	3·0	3·0

Discussion.

It is well known that a close analogy exists between the processes by which momentum and heat are transferred to a fluid through which a body is moving, so that, for example, the drag and heat-loss, expressed in non-dimensional terms, can each be plotted as a function of Reynolds' number *. The principal distinction is to be found in the absence of a sharp change in the slope of the heat-loss curve at the critical Reynolds' number such as occurs in the drag. This is due to the fact that whereas the formation of eddies involves an abnormal dissipation of motional energy the heat-loss is less affected, as the eddies simply swirl the already heated portions of fluid round the stern of the obstacle. Thus the change in the configuration of the temperature field as the speed goes up is quite a gradual process (*cf.* fig. 6) †.

Similarly it will be found that a map of the streamlines round a hot body in a fluid marches closely with a map of the isothermals at a given speed. Hermann ‡ has derived functions for the temperature and velocity gradients round a cylinder in *natural convection*, and compared his calculations with the measurements of Jodlbauer §. For *forced convection* we have a theoretical

* Precisely the heat-loss has to be plotted against the product $(vd/\nu)(c\nu/k)$, but as the latter quantity is a constant in diatomic gases it may be dismissed from the argument. The curve in question will be found in Fishenden and Saunders, ' Calculation of Heat Transmission,' fig. 22.

† The change in drag coefficient which occurs at supersonic speeds is paralleled by abnormal heat-loss as the velocity of sound is approached (*cf.* Santon, *C. R.* cxcvi. p. 625 (1933). It would be interesting to measure the drag of a hot wire at supersonic speeds.

‡ *V. D. I. Forschungsheft*, no. 379 (1936).

§ *V. D. I. Forschungsheft*, iv. p. 157 (1933).

paper by Piercy and Winny * which actually deals with the heat-loss from cylinders, but the authors have kindly supplied, in a written communication, the temperature distribution round the circular cylinder, with which the experiments now described may be tested.

In each case the temperature function is plotted against a "non-dimensional distance" measured from the cylinder surface, and the curve takes the same form for both types of convection, which is to be expected, since natural convection may be regarded as a low-speed order of forced convection entailed by density differences in the fluid adjacent to the hot body. In natural convection, however, the dimensionless distance x is expressed in terms of Grashof's number, $G=r^3g\beta\theta/\nu^2$, where g is the acceleration of gravity and β the coefficient of expansion of the fluid. (Hermann finds $x \propto G^{-\frac{1}{4}}$.) In forced convection, on the other hand, x is a function of Peclét's number, $P=Vrc/k=\cdot 7Vr/\nu$ in air, where c is the thermal capacity per unit volume and k is the thermal conductivity of the fluid. The solution given by Piercy and Winny is actually

$$f(x)=\theta/\theta_0=\frac{2}{\sqrt{\pi}}\int_x^\infty e^{-x^2}dx, \quad . \quad . \quad . \quad . \quad (1)$$

where x is written for $\frac{l}{r}\sin\frac{\xi}{2}\sqrt{P}$, l being the distance from the surface of a point where the temperature excess is θ and ξ the polar coordinate reckoned from the front stagnation point. (For the data on fig. 5, $\xi=\pi/2$.) When x is large (1) may be written $f(x)=e^{-x^2}/x\sqrt{\pi}$.

The curve (1) is shown on fig. 7 by the continuous line, while the broken line gives the velocity distribution (after Hermann). The broken line, as drawn, represents of course the velocity distribution in natural convection. In forced convection the velocity would fall to the general stream velocity at infinity. The boundary layer of velocity as indicated by the rising gradient extends to a depth at which the temperature has fallen to roughly half the surface value.

In comparing the experimental distribution with theory one is faced with the difficulty that P is not constant

* Phil. Mag. xvi. p. 390 (1933).

through the boundary layer, nor is the temperature at $x=0$ necessarily the same as that of the solid body. The work of Langmuir indicates that there is a discontinuity at the solid surface. Following Hermann we select the Peclét number corresponding to the mean temperature of the boundary layer and exterpolate the readings to find θ_0 at $x=0$ to call this the body temperature. Bearing in mind these approximations, the

Fig. 7.

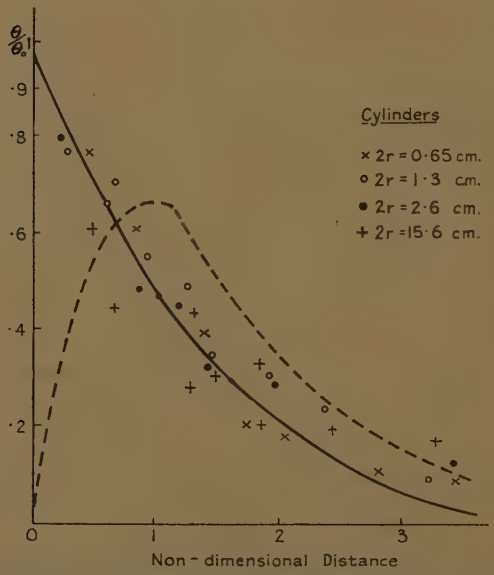

Boundary layer in horizontal plane through cylinder axes; continuous line, temperature (general convection); broken line, velocity (natural convection).

agreement between the experimental points and the curve is fair up to moderate values of x. At large values of x the temperature measured by the thermojunction does not fall as rapidly as it should. This may be ascribed to the radiation from the cylinder to the thermometer, which will be proportionally to the convection greater at greater distances. At least up to $x=2$ the general shape of the curve is followed by all results,

and at this value of x a common value ·2 for θ/θ_0 is reached, so we will define the thickness δ of the boundary layer to conform to this value of the non-dimensional distance. This makes

$$\frac{\delta}{r} = \frac{2}{\sqrt{P}} = \frac{7}{3}\sqrt{\frac{\nu}{Vr}} \quad \ldots\ldots \quad (2)$$

in terms of the Reynolds' number of the cylinder, or

$$\frac{r}{\delta} = \frac{9}{49}\frac{V\delta}{\nu} \quad \ldots\ldots \quad (3)$$

in terms of the Reynolds' number of the boundary layer. Change in the type of flow should then be expected at a critical value of r/δ for a given temperature. Comparing the results of figs. 3, 4, and 7, we obtain the following table :—

r,	θ_0.	Crit. V.	Crit. δ from (2).	$\frac{r}{\delta}$.
·325 cm.	450° C.	70 cm./sec.	·093 cm.	·28
	580° C.	90 ,,	·097 ,,	·30
·65 ,,	450° C.	40 ,,	·17 ,,	·26
	650° C.	55 ,,	·185 ,,	·28
1·3 ,,	650° C.	40 ,,	·31 ,,	·24

Within the limits of experimental error—which is quite considerable when it is a question of picking out a critical velocity from a resistance graph—we may consider the last column constant, as theory requires.

The criterion we are examining applies to the formation of alternate eddies of the Bénard-Karman type behind the cylinder. There is yet a lower critical velocity which should be apparent when the stationary vortices of the Nisi-Porter type are first formed—with a spherical obstacle this occurs at $vd/\nu = 4$ *. We have no measurements in forced convection at such low Reynolds' numbers, but the induced velocities involved in the lift curves under natural convection embraced this range—that is to say, that if a wind equal to the maximum induced velocity involved in the measurements of fig. 2 blew

* Phil. Mag. xlvi. p. 754 (1923).

upon the *cold* cylinders this lower critical velocity would have been exceeded. We may then take the absence of any sudden inflexion in the lift curves of fig. 2 as an indication that the hot boundary layer in natural convection inhibits the formation of these stationary vortices just as at higher velocities, in forced convection, the alternate shedding of the vortices is delayed. The *schlieren* photographs of Hermann confirm this aspect, since they fail to show vortices at Reynolds' numbers for which they would exist behind the normal unheated cylinder.

Hermann also shows that the velocity gradient induced by natural convection, and causing the lift through its associated skin-friction, is proportional to $\frac{\nu}{r}.\,\mathrm{G}^{\frac{1}{4}}$, *i. e.*, to $r^{\frac{1}{4}}\theta_0^{\frac{1}{4}}$ if ν be assumed to vary directly with θ_0. The reduced lift (fig. 2, dotted line) does in fact vary with $r^{\frac{1}{4}}$, but the proportionality with θ_0 does not agree with Hermann's theory. We shall find a discrepancy of the same order in the next section.

A Note on the Dust-free Space.

The dust-free space surrounding a heated cylinder in a dusty or misty atmosphere, discovered by Tyndall *, has recently been quantitatively examined by Miyake † and by Watson ‡. Whatever the ultimate origin of the phenomenon—and rival theories will be found in the papers just cited—it is obvious from the published photographs that the configuration of the dust-free space conforms to the temperature (or velocity) boundary layer. That being so, it may be of interest to compare measurements of the boundary layer with those of the dust-free space. As the measurements made by Miyake and Watson concern natural convection we will select the results of Jodlbauer-Hermann for the comparison.

The dimensionless boundary layer thickness δ/r in natural convection is inversely proportional to $(r^3 g\beta\theta_0/\nu^2)^{\frac{1}{4}}$, *i. e.*, $\delta \propto r^{\frac{1}{4}}\theta_0^{-\frac{1}{4}}\nu^{\frac{1}{2}}$. The exact value of the exponent n in the proportionality $\nu \propto \theta^n$ will depend on the range of

* Proc. Roy. Inst. vi. p. 3 (1870).
† Rep. Aero. Inst. Tokyo. x. p. 85 (1935).
‡ Trans. Farad. Soc. xxxii. p. 1073 (1936).

temperature concerned, but taking $n=1$ as an attempt to cover a moderate range, we shall get $\delta \propto r^{\frac{1}{2}}\theta_0^{\frac{1}{2}}$. Now Watson used two rods, 4·6 and 9 mm. diameter respectively, together with a wire ·001 in. diameter. The measured values of δ (*cf.* his table I.) agree moderately well with the relation $\delta \propto r^{\frac{1}{2}}$. For instance the thinner rod and wire (ratio of diameters 18 : 1) have dust-free spaces of relative thickness 1·9 : 1 at 220° C. The agreement is not so good in the temperature variation; instead of an exponent $\frac{1}{4}$ Watson (fig. 5) puts $\frac{1}{2}$, while Miyake prefers ·7. Apart from discrepancy between the experimental results of the two observers the disagreement with theory may be in part imputed to our assumption of a constant viscosity throughout the boundary layer.

LXIX. *On the Construction and Sensitivities of Short Period Platinum Thermometers.* *By* J. J. Manley, *M.A., D.Sc.Oxon.* (*Fellow of Magdalen College, Oxford*) *.

(a) *Introductory.*

CONFRONTED with the problem of determining small changes in the melting-points of certain substances consequent upon intensive drying, it appeared that the solution of the same would best be achieved by the use of platinum thermometers; and so as a preliminary to our main purpose, which is to be dealt with in another paper, some 20 thermometers were constructed and tested. In experimenting with these our chief object was the discovery of an instrument having a minimum heat capacity and, for the limited volume of its bulb, a maximum resistance; moreover, it was for our purpose, essential that the thermometer should be capable of instantaneously responding to small variations in temperature. We first describe the structures of the more satisfying of these thermometers and tabulate their respective constants, etc., our standard of reference being one of the well-known platinum-on-mica thermometers enclosed in a glass tube and made by the Cambridge Instrument Co.

* Communicated by the Author.

(b) *The Several Thermometers Described.*

(1) In fig. 1, A, is depicted our reduced replica of the Cambridge thermometer. By using an attenuated resistance wire we were able to limit the thickness of the intersecting mica plates forming the frame, to 0·1 mm. Also, the plates being thin required no notches for the reception and retention of the wire. Rightly prepared, their edges are finely irregular; and so, during the operation of the loaded wire, with the result that the wire is partially but effectively embedded and thus kept *in situ*.

Fig. 1.

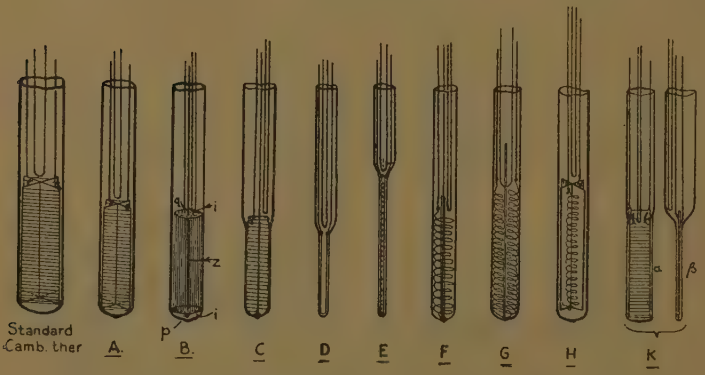

(2) In the next diagram, fig. 1, B, is shown a second plan. According to this the wire is carried by two thin ivory disks i, i, supported centrally by one of the silver wire leads and permanently held apart by a capillary glass tube z. Just within the edge of each disk is a circular row of minute and closely spaced holes through which the attenuated wire is passed from disk to disk and drawn nearly but not quite taut. The ends of the wire are fused to the leads at p and q. Arranged thus the resistance wire constitutes a vertical and cylindrical grid. The sensitivity of a thermometer of this type may be increased by a second and similar but of necessity smaller grid constructed within the other. Calculation shows that when the length and diameter of the grid are respectively 25 and 5 mm. and the distance from

hole to hole 1 mm. the required length of the wire is approximately 40 cm.

(3) For the core of the thermometer shown in fig. 1, C, use was made of a thin-walled glass tube ; and in constructing the instrument the loaded wire was first wound spiral-wise upon the core and then fused to it and so permanently fixed. Next, the ends of the wire were attached to their leads and the whole introduced into the protecting glass tube, the lower end of which had already been drawn out and blown, so that the resultant cylindrical bulb had a very thin wall and was only just wide enough to admit the core. Finally, beginning at the closed end, the containing bulb and its core were gradually softened throughout and fused together so as to form one continuous whole. Thus the resistance wire was completely embedded and at the same time permanently insulated and protected.

(4) Our fourth trial thermometer (termed No. 5 in the table) (p. 700) was built according to the plan just described and followed for the construction of thermometer no. 4. Its dimensions were, however, less ; also, the resistance wire was of smaller diameter (*vide infra*).

(5) For the core of thermometer No. 6 use was made of a slender rod of glass-blower's blue enamel. The spiral resistance wire was first fused to the core and then coated with a thin layer of the enamel.

(6) Thermometer No. 7, which was purchased, was a platinum-in-silica thermometer. The maker had constructed it according to the plan already described for the thermometer C.

(7) The resistances of thermometers D and E (fig. 1) consisted of single loops of wire contained within capillary bulbs. The limbs of the loop of E were separated by a slip of mica ; but in the case of D this precaution was uncalled for. This on account of the shortness of the loop.

(8) The resistances of thermometers F, G, and H consisted respectively of 1, 2, and 4 coreless and sufficiently taut spirals of wire. The twin serial spirals of G were separated by a thin mica plate, whilst the four serial

spirals of H, one only of which is represented, were each contained within one of the four angular spaces formed by two thin intersecting plates of mica.

(9) The last thermometer K had for its resistance a flat spiral formed by coiling the wire upon a thin mica plate. Other particulars of the various thermometers are given in the table.

It may here be added that all resistance wires used for the construction of our thermometers, were initially raised to a bright red heat and so annealed. Also, with the sole exception of the purchased Siemen's thermometer (No. 7 of the table), all thermometers had compensating leads.

Having now described our various experimental thermometers, we next outline the methods adopted for determining the several time-constants which obtain when the instruments are cooled (*a*) in air, and (*b*) in water.

(c) *Determination of the Rate of Cooling in Air.*

The time-constant $1/\epsilon$ for a thermometer cooling in air, was measured with the aid of a thermostat containing 36 *l* of water, the temperature of which was controlled within the limits of $\pm \cdot 005°$ C., and the apparatus depicted sectionally in fig. 2. This apparatus consisted of two concentric conical brass vessels V_1, V_2, kept apart by three narrow and vertically placed strips of rubber, two of which, r_1, r_2 are shown. The central brass chambers C_1, C_2 were 25 mm. in diameter and their inner surfaces were coated with Indian ink. The whole was carried by a cord-covered ring *g*, *g*, so adjusted that C_2 was completely immersed as shown. The chamber C_1 was closed with a cork having a short glass tube S, through which the thermometer to be tested passed with ease. Attached to the thermometer was a cork *k*, to the lower surface of which was cemented a polished aluminium disk having a diameter nearly equal to that of C_1 and C_2. The position of the disk was such that its distance from the end of the thermometer was $=2/3$ of the depth of C_2. The mouth of C_2 was closed by a perforated cork k_2, the upper surface of which was covered with tin-foil having four short cuts radiating from its centre. Finally, the thermometer under examination was suspended

from one end of a cord running over a pulley, its initial position being that indicated in fig. 2; the other and looped end of the cord was held by a peg placed near the electrical measuring apparatus. The procedure was as follows:—

First the thermometer was placed *in situ*, as shown in fig. 2, and connected with the Carey Foster bridge; then the vessel V_1 was filled with water having a temperature some 3·5° C. in excess of the temperature θ

Fig. 2.

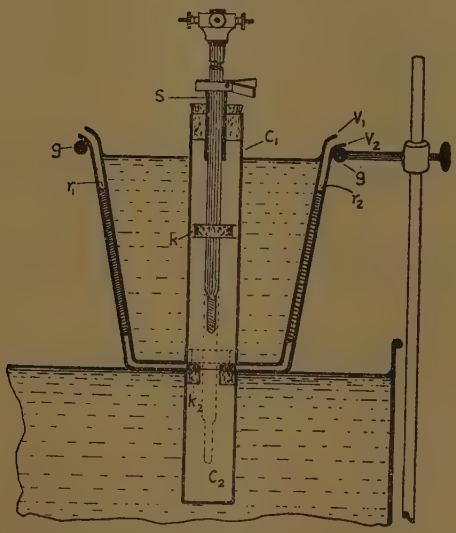

of the thermostat. Next, the slider was set so that the bridge reading corresponded to $\theta+3°$ C. and the water in the thermostat and also that in V_1 kept vigorously stirred. When the galvanometer reading $=0$ (that is, when the temperature of the thermometer $=\theta+3°$ C.), the slider was quickly reset, so that its new position corresponded to the temperature $(\theta+3)-3/\epsilon$ °C.; then the thermometer was suddenly lowered into the chamber V_2, and the time required by the galvanometer for the re-assumption of a zero reading chronometrically determined. In each case the determination was carried

TABLE.

Thermometer.	Containing tube.	Bulb. Length.	Bulb. Diameter.	Diameter of wire.	R_0° C.	Time taken in cooling $1/\epsilon$ of the diff. 23–20° C. (*a*) in air within black chamber.	Time taken in cooling $1/\epsilon$ of the diff. 23–20° C. (*b*) in water.	Ratio *a*/*b*.	Sensitivities in terms of the stand : ther.
(*a*)	(*b*)	(*c*) mm.	(*d*) mm.	(*e*) mm.	(*f*)	(*g*) sec.	(*h*) sec.	(*i*)	(*j*)
1. Cambridge thermometer	Glass	35	11	0·20	2·6	149	16	9·3	1
2. Reduced replica of Cambridge thermometer	"	30	8·2	·05	22·57	76	8	9·5	8·7
3. Wire grid carried by ivory disks	"	25	8·2	·05	16·92	185	12	15·4	6·5
4. Wire embedded in glass cylinder	"	32	8·2	·085	13·96	284	8	35·5	5·4
5. Wire embedded in glass cylinder	"	24	6·0	·05	26·65	168	4	42·0	10·3
6. Wire embedded in glass blower's blue enamel	"	20	2·5	·03	19·67	40	2·3	17·4	7·5
7. Wire embedded in fused silica.	Fused silica	28	3·2	·04	25·00	88	1·2	73·3	9·6
8. Single loop	Glass	21	2·4	·025	6·19	34	1·0	34	2·4
9. Single loop	"	38	2·0	·04	5·1	32	1·5	21·3	2
10. Single spiral	Fused silica	27	5·2	·06	8·59	51	2·5	20·4	3·7
11. Twin spirals	"	35	6·5	·05	19·49	55	3·2	17·2	7·5
12. Four spirals	"	34	7·5	·05	54·11	62	3·0	20·7	20·8
13. Spiral on mica plate.	Glass	Flat bulb 26×7×2		·05	22·88	30	2·9	10·3	8·8

out several times, and the mean value of the closely agreeing results accepted. These mean values are given in column (*g*) of the table.

(d) *Determination of the Rate of Cooling in Water.*

The above described measurements having been completed, others in kind precisely similar, were carried out for determining the rates of cooling following the immersion of the thermometers in water. For these additional experiments, the vessel V_2 was discarded and the bottom of C_1 closed by an attached tin-foil disk having central radiating cuts. Also, C_1 was so placed that its base was close to but not in actual contact with the water of the thermostat. For this second series, the initial temperature of the several thermometers was, as in the first series of experiments, 3° C. in excess of the temperature of the thermostat. The mean values $3/\epsilon$ found for the 13 thermometers are set forth in column (*h*) of the table.

We note that when the two series of values tabulated in columns (*g*) and (*h*) are compared, the descending order for the one differs from that which obtains for the other. The changes in order appear to be due to the fact that in the first series the cooling was chiefly brought about by radiation ; whilst in the second, it was almost entirely due to conduction. It will be observed that air temperatures were most quickly acquired by thermometers Nos. 8, 9, and 13, and water temperatures by Nos. 7, 8, and 9.

Our quest was now ended, and the conclusion reached that for the determination of the melting-point of a substance with the aid of a water-bath, any one of the thermometers numbered 6–13 inclusive, would prove satisfactory. It may, however, be observed that preference should be given and that in the following order, to thermometers 12, 7, and 13. This on account of their superior sensitivities.

The Gables,
Littledown Avenue,
Bournemouth.

LXX. *The Tribo-Electric Properties of a Quartz-Nickel Interface between* 120° C. *and* −78° C. *By* P. A. Mainstone, *M.Sc., F Inst P., Lecturer in Physics, University College of North Wales* *.

ATTEMPTS have been made by the author [1] to examine the frictional charges produced between a surface of fused quartz and that of a polished metal surface at temperatures up to about 350° C. The results, for various reasons, were inconclusive, the chief causes being a certain amount of contamination of the metal and a change in the nature of the quartz surface itself. This latter effect has been discussed in the last number of this Journal (p. 620). It seemed, however, desirable to re-examine the effect of temperature over a small range in which these unwanted factors did not enter. Temperatures below room temperature are obviously suitable, and the apparatus was modified so that the experimental tube could be surrounded at will by either an electric heater or a low temperature enclosure.

The experimental tube, 2 inches in diameter, was fixed vertically, and the disposition of the rubbing surfaces, and of the necessary connexions to the electroscope and to earth, is shown in the figure. The rubbing was performed through a taper joint, as in the earlier experiments.

The first measurements were made at low temperature by surrounding the tube with a vacuum vessel containing solid carbon dioxide. In order to prevent condensation of moisture in the tube at this temperature, it was necessary that only dry gas should be admitted to the apparatus. A vapour-trap, cooled by solid carbon dioxide and ether, was also introduced, and with these precautions the polished surfaces remained on the whole quite bright and free from tarnish.

The low temperature inside the tube was not actually measured simultaneously with the frictional charges, but the reading of a thermo-couple when inserted into the open tube was compared with that obtained on direct insertion into the solidified gas. No difference was observed, and the temperature at which the charges were measured was thus taken as −78° C.

* Communicated by Prof. E. A. Owen, M.A., Sc.D.

Since repetition of each reading is necessary before any weight can be attached to it, it was found convenient to compare the frictional charges at room temperature and at solid CO_2 temperature or three times in alternation, the pressure being kept constant during such a set of readings. Readings at four different pressures, viz.,

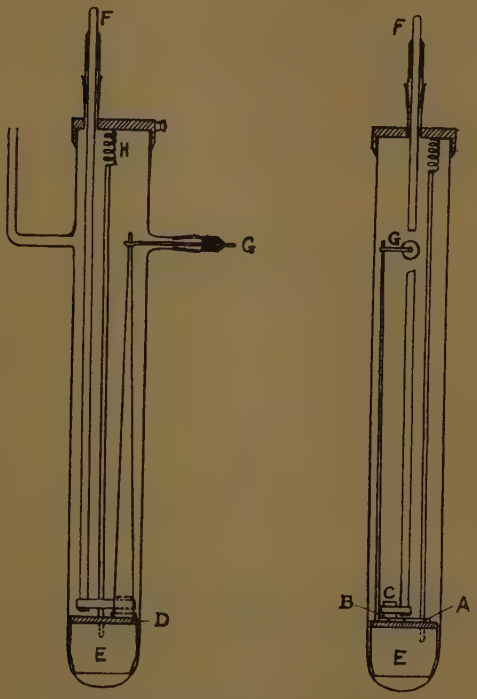

A. Earthed polished surface.
B. Insulated polished surface.
C. Quartz rubber.
D. Ebonite or mica insulator.
E. Heavy metal base.
F. External rod for controlling quartz rubber.
G. Connexion to electroscope.
H. Spring contact to earthed metal cap.

60 cm., 5 cm. 1 mm., and 10^{-4} mm., were obtained in this way. Since only small changes of the frictional

charges were to be looked for, the capacity of the electroscope system was arranged so that conveniently large electroscope deflexions were obtained in each case. At 60 cm. and 5 cm. pressure, the capacity was reduced to about one-quarter of its usual value.

The results are shown in Table I. At each pressure readings were taken at room temperature and low temperature alternately, only a short interval of from $\frac{1}{2}$ to 1 hour elapsing between one reading and the next. (As in all the previous experiments, a large number of rubs

TABLE I.

Comparison of Charges in Air at Room Temperature and at −78° C.

Pressure 60 cm.		Pressure 5 cm.		Pressure 1 mm.		Pressure 10^{-4} mm.	
Room temperature	33	Room temperature	26	Room temperature	12	Room temperature	26
−78° C. .	41	−78° C. .	33	−78° C. .	13	−78° C. .	30
Room temperature	29	Room temperature	25	Room temperature	18	Room temperature	27
−78° C. .	44	−78° C. .	33	−78° C. .	17	−78° C. .	26
Room temperature	34	Room temperature	30	Room temperature	17	Room temperature	39

were made before the ultimate steady charge per single rub was noted.) The readings at the first three pressures were all obtained with the surfaces in the same state of polish, but re-polishing was necessary before the fourth set of readings.

At pressures of 60 cm. and 5 cm. the variation with temperature agrees with the suggestions already put forward. The very light rubbing actually involves layers of adsorbed gas rather than solid surfaces, and the amount of gas so adsorbed is greater at the lower temperature. At the low pressures, however, the readings are irregular and show no relation to the temperature. The rubbing now involves solid surfaces rather than gaseous layers, and the difficulty of reproducing any

given reading is that which has always occurred in this work.

The readings at 60 cm. pressure were checked at a later stage in the work, and although the absolute values of the changes were rather higher, the variation with temperature was the same.

Following the results of Table I., the charges at room temperature were compared with those at 120° C., but at a later stage measurements were made in hydrogen at the low temperature. These at first did not yield the expected results, and it appeared that the charges were independent of temperature at all pressures. The nickel surfaces were re-ground and re-polished, and the results given in Table II. were obtained.

TABLE II.

Comparison of Charges in Hydrogen at Room Temperature and at −78° C.

Pressure 50 cm.		Pressure 10^{-4} mm.	
Room temperature ...	32	Room temperature ...	23
−78° C.	35	−78° C.	23
Room temperature ...	32	Room temperature ...	31
−78° C.	35	−78° C.	29
Room temperature ...	33	Room temperature ...	33

The results correspond with those of Table I., although at 50 cm. pressure the variation of charge with temperature is not quite so great as in the case of air.

Measurements at 120° C. were made by surrounding the tube with an electric heater which could be removed at will, and in this case a mercury thermometer was introduced into the tube. Mica insulation was used instead of ebonite, as employed in the low temperature measurements. Adopting the same procedure of measuring the charges at room temperature and at 120° C. alternately, the results for air and for hydrogen are given in Table III. The capacity was adjusted as before, so that the relative values of the charges at 60 cm. and 5 cm. must be reduced to about one-quarter of the values given.

TABLE III.

Comparison of Charges in Air and in Hydrogen at Room Temperature and at 120° C.

Air.

Pressure 60 cm.	Pressure 5 cm.	Pressure 1 mm.	Pressure 10^{-4} mm.
Room temperature } 38	Room temperature } 25	Room temperature } 11·0	Room temperature } 17·0
120° C. . . 31	120° C. . . 22	120° C. . . 11·0	120° C. . . 15·5
Room temperature } 39	Room temperature } 24·5	Room temperature } 11·5	Room temperature } 18·5
120° C. . . 30	120° C. . . . . 21·5	120° C. . . 10·0	120° C. . . 19·0
Room temperature } 40	Room temperature } 24	Room temperature } 12·0	Room temperature } 18·0

Hydrogen.

Pressure 60 cm.	Pressure 5 cm.	Pressure 1 mm.	Pressure 10^{-4} mm.
Room temperature } 25	Room temperature } 17·5	Room temperature } 12·0	Room temperature } 28
120° C. . . 22	120° C. . . 15·5	120° C. . . 14·0	120° C. . . 24
Room temperature } 25	Room temperature } 16·5	Room temperature } 17·5	Room temperature } 24
120° C. . . 22	120° C. . . 15·5	120° C. . . 17·5	120° C. . . 23
Room temperature } 26	Room temperature } 16·0	Room temperature } 18·5	Room temperature } 23

Discussion.

On the adsorption theory of Langmuir [2] the numbers of gaseous molecules condensing on and evaporating from a solid surface can each be expressed as a function of the temperature. The rate of impact of gaseous molecules is given by the kinetic theory, and at a pressure p and absolute temperature T is proportional to $(p\mathrm{T}^{-\frac{1}{2}})$ [3]. The rate of evaporation from the surface varies exponentially with the temperature, being proportional to $e^{-\frac{\lambda}{\mathrm{RT}}}$ [4] (λ=heat of adsorption). On the

assumption of the monomolecular layer, this leads to an expression for the fraction θ of the surface covered

$$\alpha_1 p T^{-\frac{1}{2}}(1-\theta)=\alpha_2 . e^{-\frac{\lambda}{RT}} . \theta,$$

or

$$\theta=\frac{\alpha_1 p T^{-\frac{1}{2}}}{\alpha_1 p T^{-\frac{1}{2}}+\alpha_2 e^{-\frac{\lambda}{RT}}}.$$

Although the constants α_1 and α_2 cannot readily be evaluated, it is clear that the value of θ diminishes with increasing temperature.

The actual variation with temperature of the amount of gas adsorbed on a nickel surface has been measured by H. S. Taylor and Burns [5]. Between 25° C. and 110° C. the relative values for nitrogen were 9·6 and 7·4 in one instance, and for hydrogen 12·35 and 10·35. If the values of the frictional charges in the present experiments are mainly dependent on those of θ, and thus on the amount of gas adsorbed, a correlation between the figures of Taylor and Burns and those of the frictional charges is to be expected. An examination of the tables shows that at the higher pressures such a correlation definitely exists. It must not be overlooked, however, that the state of the quartz surface is possibly a more important factor than that of the metal. Relevant figures for the temperature variation of adsorption on quartz do not appear to be available.

Figures for the adsorption of hydrogen on nickel at low temperatures are given by Benton and White [6], and by Maxted and Hassid [7]. At moderate pressures Benton and White find that adsorption at −100° C. is greater than at 0° C., although at a pressure of 60 cm. the temperature variation over this range is practically nil. The results of Maxted and Hassid, however, indicate that the amount of adsorption at −79° C. is considerably less than at 0° C. No support for this result is found in the present experiments.

At low pressures, when the amount of gas adsorbed is much smaller, no definite connexion between the frictional charge and the temperature can be established. It can only be concluded that under these conditions the charges are characteristic of the solid surfaces themselves rather than of the gas layers adsorbed on them.

Summary.

1. The frictional charges produced on a nickel surface by the passage of a quartz rubber have been measured at temperatures 120° C., 15° C., and −78° C.

2. In atmospheres of both air and hydrogen the charges at the three temperatures in the order given are in increasing order of magnitude at gas pressures of 60 cm. and 5 cm. At pressures of 1 mm. and 10^{-4} mm. the charges are irregular and bear no relation to the temperature.

3. The results are discussed in the light of available figures for the amounts of gases adsorbed by nickel. The unknown adsorption by the quartz is, however, a complicating factor.

In conclusion, it gives me great pleasure to express my indebtedness to Prof. E. A. Owen for the help and encouragement he has given me throughout the work.

References.

(1) Phil. Mag. xvi. pp. 1083–1096 (1933).
(2) J. Am. Chem. Soc. xxxviii. p. 2267 (1916).
(3) Adam, ' Physics and Chemistry of Surfaces,' p. 251.
(4) H. S. Taylor, ' Physical Chemistry,' 2nd ed. p. 1082.
(5) J. Am. Chem. Soc. xliii. p. 1273 (1921).
(6) J. Am. Chem. Soc. lii. p. 2325 (1930).
(7) " Adsorption of Gases by Solids " (Discussion Far. Soc. p. 253 (1932)).

LXXI. *The Effect of Trochoidal Interference on the Operation of Involute Gears.* *By* W. A. Tuplin, *M.Sc.**

IT is sometimes necessary to use involute gears of such proportions that the root circle of the teeth is of smaller diameter than the base circle from which the involute part of the tooth profile is generated. That part of the profile which lies within the base circle is of trochoidal form. It cannot make useful contact with any mating gear, and it is in fact produced by the tip of the generating cutter, which is purposely extended sufficiently far into the gear blank to ensure clearance between tips and roots of mating gear teeth.

If the radius of the root circle is less than that of the base circle by more than a certain amount depending

* Communicated by the Author.

on the pressure angle of the gears, the trochoidal part of the profile meets the involute part at a point outside the base circle, a small portion of the involute, commencing at the base circle, having been removed by the

Fig. 1.

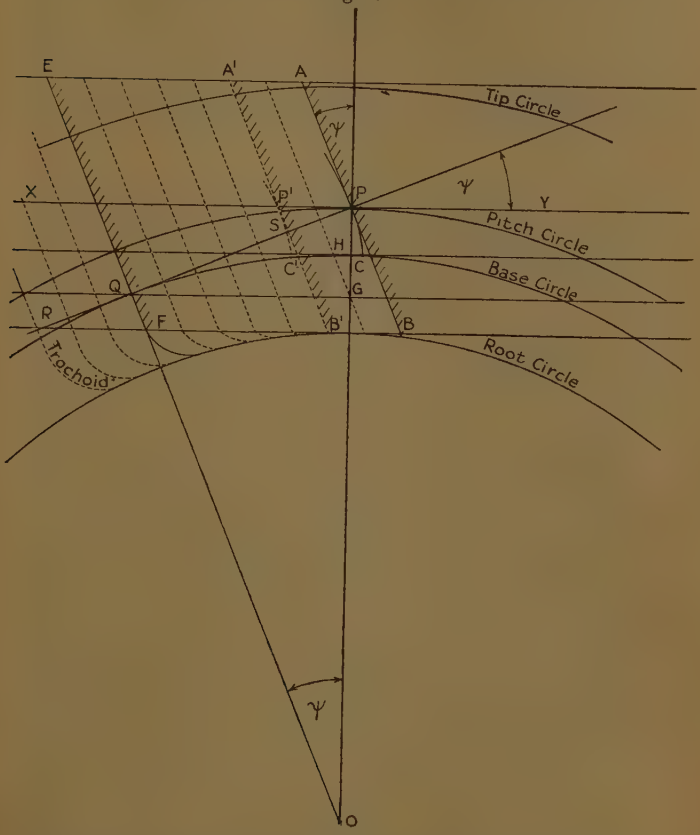

tip of the generating cutter. The effect of this interference is a tendency to reduce the length of the path of contact between the teeth of the gear and those of any mating gear.

In fig. 1, AB is a straight line which is moved horizontally in the direction YX whilst tracing its position on a

disk rotated about centre O in such a way that the circumferential displacement of the pitch circle is always equal to the linear displacement of the line AB. A straight line XY, parallel to the motion of AB, touches the pitch circle at the point P, called the "pitch point." A line PR is drawn through P, perpendicular to AB, and the circle having centre O and touching PR (in Q) is called the "base circle."

The inclination of AB to OP is the "pressure angle" ψ. The relation between the radii of base circle and pitch circle is

$$OQ = OP \cos \psi.$$

When AB takes up a position A′B′ it intersects XY in P′ and PQ in S. Then $PS = PP' \cos \psi$.

If the involutes which cut PQ orthogonally in P and S meet the base circle in C and C′

$$\text{Arc } CC' = PS = PP' \cos \psi;$$

but the circumferential displacement of the pitch circle is equal to PP′, and that of the base circle is therefore $PP' \cos \psi$, since $\cos \psi$ is the ratio of the radii of these circles. Hence the point C moves through a circumferential distance CC′, and so coincides with C′. In other words, the point of intersection of AB and PQ lies always on the same involute, and since the involute intersects PQ orthogonally it is therefore tangent to AB. Hence the envelope of the trace of AB on the plane of the disk is an involute so far as concerns that part which lies outside the base circle. The part within the base circle is a "trochoid."

When AB has reached the position EF the point of intersection with PQ is Q, and the involute is generated right the way down to the base circle. Further movement of AB to the left causes outward extension of the trochoid, and ultimately intersection with the previously generated involute.

Regarding AB as the straight edge of a cutter producing teeth by reciprocation perpendicular to the plane of the disk, this "interference" by the tip of the cutter removes part of the involute profile in the manner indicated in fig. 2.

The nature of the contact between a pair of straight-tooth involute gears is indicated in fig. 3. If an involute to the upper base circle passes through a point Q the normal at Q to the involute touches the upper base

Fig. 2.

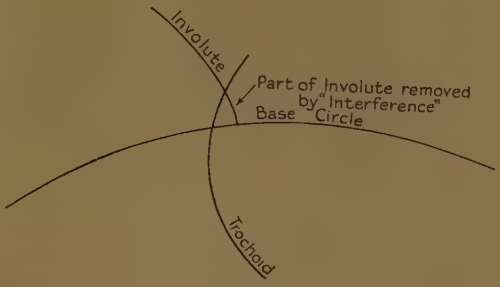
Involute
Part of Involute removed by "Interference"
Base Circle
Trochoid

Fig. 3.

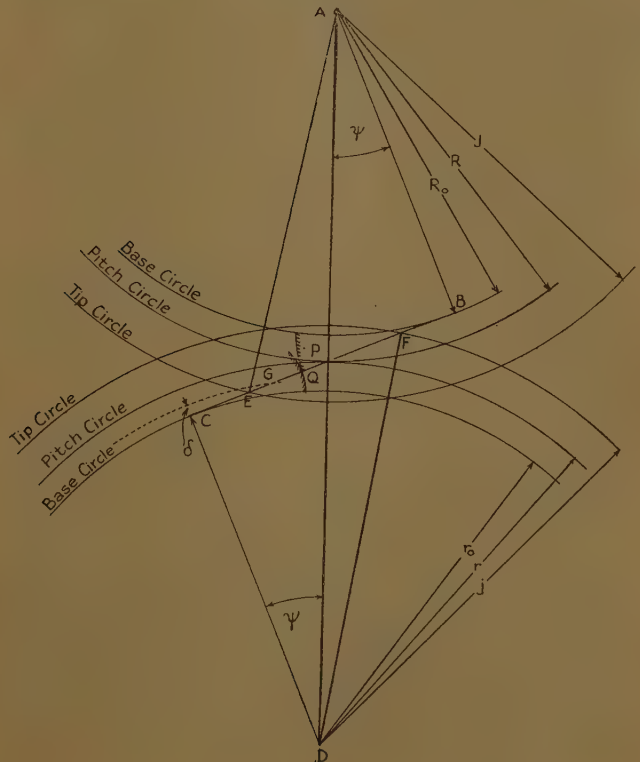
A
ψ
J
R
Ro
B
Base Circle
Pitch Circle
Tip Circle
P
F
G
Q
E
C
δ
Tip Circle
Pitch Circle
Base Circle
ψ
D

circle. If an involute to the lower base circle touches the first involute at Q, the common normal at Q to the two involutes touches the lower base circle. Hence Q lies on the common tangent BC to the two base circles, and contact between clockwise-leading flanks of teeth of the lower gear and clockwise-leading flanks of teeth of the upper gear is confined to the straight line BC. Contact between the opposite sets of flanks is confined to the other transverse common tangent.

Hence the length of the path of the point of contact cannot in any circumstances exceed

$$BC=(r_0+R_0)\tan\psi.$$

If the tip circles of the gears intersect BC in E and F the length of the path of contact cannot exceed EF. From the right angle triangles ABP, ABE, DCP, and DCF it is seen that

$$FE=FP+PE=[\sqrt{(j^2-r_0^2)}-r_0\tan\psi]+[\sqrt{(J^2-R_0^2)}-R_0\tan\psi], \quad . \quad . \quad (1)$$

provided that the term in the first square bracket does not exceed $R_0\tan\psi$ and that that in the second square bracket does not exceed $r_0\tan\psi$.

A further limitation may be imposed by the effect of trochoidal interference. If this occurs in (say) the lower gear the involute profiles of that gear terminate on a circle (radius $(r_0+\delta)$ where δ is positive) intersecting BC in some such point as G (fig. 3). Then if δ is small compared with r_0 the length CG is connected with δ by the very nearly exact relation

$$CG^2=2r_0\delta. \quad . \quad . \quad . \quad . \quad . \quad . \quad . \quad (2)$$

The object of the present investigation is to express the shortening CG of the path of contact in terms of the addendum of the cutter, *i. e.*, the distance by which the generating cutter extends inside the pitch circle of the gear. From fig. 1 it is seen that even if the addendum of the cutter is as great as PG there is no interference, because when the tip of the cutter reaches Q, generation of involute and trochoid terminate simultaneously at the base circle. If the addendum of the cutter is less than PH the generated tooth is entirely of involute form.

From the right-angle triangles PQG and PQO it will be seen that

$$PG=PQ\sin\psi=r_0\tan\psi\sin\psi.$$

Interference occurs if the addendum of the cutter exceeds this amount, *i. e.*, if the path of the tip of the cutter lies below Q. Because of its significance in this connexion, Q is known as the "interference point."

Fig. 4 represents the condition in which the tooth of a cutter overlapping the interference point Q, by an

Fig. 4.

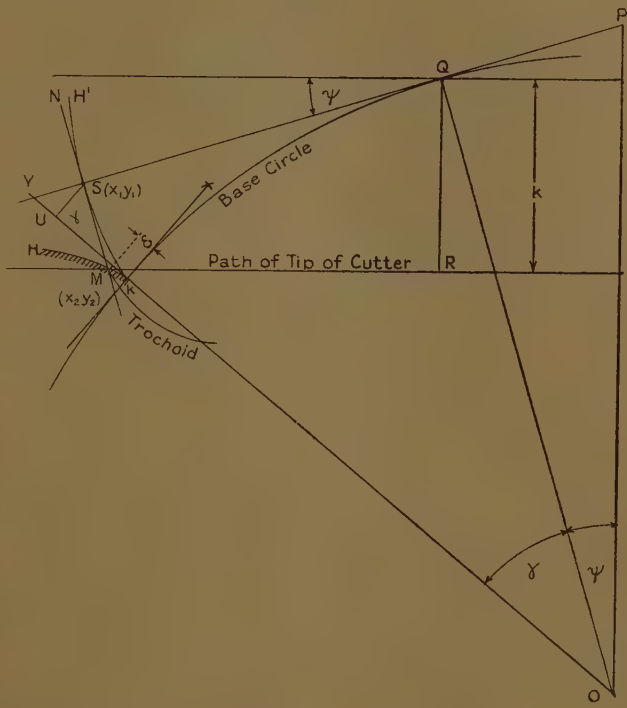

amount k is just ceasing to make contact with a gear tooth which it has generated. During its approach to Q from the right the edge NM of the cutter generates the involute HK, the point of tangency of edge and involute lying always on PQ. During the further movement of the cutter, the edge NM maintains tangency with the involute KH′, originating at the same point K as the generated involute. Throughout this later period,

the point of tangency of edge and involute similarly lies on PQ produced. The tip M generates the trochoid which ultimately intersects KH in the point M, whose distance from the centre of the base circle is $(r_0+\delta)$. It is required to find the relation between δ and k, and this involves a knowledge of the relation between the length MS of the tangent to involute KH′ from a point M on the associated involute KH, the radial distance of M from the base circle, and the inclination of the tangent MS to the radius of the base circle at K.

As in all practical cases KS is small compared with r_0 it is sufficiently accurate to use approximate equations for the involutes KH and KH′ in terms of Cartesian coordinates with origin at K and axes tangential and normal to the base circle at K.

Let the radius OK make an angle γ with OQ, the radius at the interference point.

Now $\mathrm{SQ} = \text{arc KQ} = r_0\gamma$.

Hence $x_1 = \mathrm{US} = \mathrm{OQ}\sin\gamma - \mathrm{SQ}\cos\gamma$

$$= r_0\sin\gamma - r_0\gamma\cos\gamma,$$

and $$\frac{x_1}{r_0} = \sin\gamma - \gamma\cos\gamma = \gamma - \frac{\gamma^3}{3!} + \frac{\gamma^5}{5!} - \text{etc.}$$

$$-\gamma + \frac{\gamma^3}{2!} - \frac{\gamma^5}{4!} + \text{etc.}$$

$$= \frac{\gamma^3}{3} \text{ approximately, since } \gamma \text{ is small.} \quad . \quad (3)$$

Similarly, $y_1 = \mathrm{KU} = \mathrm{OU} - \mathrm{OK} = \mathrm{OQ}\cos\gamma$

$$+\mathrm{SQ}\sin\gamma - r_0,$$

and $$\frac{y_1}{r_0} = \cos\gamma + \gamma\sin\gamma - 1 = 1 - \frac{\gamma^2}{2!} + \frac{\gamma^4}{4!} + \text{etc.}$$

$$+\gamma^2 - \frac{\gamma^4}{3!} + \frac{\gamma^6}{5!} - \text{etc.} - 1$$

$$= \frac{\gamma^2}{2} \text{ approximately, since } \gamma \text{ is small.} \quad . \quad (4)$$

Hence $x_1 = \frac{r_0}{3}\gamma^3 = \frac{r_0}{3}\left(\frac{2y}{r_0}\right)^{3/2} = 0{\cdot}943\, r_0^{-1/2} y_1^{3/2}$, . . (5)

or $$y_1 = 1{\cdot}04\, r_0^{1/3} x_1^{2/3}. \quad . \quad . \quad . \quad . \quad . \quad (6)$$

When the suffixes of x and y are suppressed this relation becomes the approximate equation of KH′ in terms of Cartesian coordinates measured from KX and KY.

The equation of KH is identical except for reversal in sign of the numerical factor.

The inclination γ to KY of the tangent SM to the involute KH′ is expressed by

$$\cot\gamma = \left(\frac{dy}{dx}\right)_{x=x_1} = 0{\cdot}694 r_0^{1/3} x_1^{-1/3}.$$

If the coordinates of M be (x_2, y_2),

$$\frac{(y_1-y_2)}{(x_1-x_2)} = 0{\cdot}694\, r_0^{1/3} x_1^{-1/3},$$

whence $$x_1^{1/3} y_1 - x_1^{1/3} y_2 = 0{\cdot}694\, r_0^{1/3} (x_1-x_2).$$

Substituting $y_1 = 1\,04\, r^{1/3} x_1^{2/3}$ and $x_2 = -0{\cdot}943\, r_0^{-1/2} y_2^{3/2}$.

$$1{\cdot}04\, r_0^{1/3} x_1 - x_1^{1/3} y_2 = 0{\cdot}694\, r_0^{1/} \quad +0{\cdot}655\, r_0^{-1/6} y_2^{3/2},$$

whence $$\frac{x_1}{r_0} - 2{\cdot}89\left(\frac{y_2}{r_0}\right)\left(\frac{x_1}{r_0}\right)^{1/3} - 1{\cdot}89\left(\frac{y_2}{r_0}\right)^{3/2} = 0,$$

and, solving by the method of successive approximation.

$$\frac{x_1}{r_0} = 7{\cdot}55\left(\frac{y_2}{r_0}\right)^{3/2}.$$

Hence $$y_1 = 1{\cdot}04\, r_0^{1/3} x_1^{2/3} = 4y_2 \text{ and } y_1 - y_2 = 3y_2.$$

Also $$x_2 = -0{\cdot}943\, r_0^{-1/2} y_2^{3/2},$$

and $$x_1 - x_2 = (7{\cdot}55+0{\cdot}943) r_0^{-1/2} y_2^{3/2} = 8{\cdot}493\, r_0^{-1/2} y_2^{3/2}.$$

Therefore
$$\begin{aligned} \text{SM} &= \sqrt{[(y_1-y_2)^2+(x_1-x_2)^2]} \\ &= \sqrt{[(3y_2)^2+(8{\cdot}493)^2 r_0^{-1} y_2^3]} \\ &= 3y_2\sqrt{\left[1+\frac{8y_2}{r_0}\right]}. \quad . \quad . \quad . \quad . \quad . \quad . \quad (7) \end{aligned}$$

Now $\cot\gamma = 0{\cdot}694 r_0^{1/3} x_1^{-1/3} = 0{\cdot}694\, r_0\ [7{\cdot}55\, y_2^{3/2} r_0^{-1/2}]^{-1/3}$.

whence

$$\tan\gamma = 2{\cdot}83\left(\frac{y_2}{r_0}\right)^{1/2}$$

and $$\gamma = \tan^{-1}\left[2{\cdot}83\left(\frac{y_2}{r_0}\right)^{1/2}\right]$$

$$= 2{\cdot}83\left(\frac{y_2}{r_0}\right)^{1/2} - 7{\cdot}55\left(\frac{y_2}{r_0}\right)^{3/2} + 36{\cdot}2\left(\frac{y_2}{r_0}\right)^{5/2} \quad . \quad . \quad (8)$$

approximately, since in all practical cases y_2/r_0 is much less than unity.

Now y_2 is very nearly equal to δ, the radial distance of M from the base circle. Hence, if l be the amount by which the path of contact is shortened, we have from (2)

$$\frac{l^2}{2r_0} = \delta = y_2, \quad \frac{y_2}{r_0} = \frac{l^2}{2r_0^2} \text{ and } \tan\gamma = 2{\cdot}83\,\frac{l}{r_0\sqrt{2}}.$$

Now, from fig. 4,

$$k = \mathrm{QR} = \mathrm{QS}\sin\psi + \mathrm{SM}\cos\psi$$

$$= r_0\gamma\sin\psi + \left[3y_2\sqrt{\left(1+\frac{8y_2}{r_0}\right)}\right]\cos\psi,$$

$$\frac{k}{r_0\sin\psi} = \gamma + \left[\frac{3y_2}{r_0}\sqrt{\left(1+\frac{8y_2}{r_0}\right)}\right]\cot\psi$$

$$= 2{\cdot}83\,\frac{l}{r_0\sqrt{2}} - 7{\cdot}55\left(\frac{l}{r_0\sqrt{2}}\right)^3 + 36{\cdot}2\left(\frac{l}{r_0\sqrt{2}}\right)^5$$

$$+\left[\frac{3l^2}{2r_0^2}\sqrt{\left(1+\frac{8y_2}{r_0}\right)}\right]\cot\psi,$$

$$\frac{k}{r_0\tan\psi\sin\psi} = 2\left(\frac{l}{r_0\tan\psi}\right) - 2{\cdot}67\tan^2\psi\left(\frac{l}{r_0\tan\psi}\right)^3$$

$$+6{\cdot}4\tan^4\psi\left(\frac{l}{r_0\tan\psi}\right)$$

$$+1{\cdot}5\left(\frac{l}{r_0\tan\psi}\right)^2\sqrt{\left(1+\frac{4l^2}{r_0^2}\right)}. \quad . \quad . \quad . \quad (9)$$

The magnitude of the cutter addendum which just produces trochoidal interference is $r_0\tan\psi\sin\psi$. Denoting this by a_0, and writing

$$\frac{\text{Shortening of path of contact}}{\text{Path from base circle to pitch point}} = \frac{l}{r_0\tan\psi} = s,$$

we have

$$\frac{k}{a_0} = 2s - (2{\cdot}67 \tan^2 \psi)\, s^3 + (6{\cdot}4 \tan^4 \psi) s^5 + 1{\cdot}5s^2 \sqrt{[1 + (2 \tan \psi)^2 s^2]}. \quad . \quad . \quad . \quad . \quad . \quad (10)$$

For the range of values of ψ used in practice this relation between k/a_0 and s is almost independent of ψ. Between $\psi = 20°$ and $\psi = 14\frac{1}{2}°$ (the pressure angles in common use) the proportional difference in k/a_0 ranges from zero when $s = 0$ to 0·047 when $s = 1{\cdot}0$.

From the curve which corresponds to (10) for $\psi = 20°$ it is found that a closely approximate converse relation between k/a_0 and s may be expressed by

$$s = 0{\cdot}489 \frac{k}{a_0} - 0{\cdot}1082 \left(\frac{k}{a_0}\right)^2 + 0{\cdot}0153 \left(\frac{k}{a_0}\right)^3, \quad (11)$$

and this may be accepted for any pressure angle between $14\frac{1}{2}°$ and 20°.

By means of this relation the shortening of the path of contact may be calculated directly from the addendum of the cutter with an error not exceeding 1 per cent. at any point in the range from $s = 0$ to $s = 0{\cdot}5$, which corresponds (approximately) to the range $k = 0$ to $k = 1{\cdot}35$.

The length of the path of contact may be determined from (1) in conjunction with a proviso associated with the effect of trochoidal interference. We have :

Length of path of contact =

$$\left\{ \begin{array}{l} \sqrt{(j^2 - r_0^2)} - r_0 \tan \psi, \\ \text{or } \mathrm{SR}_0 \tan \psi, \text{ which-} \\ \text{ever is the less} \end{array} \right\} + \left\{ \begin{array}{l} \sqrt{(\mathrm{J}^2 - \mathrm{R}_0^2)} - \mathrm{R}_0 \tan \psi, \\ \text{or } sr_0 \tan \psi, \text{ which-} \\ \text{ever is the less} \end{array} \right\}, \quad . \quad . \quad . \quad . \quad (12)$$

where the values of s and S are obtained by inserting in (11) numerical values of k and a_0 applying respectively to the two gears.

This method of calculating the length of the path of contact is useful when consideration is being given to the design of gears which are to have specially long teeth for the purpose of permitting variation in working centre distance.

LXXII. *The Effect of Air Velocity on the Spark between Point-Plate and Two-Point Electrode Systems in Atmospheric Air. By* Prof. E. L. E. Wheatcroft, *M.A.*, R. B. Smith, *Ph.D.*, *and* E. L. Hoyle, *B.Sc.**

1. *Introductory.*

THE first discharge as the potential difference is slowly raised in an electrode system consisting of two points, or point and plate, takes the form of corona. This is initially stable, and exhibits a "rising" current-potential characteristic. With still further increasing current, however, the slope of the characteristic curve decreases, and eventually the conduction becomes unstable and passes over violently to a spark. It has long been known that with the point-plate system the transition depends upon the polarity of the electrodes, occurring at lower voltage when the point is positive. When attempt is made to use this property for rectification of alternating current it is found that the current which can be so handled is small, of the order of 1 milliampère with a point of 1 mm. diameter. With any current in excess of this rectification ceases and the point is rapidly heated to incandescence. Woolcott and Erickson †, however, showed that if a blast of air be directed from point to plate the current which can be rectified before breakdown is increased greatly, being now of the order of 20 or 30 milliampères with the same electrodes.

We undertook the investigation described in this paper with a view to elucidating the action of the air-blast, and in the hope that it might throw light upon the mechanism of the transition from corona to spark. In this last aim we have not succeeded, nor have we been able to interpret our results quantitatively in terms of ionic mobilities and air velocities, for in general the distribution of air-flow and of the electrostatic field is too complicated to allow of computation. We have, however, made many tests which throw light upon the action of the air in the rectifier, and these, together with some of our conclusions, are given below.

* Communicated by Prof. E. L. E. Wheatcroft, M.A.

† Phys. Rev. ix. p. 480 (1917).

Fig. 1 shows the form of the point electrodes and the arrangements for directing the flow of air, which was always co-axial to the point, as shown by the arrows. The point was made from an electroplated iron pin of 0·775 mm. diameter, the sharp point cut off and the end rounded by emery. It was mounted in a brass holder with axial adjustment, and the end was always

Fig. 1.

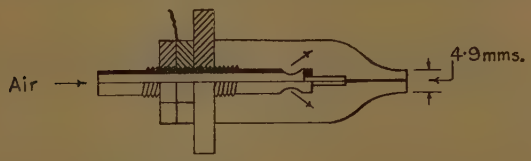

set in line with the open end of the surrounding glass nozzle. In the two-point experiments the two electrodes were identical, the air flowing out of one nozzle into the other. In the other experiments a simple brass disk of 3 cm. diameter was used for the second electrode.

The axial air velocity just outside the nozzle was calibrated against h, where h is the head of air as measured by a manometer.

2. *Effect of Air Velocity on Corona Characteristic.*

Fig. 2 shows the result of a corona test upon the point-plate arrangement. It will be seen that the air blast

Fig. 2.

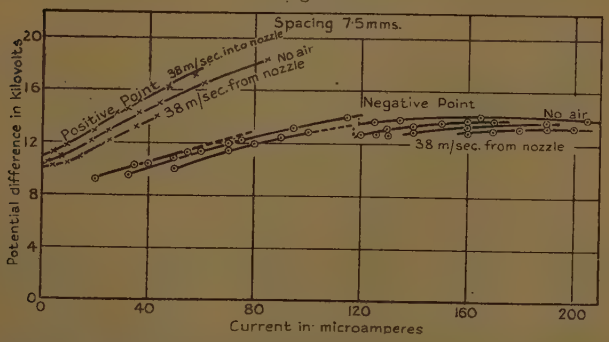

has little effect on the current or even upon the sparking point in this case. The corona characteristic has no

obvious bearing upon the operation of the rectifier, but it is given here as being interesting in any theoretical study of sparkover. The tests were made with direct current taken from a 25 kv. source through a stabilizing resistance, and the measurements were made with suitable moving-coil instruments. The characteristic of the negative point was irregular, as is clear from the figure.

3. *Effect of Air Velocity on the Sparkover.*

Figs. 3 and 4 show the effect of air velocity on the sparkover potential for two points and point-plate.

Fig. 3.

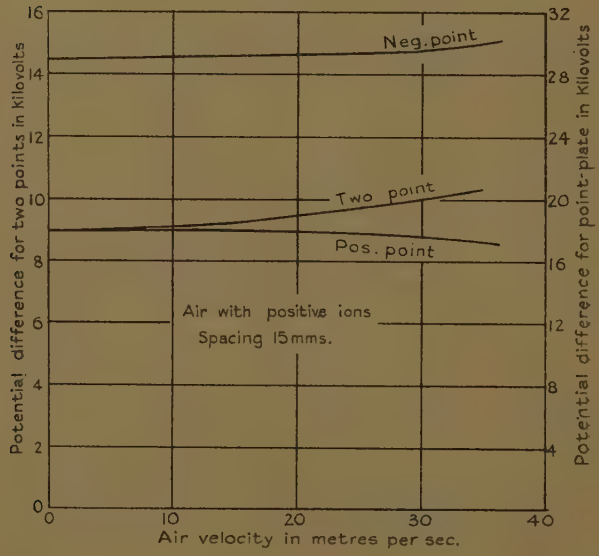

In fig. 3 the motion of the air is *with* the travel of the positive ions, and the effect is small. In fig. 4 the motion of the air is *against* the positive ions. The effect on the negative point is negligible ; on the positive point it is small except with high velocities, where the effect is to raise the striking potential up to that of the negative point. With two points quite a small nozzle velocity

is capable of polarizing the system and making it equivalent to point-plate. It is unfortunately, however, not possible to correlate the air velocities in the two cases, because with two points the velocity is nearly uniform and axial right across the gap, whereas with the point-plate system it must turn outwards, parallel to the plate, and as a result the effect on the ions must be considerably less for a given head of air.

Fig. 4.

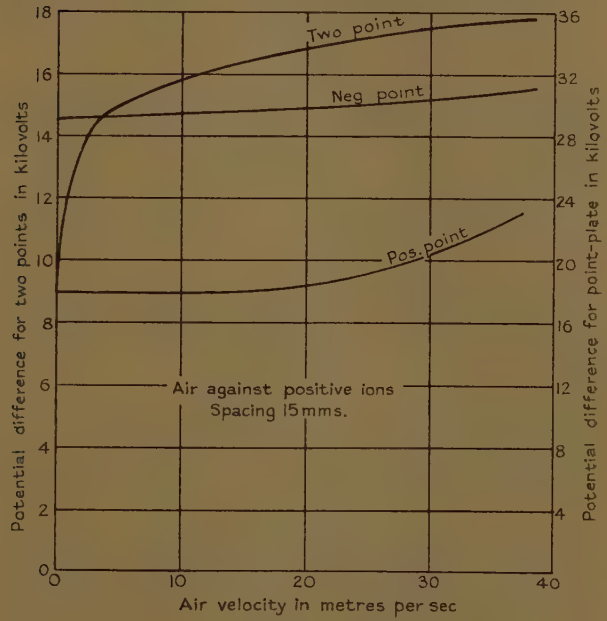

4. *Effect of Air Velocity on Spark Maintenance.*

Fig. 5 (*a*), (*b*), (*c*), and (*d*) show the effect of air-velocity on the volt-ampère characteristic of the conducting "arc." The effect of increasing air blast in either direction is to raise the maintenance potential, so presumably the effect in this case is largely due to cooling. The curves are of interest, since the stability of the arc depends upon its volt-ampère characteristic.

5. *Operation of Point-plate Rectifier.*

(a) *Preliminary Tests.*

In the preliminary experiments the rectifier was operated from an induction coil, of which the primary winding was connected through a variable resistance to a source of current at 50 cycles per sec., and the secondary side connected without load resistance directly across the rectifier. The internal resistance of the secondary winding was about 25,000 ohms. In order to observe the effect of the air blast the current through, and voltage

Fig. 5.

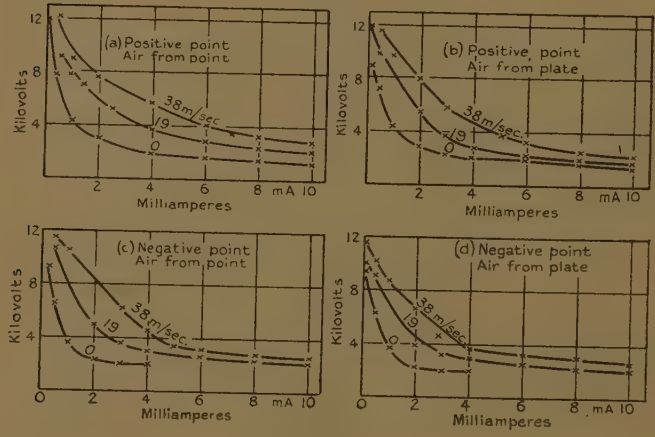

Spacing 7·5 mm.

across, the discharge were measured by bifilar oscillographs, electromagnetic for the current wave and electrostatic for the voltage wave. A 50 megohm potential divider was used with the latter.

As the air blast (from point to plate) was increased, the discharge passed through four stages, which appear on the oscillograms shown in fig. 6 (*a*), (*b*), (*c*), and (*d*). With no air blast there is no rectification, as shown in fig. 6 (*a*) ; with slight air blast there is a small net current from plate to point as in fig. 6 (*b*) ; with still more blast there is complete rectification from plate to point as in fig. 6 (*c*) ; and with more blast still the current direction

reverses, and there is complete rectification from point to plate as in fig. 6 (*d*). The accompanying visible changes are as follows :—

Fig. 6 (*a*). The discharge is yellow in colour, terminating in a single steady blue spot on the plate. The point is raised to a very bright incandescence.

Fig. 6 (*b*). The flame is blown much thinner, and follows to some extent the lines of flow of the air blast. The single steady blue spot on the plate changes to many blue spots moving rapidly about over the plate. The incandescence becomes less. The current is slightly rectified, its direction being from plate to point.

Fig. 6

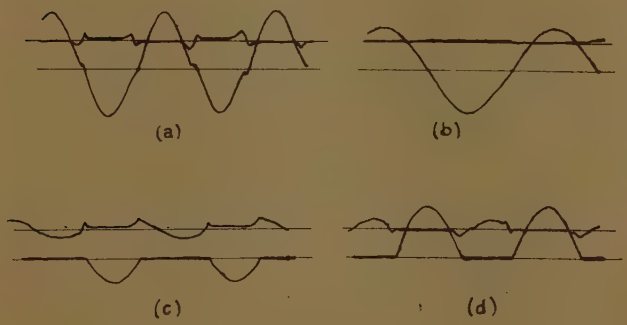

Fig. 6 (*c*). With further reduction of the current a stage is eventually reached at which a distinct change takes place in the character of the discharge, and which results in complete suppression of one half wave of the current. Conduction is still from plate to point.

Fig. 6 (*d*). At a certain stage the incandescence of the point is suddenly and completely extinguished, and the discharge then consists mainly of blue and thick mauve " bushy " streamers, the blue streamers ending in intense blue spots moving about the plate. There is a complete change over in the direction of the rectification, the current now proceeding from the point to the plate.

In using the point-plate arrangement as a rectifier to supply direct current the conduction is from point to plate, as in fig. 6 (*d*), sufficient air being always used for this purpose.

(b) *Working Tests.*

For these tests the rectifier was connected through a loading resistance to a 15 kva. 50-cycle transformer. The primary current of the transformer was supplied through an induction regulator, so that the output voltage could be varied from zero up to 50 kv. : the operating voltage used was generally in the neighbourhood of 20 kv. The loading resistance consisted of banks of woven wire nets, and had a maximum value of 367,000 ohms. The resistance and reactance of the

Fig. 7.

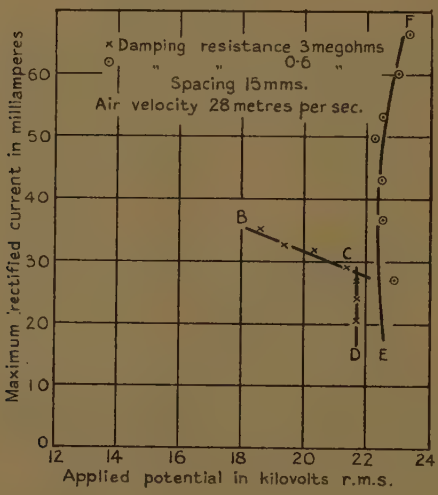

transformer and regulator together were found to be equivalent to 23,000 ohms and 117,000 ohms respectively. The self-capacity of the transformer was calculated to be equivalent to 426 micro microfarads in parallel with the secondary winding. A damping resistance was also connected across the secondary terminals, in order to reduce the peak of the voltage wave during the non-conducting half cycle. The value of this resistance is given on the various diagrams.

The results of the operating tests under typical conditions of air blast are given in fig. 7. There are three

limits to the operating range at any given value of air blast. At a lower limit (not shown) the applied potential is too low to initiate the discharge in either direction. The value in our case was in the neighbourhood of 13 kilovolts r.m.s. The explanation of the two limits, BC and CD, is given in fig. 8, which shows two forms

Fig. 8.

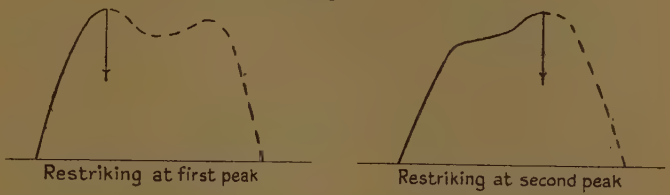

of the observed potential difference across the rectifier in the non-conducting half-cycle. Owing to the inherent resonance of the circuit the voltage wave has a double peak, as shown in the figure, and the boundary BC represents the case where breakdown occurs on the first

Fig. 9.

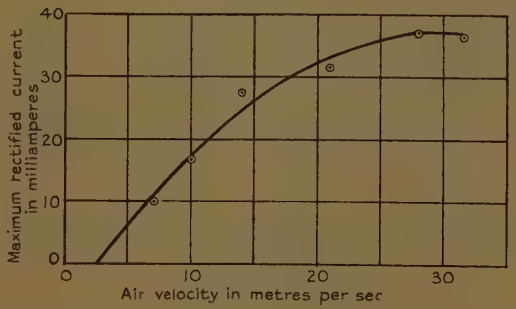

peak and CD where breakdown occurs on the second peak. The re-striking voltage is the same in the two cases. The magnitude of the first peak for given circuit constants depends chiefly on the transient rise caused by the current extinction, and therefore the limit BC is nearly a constant current line. On the other hand, the second peak, occurring later in the cycle when the

transient part is practically damped out, is chiefly dependent on the applied voltage, and therefore the limit CD is nearly a constant voltage line. It follows then that if the circuit can be damped so that the first peak disappears the limit BC is also removed. This is clearly demonstrated by the line EF of fig. 7, where the shunt damping resistance is decreased to 0·6 megohms.

The effect of the air in raising the limit line BC is shown in fig. 9, which gives, for different air-velocities, the maximum rectified current with an r.m.s. potential

Fig. 10.

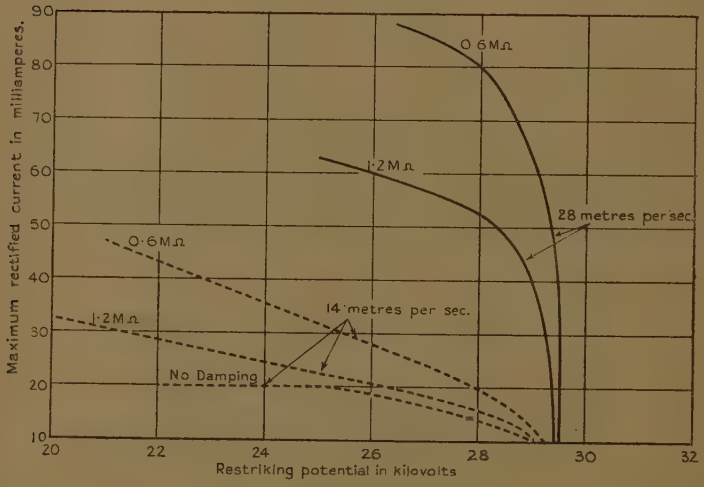

of 20 kilovolts and a damping resistance of 3 megohms.

In fig. 10 the results are given in yet another form.

6. *Conclusions.*

The air flow has little effect on the spark-over potential of the point-plate system, and therefore we conclude that in the rectifier the action of the air-blast is that of "scavenging," as in the case of an air-blast circuit breaker *.

* Compare Kesselring and Koppelmann, *Arch. f. Elektrotechnik.* xxx. p. 71 (1936).

LXXIII. *The Plane Jet.* *By* W. G. Bickley, *D.Sc.*, *Imperial College of Science and Technology* *.

1. Some time ago Dr. H. Schlichting published a paper [1] in which he examined the propagation of a jet issuing from a small hole into stationary fluid, in two cases. The case of axial symmetry led to equations which were integrated in closed form. In the case of the plane jet (*i. e.*, when the fluid issues from a long narrow orifice and the motion is taken to be two-dimensional) the equations were integrated by an approximate numerical method. In going through Schlichting's work the present writer noticed that in the plane case also the equations are integrable in closed form, and discovered small numerical errors in the results given †.

Since the problem is of interest, and also because simple exact solutions of Prandtl's boundary layer equations are rare, it has been thought desirable to give the details of this exact solution.

(2) We consider the steady two-dimensional motion of an incompressible viscous fluid due to a jet issuing from a long narrow orifice. We use coordinates (x, y) in the plane of motion, the origin being at the orifice and the x-axis being in the plane of symmetry of the jet; we denote by u and v the x- and y-components respectively of the fluid velocity at any point. If we assume that the Prandtl boundary layer equations give a sufficiently good approximation, and that the pressure is independent of x as well as of y, the equations of the problem are

$$u\frac{\partial u}{\partial x}+v\frac{\partial u}{\partial y}=\nu\frac{\partial^2 u}{\partial y^2}, \quad \ldots \quad (2.1)$$

$$\frac{\partial u}{\partial x}+\frac{\partial v}{\partial y}=0, \quad \ldots \quad (2.2)$$

with the boundary conditions

$$\left.\begin{aligned} &\partial u/\partial y=0, \quad \text{and} \quad v=0, \quad \text{when } y=0 \\ &u\to 0, \quad \text{as} \quad y\to\infty . \end{aligned}\right\} \quad \ldots \quad (2.3)$$

* Communicated by the Author.

† Dr. Schlichting has informed the present writer that he discovered the possibility of exact integration after publication of his paper.

Further, the total x-component of the fluid momentum must be constant, or

$$M=2\int_0^\infty \rho u^2\,dy=\text{const.} \quad . \quad . \quad . \quad . \quad (2.4)$$

In these equations ν stands for the kinematic viscosity of the fluid and ρ for its density.

(3) Following Schlichting, we seek a solution of these equations in the form

$$u=x^p f(y/x^q)=x^p f(\eta). \quad . \quad . \quad . \quad . \quad (3.1)$$

Substituting in equation (2.4), we find that in order that M may be constant we must have

$$2p+q=0. \quad . \quad . \quad . \quad . \quad . \quad . \quad (3.2)$$

Again, if the term $u\,.\,\partial u/\partial x$ is to have the same degree in x as the term $\nu\partial^2 u/\partial y^2$, then

$$2p-1=p-2q, \quad . \quad . \quad . \quad . \quad . \quad . \quad (3.3)$$

or

$$p=-1/3, \quad q=2/3. \quad . \quad . \quad . \quad . \quad (3.4)$$

The equation of continuity (2.2) is automatically satisfied if we introduce a stream-function ψ given by

$$\partial\psi/\partial y=u, \quad -\partial\psi/\partial x=v, \quad . \quad . \quad . \quad (3.5)$$

and the results of equations (3.1) and (3.4) are incorporated if we write

$$\left.\begin{aligned}\psi&=x^{1/3}F(\eta)\\ \text{with}\qquad \eta&=yx^{-2/3},\end{aligned}\right\} \quad . \quad . \quad . \quad . \quad . \quad (3.6)$$

and then

$$u=x^{-1/3}F'(\eta), \quad v=\tfrac{1}{3}x^{-2/3}\{2\eta F'(\eta)-F(\eta)\}, \quad . \quad (3.7)$$

where dashes denote differentiation of $F(\eta)$ with respect to its argument. Substituting these values in equation (2.1), we find that

$$F'^2+FF''+3\nu F'''=0. \quad . \quad . \quad . \quad . \quad (3.8)$$

(4) This last equation can be put into a non-dimensional form by writing

$$\left.\begin{aligned}\xi&=\alpha\eta/3\\ \text{and}\qquad F(\eta)&=\beta G(\xi),\\ \text{if}\qquad \beta&=2\nu\alpha,\end{aligned}\right\} \quad . \quad . \quad . \quad . \quad . \quad (4.1)$$

where the factor 2 has been introduced for later convenience. Making this substitution, we find that

$$2(G'^2+GG'')+G'''=0. \quad . \quad . \quad . \quad . \quad (4.2)$$

In terms of G, the boundary conditions (2.3) become

$$\left.\begin{aligned} G=0 \quad &\text{and} \quad G''=0, \text{ when } \xi=0, \\ G\to 0 \quad &\text{as} \quad \xi\to\infty, \end{aligned}\right\} \quad . \quad (4.3)$$

while (2.4) becomes

$$M=\frac{8\rho\nu^2\alpha^3}{3}\int_0^\infty G'^2\,d\xi. \quad . \quad . \quad . \quad . \quad (4.4)$$

If we put

$$\gamma=\int_0^\infty G'^2\,d\xi,$$

we find that

$$\alpha=(3M/8\rho\nu^2\gamma)^{1/3}. \quad . \quad . \quad . \quad . \quad . \quad (4.5)$$

The equation (4.3) for G can be written

$$2\frac{d}{d\xi}(GG')+G'''=0.$$

Integrating, and using the conditions at $\xi=0$ from (4.3),

$$G''=-2GG'.$$

Integrating again, we have

$$G'=-G^2+\text{const.}$$

Since we have one constant, α, which will not be determined by the boundary conditions, but subsequently by (4.5), the value of the constant of integration in the equation last written is at our choice; we choose it to be unity, so that

$$G'=1-G^2.$$

The integral of this which vanishes when $\xi=0$ is

$$G=\tanh\xi. \quad . \quad . \quad . \quad . \quad . \quad . \quad (4.6)$$

This value of G gives

$$\gamma=\int_0^\infty \operatorname{sech}^4\xi\,d\xi=2/3,$$

$$\alpha=(9M/16\rho\nu^2)^{1/3}=0{\cdot}8255..(M/\rho\nu^2)^{1/3},$$

$$\psi=1{\cdot}6510..(M\nu x/\rho)^{2/3}\tanh\xi,$$

$$u = 0{\cdot}4543..(M^2/\rho^2\nu x)^{1/3}\,\mathrm{sech}^2\,\xi.$$

$$v = 0{\cdot}5503..(M\gamma/\rho x^2)^{1/3}\{2\xi\,\mathrm{sech}^2\,\xi - \tanh\,\xi\},$$

with

$$\xi = 0{\cdot}2751..(M/\rho\nu^2)^{1/3}.y/x^{2/3}.$$

The total flux of matter across any plane perpendicular to the jet, per unit width, is

$$Q = 2\rho\int_0^\infty u\,dy = 3{\cdot}3019.\rho(M\nu x/\rho)^{1/3}\int_0^\infty G'\,d\xi$$
$$= 3{\cdot}3019..(M\nu x\rho^2)^{1/3}.$$

Stream-lines and velocity profiles for the plane jet.

We thus see that the progress of the jet is accompanied by the entrainment of a progressively increasing mass of fluid, the velocity of course decreasing so that the total momentum remains constant.

A drawing of the stream-lines, upon which have been superimposed graphs of the velocity profile at several sections, is given, and this should make the progress of the jet clear.

An *à posteriori* examination of the approximations made shows them to be adequate for moderate and large values of x. It was not to be expected that the formulæ would hold in the close neighbourhood of the origin. It is also seen that $x=0$ is a line of singularities for the solution ; the occurrence of such a line is a common feature of the solutions of the boundary layer equations, and can be traced to the omission of the term $\partial^2 u/\partial x^2$ from the equations of motion. As the present writer has pointed out in another connexion [2], the omission of such a term is equivalent to the neglect of conduction or diffusion against the stream.

References.

(1) H. Schlichting, ' Laminare Strahlausbreitung,' ZAMM, xiii. pp. 260–263 (1933).
(2) W. G. Bickley, " Some Solutions of the Problem of Forced Convection," Phil. Mag. (7) xx. pp. 322–343 (1935).

LXXIV. *Methods for the Calculation of Lift Distributions of Aerofoils.* *By* Prof. R. C. J. Howland, *M.A.*, *D.Sc.**

A SHORT while before his untimely death on August 16th, 1936, the late Prof. R. C. J. Howland, M.A., D.Sc., University College, Southampton, had been working on methods of calculating the lift distribution of aeroplane wings. A paper † written jointly with another had already been published and showed his keen interest in the problem. The following contribution is a first draft of some further work on the subject and is in the form in which he left it. With it were left a series of calculations which showed his intention of applying the methods here given to a particular wing form. Unfortunately they were not finished, and so this paper is not in its proposed completeness.

I have added a list of symbols, as was done in the earlier paper, that this communication may be more easily read. In addition I have supplied a footnote where I considered it necessary. Apart from this,

* Communicated by R. C. Knight.

† R. C. J. Howland and B. S. Shenstone, " The Inverse Method for Tapered and Twisted Wings," Phil. Mag. ser. 7, vol. xxii. p. 1 (1936).

and checking the results, I have made no addition or alteration.

I feel sure that Prof. Howland would have wished this paper to be published, and in submitting this paper I pay tribute to his memory. He was known as a research worker in more than one branch of Applied Mathematics and was a most inspiring teacher.

R. C. KNIGHT.

King's College,
London.
October 29th, 1936.

Symbols to be employed.

V = velocity of wing relative to still air.

α = angle of incidence, usually a function of x.

c = chord of wing, a function of x.

c_0 = chord at mid-span.

s = semi-span.

x = distance from central section measured along the span.

ξ = same as x, when a second point of the wing is indicated.

K = circulation round the wing, a function of x.

K_ξ = the same, expressed as a function of ξ.

a_0 = slope of lift curve ; its theoretical value is π.

β = angle of taper.

$\mu = (s/c_0) \tan \beta$.

θ, ϕ, defined by $x = -s \cos \theta$; $\xi = -s \cos \phi$.

A_n = coefficient in Fourier Series for K.

y_r = value of $K/4sV$ at the point $\theta = r\pi/2p$.

η_r = value of $K/4sV$ at the point $x = rs/n$.

p = number of divisions of the semi-span in method 1.

n = number of divisions of the semi-span in method 2.

$\alpha_{rs} = \dfrac{a_0 c_r}{4s}\left(\dfrac{2A_{rs}}{\pi p}\right)$ are the coefficients in the final equations for y_r in method 1.

$= \dfrac{a_0 c_r}{4s}\left(\dfrac{na}{\pi}\right)$ in method 2.

Values of A_{rs}, a_{rs} are given in the tables.

Methods for the Calculation of Lift Distributions of Aerofoils.

The equation to be solved is *

$$\frac{K}{a_0 c} = V\alpha - \frac{1}{4\pi}\int_{-s}^{s} \frac{dK_\xi}{d\xi}\frac{d\xi}{x-\xi}, \quad \ldots \quad (1)$$

when c, α are given functions of x.

For simplicity assume symmetry about $x=0$. The methods are based on the expectation that the integral on the right gives, at most points of the wing, a small correction, so that

$$K = Va_0 c\alpha$$

is a first approximation. An exception will arise at the wing tips if $c\alpha$ does not vanish there as, for example, in the case of an untwisted rectangular wing. The first approximation will then be bad near the wing tip.

In the ordinary method of Fourier Series the advantage of using this first approximation is best, since the Fourier coefficients of the first approximation may differ widely from those of the correct solution. We therefore work in terms of the ordinates of the curve for K. This curve is supposed to be given by an approximate formula.

Method 1.

Using Finite Fourier Series.

As in Glauert's † method, write

$$K = 4sV\sum_{n=0}^{p-1} A_n \sin(2n+1)\theta, \quad \ldots \quad (2)$$

and let the values of $K/4sV$ at the points

$$\theta = 0, \quad \pi/2p, \ldots r\pi/2p, \ldots (p-1)\pi/2p, \quad \pi/2,$$

be

$$0, \quad y, \quad y_r, \quad y_{p-1}, \quad y_p.$$

Then

$$y_r = \sum_{n=0}^{p-1} A_n \sin\frac{(2n+1)r\pi}{2p}, \quad r=1, \ldots p. \quad \ldots \quad (3)$$

* Prandtl's fundamental equation. See Prandtl, ' Vier Abhandlungen zur Hydrodynamik und Aerodynamik ' (Berlin, 1927); " Tragfluegeltheorie," *Göttingen Nachrichten*, 1918, 1919.

† Glauert, ' Aerofoil and Airscrew Theory,' p. 138 (Cambridge, 1930).

To express the coefficients A_n in the terms of the y_r, consider the sum

$$\sum_{r=1}^{p-1} y_r \sin\frac{(2n+1)r\pi}{2p} + \frac{1}{2} y_p \sin\frac{(2n+1)\pi}{2}.$$

In this the coefficient of A_m is

$$\sum_{r=1}^{p-1} \sin\frac{(2n+1)r\pi}{2p} \sin\frac{(2m+1)r\pi}{2p} + \frac{1}{2}\sin\frac{(2n+1)\pi}{2}\sin\frac{(2m+1)\pi}{2}$$

$$= \frac{1}{2}\sum_{r=1}^{p-1}\left[\cos\frac{(n-m)r\pi}{p} - \cos\frac{(n+m+1)r\pi}{p}\right] + \tfrac{1}{2}(-1)^{n+m}.$$

Now, if

$$c = \sum_{r=1}^{p-1} \cos\frac{kr\pi}{p},$$

we have

$$2c\sin\frac{k\pi}{2p} = \sum_{r=1}^{p-1}\left[\sin\frac{(2r+1)k\pi}{2p} - \sin\frac{(2r-1)k\pi}{2p}\right]$$

$$= \sin\frac{(2p-1)k\pi}{2p} - \sin\frac{k\pi}{2p}$$

$$= 2\cos\frac{k\pi}{2}\sin\frac{(p-1)k\pi}{2p}.$$

This vanishes when k is odd; when k is even

$$c = \frac{1}{2}\left[\frac{\sin\frac{(2p-1)k'\pi}{p}}{\sin\frac{k'\pi}{p}} - 1\right], \quad k' = \tfrac{1}{2}k$$

$$= \frac{1}{2}\left[\frac{\sin\left(2k'\pi - \frac{k'\pi}{p}\right)}{\sin\frac{k'\pi}{p}} - 1\right]$$

$$= -1.$$

Now if $n+m+1$ is even, $(n-m)$ is odd, and conversely; it follows that the coefficient of A_m vanishes if $n=m$.

When $n=m$, $(n+m+1)$ is odd, and the coefficient of A_n is $\frac{1}{2}p$.

We now have

$$A_n = \frac{2}{p}\left[\sum_{r=1}^{p-1} y_r \sin\frac{(2n+1)r\pi}{2p} + \tfrac{1}{2}(-1)^n y_p\right]. \quad . \quad (4)$$

On substituting the value of K in (2) into the equation (1) we have

$$\frac{K}{4sV} = \frac{a_0 c}{4s}\left[\alpha - \frac{1}{\pi}\sum_{n=0}^{p-1}(2n+1)A_n \frac{\sin(2n+1)\theta}{\sin\theta}\right],$$

$$y_r = \frac{a_0 c_r}{4s}\left[\alpha_r - \frac{1}{\pi}\sum_{n=0}^{p-1}(2n+1)A_n \frac{\sin\dfrac{(2n+1)r\pi}{2p}}{\sin\dfrac{r\pi}{2p}}\right]$$

$$= \frac{a_0 c_r}{4s}\left[\alpha_r - \frac{2}{\pi p}\sum_{n=0}^{p-1}(2n+1)\frac{\sin\dfrac{(2n+1)r\pi}{2p}}{\sin\dfrac{r\pi}{2p}} \times \left\{\sum_{s=1}^{p-1} y_s \sin\frac{(2n+1)s\pi}{2p} + \tfrac{1}{2}(-1)^n y_p\right\}\right]$$

$$= \frac{a_0 c_r}{4s}\left[\alpha_r - \frac{2}{\pi p}\sum_{s=1}^{p} A_{rs} y_s\right], \quad . \quad . \quad . \quad . \quad . \quad . \quad . \quad . \quad (5)$$

where, except for $s=p$,

$$A_{rs} = \frac{1}{\sin\dfrac{r\pi}{2p}}\sum_{n=0}^{p-1}(2n+1)\sin\frac{(2n+1)r\pi}{2p}\sin\frac{(2n+\pi)s\pi}{2p}, \quad (6)$$

while

$$A_{rp} = \frac{1}{2\sin\dfrac{r\pi}{2p}}\sum_{n=0}^{p-1}(-1)^n(2n+1)\sin\frac{(2n+1)r\pi}{2p}. \quad . \quad (7)$$

To evaluate these sums, first notice that A_{rp} is obtainable from A_{rs} by putting $s=p$ and halving the result, so that we have only to deal with (6). Write this

$$A_{rs} = \frac{1}{2\sin\dfrac{r\pi}{2p}}\sum_{n=0}^{p-1}(2n+1) \times \left[\cos\frac{(2n+1)(r-s)\pi}{2p} - \cos\frac{(2n+1)(r+s)\pi}{2p}\right]$$

and then consider the sum

$$Z = \sum_{n=0}^{p-1} (2n+1)z^{2n+1},$$

where $z = e^{ik\pi/2p}$ and k is an integer. We have

$$(1-z^2)Z = z + 2\sum_{n=1}^{p-1} z^{2n+1} - (2p-1)z^{2p+1}$$

$$= z + \frac{2z^3(z^{2p-2}-1)}{z^2-1} + (2p-1)z^{2p+1}$$

$$= \frac{2z^{2p+1} - z^3 - z - (2p-1)(z^{2p+3} - z^{2p+1})}{z^2-1};$$

$$\therefore \quad Z = \frac{(2p-1)z^{2p+3} - (2p+1)z^{2p+1} + z^3 + z}{(1-z^2)^2}$$

$$= \frac{(2p-1)z^{2p+1} - (2p+1)z^{2p-1} + z + z^{-1}}{(z-z^{-1})^2}$$

$$= \frac{(2p-1)z^{2p+1} - (2p+1)z^{2p-1} + 2\cos k\pi/2p}{\left(2i \sin \frac{k\pi}{2p}\right)}.$$

Taking the real part

$$\sum_{n=0}^{p-1} (2n+1)\cos\frac{(2n+1)k\pi}{2p}$$

$$= \frac{1}{4\sin^2\frac{k\pi}{2p}}\left[(2p+1)\cos\frac{(2p-1)k\pi}{2p} - (2p-1)\cos\frac{(2p+1)k\pi}{2p} - 2\cos\frac{k\pi}{2p}\right]$$

$$= \frac{1}{4\sin^2\frac{k\pi}{2p}}\left[(2p+1)\cos\left(k\pi - \frac{k\pi}{2p}\right) - (2p-1)\cos\left(k\pi + \frac{k\pi}{2p}\right) - 2\cos\frac{k\pi}{2p}\right]$$

$$= \frac{[(-1)^k - 1]\cos\frac{k\pi}{2p}}{2\sin^2\frac{k\pi}{2p}}$$

$$= 0, \text{ when } k \text{ is even}$$

$$= -\cot\frac{k\pi}{2p}\operatorname{cosec}\frac{k\pi}{2p}, \text{ when } k \text{ is odd.}$$

When $(r-s)$ is even, so is $(r+s)$;

$$\therefore\ A_{rs}=0, \text{ when } (r-s) \text{ is even}, \quad r\neq s,$$

while

$$A_{rr}=\tfrac{1}{2}\operatorname{cosec} r\pi/2p \sum_{n=0}^{p-1}(2n+1)=\tfrac{1}{2}p^2\operatorname{cosec} r\pi/2p.$$

When $(r-s)$ is odd,

$$A_{rs}=\frac{1}{2}\operatorname{cosec}\frac{k\pi}{2p}\left[\cot\frac{(r+s)\pi}{2p}\operatorname{cosec}\frac{(r+s)\pi}{2p} - \cot\frac{(r-s)\pi}{2p}\operatorname{cosec}\frac{(r-s)\pi}{2p}\right].$$

Collecting these results, and adding those for $s=p$,

$$\left.\begin{aligned} &A_{rs}=0, \ (r-s) \text{ even}, \quad r\neq s,\\ &A_{rr}=\tfrac{1}{2}p^2\operatorname{cosec} r\pi/2p, \quad r\neq p,\\ &A_{pp}=\tfrac{1}{4}p^2,\\ &A_{rs}=\tfrac{1}{2}\operatorname{cosec} r\pi/2p[C_{r+s}-C_{r-s}], \ (r-s) \text{ odd}, \quad s\neq p,\\ &A_{rp}=\tfrac{1}{4}\operatorname{cosec} r\pi/2p[C_{r+p}-C_{r-p}], \ (r-p) \text{ odd}, \end{aligned}\right\} \quad (8)$$

where
$$C_k=\cot k\pi/2p\operatorname{cosec} k\pi/2p. \quad (9)$$

The first step in applying these results is to calculate $2A_{rs}/\pi p$ for different values of p, say $p=6$, 8, 10.

Then write (5) in the form

$$y_r=\frac{a_0c_0}{4s}\left[\gamma_r\alpha_r-\frac{2\gamma_r}{\pi p}\sum_{s=1}^{p}A_{rs}y_s\right]$$

$$=y_r^{(0)}+\sum_{s=1}^{p}\alpha_{rs}y_s, \quad (10)$$

when

$$\left.\begin{aligned} &\gamma_r=\frac{c_r}{c_0},\\ &y_r^{(0)}=\frac{a_0c_0}{4s}\gamma_r\alpha_r,\\ &\alpha_{rs}=-\frac{a_0c_0}{4s}\gamma_r\left(\frac{2A_{rs}}{\pi p}\right). \end{aligned}\right\} \quad (11)$$

The values of $y_r^{(0)}$ and α_{rs} are then found and the equations are solved by using the iteration formulæ

$$\left.\begin{aligned} y_r &= \sum_{k=0}^{\infty} y_r^{(k)}, \\ \text{where} \qquad y_r^{(k)} &= \sum_{s=1}^{p} \alpha_{rs} y_s^{(k-1)}, \quad k \geqslant 1. \end{aligned}\right\} \quad . \quad . \quad . \quad (12)$$

The method should be most useful in the investigation of a class of wings, *e. g.*, straight-tapered wings, for which the α_{rs} can be standardized and only the effects of variation in twist are to be studied.

When the y_r have been found, the A_r may be deduced from the formula (4), which may be written

$$A_n = \sum_{r=1}^{p} B_{rn} y_r, \quad . \quad . \quad . \quad . \quad . \quad (13)$$

when

$$\left.\begin{aligned} B_{rn} &= (2/p) \sin \frac{(2n+1)r\pi}{2p}, \quad r \neq p, \\ B_{pn} &= (-1)^n/p. \end{aligned}\right\} \quad . \quad . \quad . \quad (14)$$

These coefficients should be tabulated for each value of p. The whole calculation is then in the most convenient form for use with a machine.

Method 2.

Using Parabolic Arcs.

The first method should have a considerable advantage over Glauert's method in that it gives a convenient method of solving the equations when the number of ordinates is large. But it has the same disadvantage, that the ordinates are irregularly spaced. It must give results identical with these given by Glauert's method with the same number of ordinates.

An alternative method is to use equally spaced ordinates and represent K by algebraic curves. This will have two serious disadvantages: (1) the formulæ initially required are clumsy; (2) a new and much less simple formula will be needed for the induced drag, since the A's are not given by this method.

These disadvantages may, however, be offset by a considerable gain if it is found that accurate results

can be obtained with a smaller number of ordinates. Only experience in the use of the two methods can settle this point.

Still assuming symmetry, divide the half space from $x=0$ to s into n equal parts by placing ordinates at

$$x=0, \quad \frac{s}{n}, \quad \frac{2s}{n}, \ldots s.$$

Write $K=4Vsy$, as before, and let y have the values

$$\eta_0, \ \eta_1, \ \ldots \ \eta_{n-1}, \ 0,$$

at these values of x (η is used to avoid confusion, with the y of the previous method, which are taken at different values of x).

In the pth section where

$$\frac{p-1}{n}s<x<\frac{p}{n}s,$$

write

$$x_p=\frac{n}{s}\left(x-\frac{p-1}{n}s\right), \quad \ldots \quad (15)$$

so that x_p varies from 0 to 1 in this section, and assume that

$$\left.\begin{aligned} \frac{s}{n}\frac{dy}{dx}=\frac{dy}{dx_p}&=b_p+2c_px_p, \quad 0\leqslant x_p\leqslant 1, \\ y&=\eta_{p-1}+b_px_p+c_px_p^2. \end{aligned}\right\} \quad (16)$$

Continuity requires that

$$\left.\begin{aligned} b_{p+1}&=b_p+2c_p \\ \text{and} \quad b_p+c_p&=\eta_p-\eta_{p-1}, \end{aligned}\right\}$$

$$\therefore \quad b_{p+1}-b_p=2(\eta_p-\eta_{p-1}-b_p),$$

$$\text{or} \quad b_{p+1}+b_p=2(\eta_p-\eta_{p-1})=2\delta_p \quad \text{(say)},$$

$$\therefore \quad b_p=2[\delta_{p-1}-\delta_{p-2}+\ldots+(-1)^r\delta_1], \quad \ldots \quad (17)$$

since $b_1=0$ on account of the symmetry and continuity at $x=0$.

Also

$$c_p = \tfrac{1}{2}[b_{p+1} - b_p]$$
$$= \delta_p - 2\delta_{p-1} + 2\delta_{p-2} - \ldots + 2(-1)^{p-1}\delta_1. \quad . \quad (18)$$

Consider now the integral

$$\int_{-s}^{s} \frac{d\mathrm{K}_\xi}{d\xi} \frac{d\xi}{x-\xi} = 4\mathrm{V}s \int_{-s}^{s} \frac{dy}{d\xi} \frac{d\xi}{x-\xi},$$

when in y we suppose x changed to ξ.

Take the first range $\frac{p-1}{n}s < \xi < \frac{p}{n}s$, in which

$$\frac{dy}{d\xi_p} = \frac{n}{s}(b_p + 2c_p\xi_p).$$

We have also $\xi = \frac{s}{n}(\xi_p + p - 1)$, from (15), and we write

$$x = sx'/n. \quad . \quad . \quad . \quad . \quad . \quad (19)$$

Then

$$\int_{\frac{p-1}{n}s}^{\frac{p}{n}s} \frac{dy}{d\xi} \frac{d\xi}{x-\xi} = \frac{n}{s} \int_0^1 \frac{b_p + 2c_p\xi_p}{x' - \xi_p - (p-1)} d\xi_p.$$

Next take the range $-\frac{p}{n}s < \xi < -\frac{p-1}{n}s$, in which

$$\frac{dy}{d\xi} = -\frac{n}{s}(b_p + 2c_p\xi_p),$$

$$\xi = -\frac{s}{n}(\xi_p + p - 1).$$

Hence

$$\int_{-\frac{p}{n}s}^{-\frac{p-1}{n}s} \frac{dy}{d\xi} \frac{d\xi}{x-\xi} = -\frac{n}{s} \int_0^1 \frac{b_p + 2c_p\xi_p}{x' + \xi_p + (p-1)} d\xi_p.$$

Continuing these

$$\int_{-s}^{s} \frac{dy}{d\xi} \frac{d\xi}{x-\xi}$$
$$= \frac{n}{s} \sum_{p=1}^{n} \int_0^1 \left\{ \frac{b_p + 2c_p\xi_p}{x' - \xi_p - (p-1)} - \frac{b_p + 2c_p\xi_p}{x' + \xi_p + (p-1)} \right\} d\xi_p$$

$$= \frac{n}{s} \sum_{p=1}^{n} \int_0^1 \left[\frac{b_p + 2c_p(x' - p - 1) - 2c_p(x' - \xi_p - p - 1)}{x' - \xi_p - (p-1)} \right.$$

$$\left. - \frac{b_p - 2c_p(x' + p - 1) + 2c_p(x' + \xi_p + p - 1)}{x' + \xi_p + (p-1)} \right] d\xi_p$$

$$= \frac{n}{s} \sum_{p=1}^{n} \left[\{b_p + 2c_p(x' - p - 1)\} \int_0^1 \frac{d\xi_p}{x' - \xi_p - (p-1)} \right.$$

$$\left. - \{b_p - 2c_p(x' + p - 1)\} \int_0^1 \frac{d\xi_p}{x' + \xi_p + (p-1)} - 4c_p \right].$$

Suppose, now, that x lies in the rth section : *i. e.*,

$$\frac{r-1}{n} s < x < \frac{r}{n} s,$$

or $\quad (r-1) < x' < r.$

Then for $p < r$,

$$\int_0^1 \frac{d\xi_p}{x' - \xi_p - (p-1)} = -[\log\{x' - \xi_p - (p-1)\}]_0^1$$

$$= \log \frac{x' - (p-1)}{x' - p}.$$

When $p > r$ the result may be written :

$$\log \frac{(p-1) - x'}{p - x'}.$$

Finally, when $p = r$, the integral is improper, and the principal value is to be taken. This is

$$- \lim_{\epsilon \to 0} \log \frac{\epsilon}{x' - (r-1)} \cdot \frac{x' - r}{-\epsilon} = \log \frac{x' - (r-1)}{r - x'}.$$

Hence in every case we may write

$$\int_0^1 \frac{d\xi_p}{x' - \xi_p - (p-1)} = \log \frac{|x' - (p-1)|}{|x' - p|},$$

and we have

$$\int_{-s}^{s} \frac{dy}{d\xi} \frac{d\xi}{x - \xi} = \frac{n}{s} \sum_{p=1}^{n} \left[\{b_p + 2c_p(x' - [p-1])\} \log \frac{|x' - (p-1)|}{|x' - p|} \right.$$

$$\left. - \{b_p - 2c_p(x' + [p-1])\} \log \frac{x' + p}{x' + p - 1} - 4c_p \right].$$

If we now let $x \to r$ there will be two critical terms. When $x = r - \epsilon$ these are

$$\{b_{r+1} + 2c_{r+1}(-\epsilon)\} \log \epsilon - \{b_r + 2c_r(\epsilon + 1)\} \log \epsilon$$
$$= \{b_{r+1} - b_r) - 2c_r - 2c(c_{r+1} - c_r)\} \log \epsilon$$
$$= -2\epsilon(c_{r+1} - c_r) \log \epsilon$$

and $\to 0$ when $\epsilon \to 0$.

The value of integral therefore becomes

$$\frac{n}{s}\left[\sum_{p=1}^{n}{}' \{b_p + 2c_p(r-p-1)\} \log \left|\frac{r-p+1}{r-p}\right|\right.$$
$$\left. - \sum_{p=1}^{r} \{b_p - 2c_p(r+p-1)\} \log \frac{r+p}{r+p-1} - 4 \sum_{p=1}^{n} c_p\right],$$

the Σ' denoting a summation in which the terms which are not finite are omitted.

When the values of the b_p and c_p are put in we now have a result of the form

$$-\frac{n}{s} \sum_{t=1}^{n} a_{rt} y_t,$$

and the integral equation becomes

$$\frac{y_r}{a_0 c_r} = \frac{\alpha_r}{s} + \frac{n}{4\pi s} \sum_{t=1}^{n} a_{rt} y_t$$

or
$$y_r = y_r^{(0)} + \Sigma \alpha_{rt} y_t, \quad \ldots \ldots \quad (20)$$

when

$$\left.\begin{aligned} y_r^{(0)} &= \frac{a_0 c_r \alpha_r}{s}, \\ \alpha_{rt} &= \frac{n a_0 c_r}{4\pi s} a_{rt}. \end{aligned}\right\} \quad \ldots \ldots \quad (21)$$

As before, the process is first to calculate

$$\frac{n a_0}{4\pi} a_{rt} \sim \tfrac{1}{4} n a_{rt}$$

for chosen values of n. Then tabulate α_{rt} for certain classes of wing The calculation then proceeds by iteration as before.

Values of a_{rs} for $n=6$.

	$r=0.$	1.	2.	3.	4.	5.
$s=0..$	4·25255	−1·46097	−0·24260	−0·09214	−0·02377	+0·08305
1..	−2·95992	3·96826	−1·60780	−0·35688	−0·22935	−0·33655
2..	−0·49227	−1·56275	4·20614	−1·47184	−0·20537	+0·11410
3..	−0·24154	−0·33760	−1·53618	4·17661	−1·56891	−0·51705
4..	−0·10697	−0·13193	−0·25773	−1·45221	4·30546	−1·23701
5..	−0·09829	−0·11014	−0·15736	−0·30993	−1·56084	3·98726

Values of a_{rs} for $n=4$.

	$r=0.$	1.	2.	3.
$s=0...$	4·26356	−1·44684	−0·21352	0·01342
1...	−2·98194	3·94017	−1·66595	−0·56799
2...	−0·47024	−1·53449	4·26428	−1·26073
3...	−0·26356	−0·36586	−1·59432	3·96550

Values of $2A_{rs}/\pi p$ for $p=6$.

	$r=1.$	2.	3.	4.	5.	6.
$s=1..$	7·3791	−1·3799	0	−0·06964	0	−0·02943
2..	−2·6658	3·8197	−1·0610	0	−0·09291	0
3..	0	−1·5005	2·7010	−0·90032	0	−0·15005
4..	−0·23302	0	−1·1027	2·2053	−0·86964	0
5..	0	−0·17949	0	−0·96996	1·9772	−1·5300
6..	−0·05686	0	−0·10610	0	−0·79197	0·95493

$2A_{rs}/\pi p$ for $p=8$.

	$s=1.$	2.	3.	4.	5.	6.	7.	8.
$r=1$.....	13·0528	−4·7063	0	−0·38551	0	−0·12253	0	−0·04136
2.....	−2·3992	6·6543	−2·5958	0	−0·25899	0	−0·10464	0
3.....	0	−1·7880	4·5836	−1·8310	0	−0·20745	0	−0·05755
4.....	−0·10636	0	−1·4386	3·6013	−1·4615	0	−0·19680	0
5.....	0	−0·11920	0	−1·2429	3·0627	−1·2716	0	−0·12891
6.....	−0·02587	0	−0·12475	0	−1·1444	2·7563	−1·2258	0
7.....	0	−0·04083	0	−0·14189	0	−1·1547	2·5964	−1·0454
8.....	−0·01614	0	−0·06416	0	−0·21437	0	−2·0507	1·2732

LXXV. *Symmetrical Flexure of an Angle-Iron.*

By B. R. Seth, *M.A., M.Sc., Ph.D.* *

1. *Introduction.*

PHYSICAL problems connected with rectilinear boundaries having one or more re-entrant angular points have received attention from very few authors despite their important technical applications. In this connexion the first mathematical solution was obtained by F. Kötter † in 1908 for the torsion of a beam of L-section, both of whose arms are infinite. He attacked the problem by the use of the known solution of the rectangle and by application of the scheme of conformal transformation. E. Trefftz ‡ published in 1921 the torsion solution for a beam of rectilinear polygonal cross-section, and also applied his method to an infinite L-section. I. S. Sokolnikoff § has laboriously worked out an approximate solution for the torsion of a ⊥-section whose flange and web are both infinite. Recently we || have obtained a very general solution for two-dimensional problems which require the solution of Laplace's equation satisfying a given boundary condition, the boundary consisting only of straight lines. The object of the present paper is to deal with the interesting problem of the symmetrical flexure of an angle-iron with the help of this general solution.

The sections considered by Kötter and others are all infinite; the one we are going to take up is finite. Again, in general the stress (or velocity) in a physical problem becomes infinite at a re-entrant angle; in the present case it does not. But if the angle-iron is subjected to an asymmetrical flexure an infinite stress is introduced at the re-entrant angle, this being due to the "associated flexural torsion" with which it is accompanied.

2. *Conformal Transformation of the z-area.*

In the z-plane the section of the angle-iron is shown in fig. 1. It is symmetrical about the x-axis. The

* Communicated by the Author.

† F. Kötter, *Sitzungsberichte der Preuss. Akad. der Wiss.* pp. 935–955 (1908).

‡ E. Trefftz, *Math. Ann.* lxxxii. pp. 97–112 (1921).

§ I. S. Sokolnikoff, Trans. American Math. Soc. xxxiii. pp. 719–732 (1931).

|| Seth, Phil. Mag. (7) xx. pp. 632–640 (1935).

angles at O, A, E are taken each equal to $\frac{2}{3}\pi$, those at B and D equal to $\frac{1}{3}\pi$, and the one at C equal to $\frac{4}{3}\pi$.

If we take the points on the ξ-axis in the ζ-plane that correspond to O, A, B, C, D, E in the z-plane as 0, 1, $\sqrt{2}$, ∞, $-\sqrt{2}$, -1 respectively, our conformal transformation of the z-area into the upper half of the ζ-plane bounded by the real axis gives

$$z = \mathrm{A}\int \frac{d\zeta}{\zeta^{\frac{1}{3}}(\zeta^2-1)^{\frac{1}{3}}(\zeta^2-2)^{\frac{1}{3}}} + \mathrm{B}, \quad . \quad . \quad . \quad (1)$$

Fig. 1.

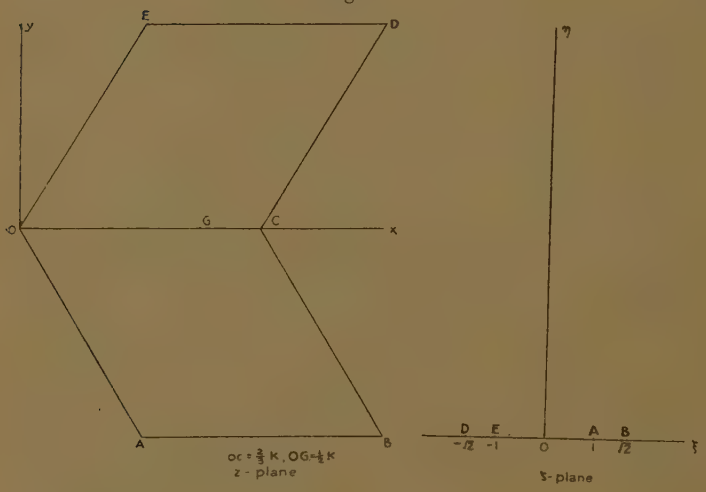

A and B being constants.

Putting $(\zeta^2-1)^2 = \lambda^3$ and $h^3 = \lambda^3/(\lambda^3-1)^2$, we get

$$z = \mathrm{A}_1\int \frac{dh}{(4h^3+1)^{\frac{1}{3}}} + \mathrm{B}_1. \quad . \quad . \quad . \quad . \quad (2)$$

If we take $\mathrm{A}_1=1$, $\mathrm{B}_1=0$, we have

$$h = \wp(z), \quad g_2=0, \quad g_3=-1. \quad . \quad . \quad . \quad . \quad (3)$$

But if we put $\mathrm{A}_1 = 3^{\frac{1}{3}}/2^{\frac{1}{3}}$, $\mathrm{B}_1=0$, we get

$$\mathrm{cn}\, 2z = \frac{\sqrt[3]{4h}-(\sqrt{3}-1)}{\sqrt[3]{4h}+(\sqrt{3}+1)}, \quad . \quad . \quad . \quad . \quad (4)$$

the modulus k of the elliptic function being $\sin 75°$.

If 4K, $4iK'$ be the complete periods corresponding to $k=\sin 75°$, we know that $K=K'\sqrt{3}$. The coordinates of the angular points O, A, B, C, D, E in the z-figure are now respectively seen to be 0, $\frac{1}{3}K-iK'$, $K-iK'$, $\frac{2}{3}K$, $K+iK'$, $\frac{1}{3}K+iK'$, the length of each side being $\frac{2}{3}K$.

3. *Form of the Boundary Condition.*

Let a load W be supposed to act along the x-axis about which the section is symmetrical. Let $(\bar{x}, 0)$ be the coordinates of G, the centre of gravity of the section, then the three non-vanishing stress-components of Saint-Venant's solution, are

$$\widehat{xz}=\frac{\mu W}{EI_y}\left[\frac{\partial\chi}{\partial x}-\tfrac{1}{2}\sigma(x-\bar{x})^2-(1-\tfrac{1}{2}\sigma)y^2\right], \quad . \quad (5.1)$$

$$\widehat{yz}=\frac{\mu W}{EI_y}\left[\frac{\partial\chi}{\partial y}-(2+\sigma)(x-\bar{x})y\right], \quad . \quad . \quad . \quad . \quad (5.2)$$

$$\widehat{zz}=-\frac{W}{I_y}(x-\bar{x})(l-z), \quad . \quad . \quad . \quad . \quad . \quad . \quad . \quad (5.3)$$

where $\chi(x, y)$ is the flexure solution, I_y the moment of inertia of the section about an axis through G parallel to the y-axis, and l the length of the beam.

If we put

$$\chi=\chi_1+\tfrac{1}{2}\sigma x\bar{x}^2-\tfrac{1}{2}\sigma\bar{x}(x^2-y^2)-\tfrac{1}{3}(1-\tfrac{1}{2}\sigma)(x^3-3xy^2), \quad (6)$$

and assume ψ_1 to be the function conjugate to χ_1, the boundary condition

$$\widehat{xz}\cos(xv)+\widehat{yz}\cos(yv)=0 \quad . \quad . \quad . \quad . \quad (7)$$

becomes

$$\frac{\partial\psi_1}{\partial s}=x^2\sin\alpha_p-[2\sigma xy-2(1+\sigma)xy]\cos\alpha_p, \quad . \quad (8)$$

s being measured along the boundary and α_p being the argument of dz when the pth side of the section is described in the positive sense by the point whose affix is z.

Again, putting

$$X_3=\frac{\partial^3\chi_1}{\partial x^3}, \qquad Y_3=\frac{\partial^3\psi_1}{\partial x^3},$$

we know * that (8) can be written as

$$X_3\sin 3\alpha_p+Y_3\cos 3\alpha_p=(1-2\sigma)\cos\alpha_p\sin 2\alpha_p. \quad (9)$$

* Seth, *loc. cit.* pp. 634, 639.

Also $\Omega_3 = X_3 + iY_3$, which is a function of z only, is given by *

$$\Omega_3 = \frac{d^3(\chi_1 + i\psi_1)}{dz^3} = C\int \frac{R(\zeta)\, d\zeta}{\zeta^2(\zeta^2-1)^2(\zeta^2-2)} + D, \quad (10)$$

where $R(\zeta)$ is a rational, integral function of the tenth degree in ζ with real coefficients.

4. *Form of* $R(\zeta)$.

Let

$$R(\zeta) = A_1\zeta^{10} + A_2\zeta^9 + A_3\zeta^8 + A_4\zeta^7 + \ldots + A_{10}\zeta + A_{11}.$$

Since the section is symmetrical about Ox along which the load acts, two zeros of $R(\zeta)$ must coincide with the angular points O and A. This requires

$$A_1 = A_{11} = 0.$$

Again, the condition that Ω_3 is to be even in ζ gives

$$A_3 = A_5 = A_7 = A_9 = 0.$$

If we now write $\zeta^2 = t$, we have

$$R(\zeta) = \zeta(A_2t^4 + A_4t^3 + A_6t^2 + A_8t + A_{10}).$$

The remaining zeros of $R(\zeta)$ can lie on the straight line through G perpendicular to the x-axis. They are seen to be the point G, the two centres of gravity of the rhombuses into which Ox divides the section, and the two points in which the straight line meets the sides AB and DE. These points are respectively given by $t = -2{\cdot}4809$, $t = 1 \pm i$, and $t = 1{\cdot}2873$. Thus

$$\begin{aligned} R(\zeta) &= A_2\zeta[(t-1)^2+1][t+2{\cdot}4809][t-1{\cdot}2873] \\ &= B\zeta[(t-1)^2+1][t-1+0{\cdot}3131t(t-2)] \quad . \quad . \quad (11) \end{aligned}$$

Absorbing the constant B in C we see that (10) becomes

$$\Omega_3 = \tfrac{1}{2}C\left[\log\frac{t(t-2)}{t-1} + 0{\cdot}3131\left(t - \frac{1}{t-1}\right)\right] + D. \quad (12)$$

From the boundary condition (9) we get the increment in iY_3 as ζ passes through the angular points O, A, B, C, D, E, as $\frac{1}{2}i(1-2\sigma)\sqrt{3}$, $-\frac{1}{4}i(1-2\sigma)\sqrt{3}$, $\frac{1}{4}i(1-2\sigma)\sqrt{3}$, $-\frac{1}{2}i(1-2\sigma)\sqrt{3}$, $\frac{1}{4}i(1-2\sigma)\sqrt{3}$, and $-\frac{1}{4}i(1-2\sigma)\sqrt{3}$ respectively. Their values are also seen from (12) to be $-iC\pi$, $\frac{1}{2}iC\pi$, $-\frac{1}{2}iC\pi$, $iC\pi$, $-\frac{1}{2}iC\pi$, and $\frac{1}{2}iC\pi$. Thus we get

$$C = -\frac{(1-2\sigma)\sqrt{3}}{2\pi},$$

and incidentally verify the result in (11).

* Seth, *loc. cit.* pp. 634, 639.

Again, we have

$$h^3 = \left[\frac{t-1}{t(t-2)}\right]^2,$$

and hence

$$\Omega_3 + \mathrm{E} = \frac{(1-2\sigma)\sqrt{3}}{4\pi}\left[\log\sqrt{h^3} + \frac{0{\cdot}3131}{\sqrt{h^3}}\right], \quad (13)$$

where E is a constant, and the plus or minus sign is understood before the under-root sign.

Ω_3 is infinite at all the angular points of the section. Ω_2, the first integral of Ω_3 with respect to z, is seen to be infinite only at the points A and C. Ω_1, the second integral with respect to z, is finite at all the angular points. These results can be easily obtained with the help of (12) and (1). In fact (7) shows that $\widehat{xz}$ and $\widehat{yz}$ both vanish at all the angular points, and hence at such a point

$$\mathrm{X}_1 = \frac{\partial\chi_1}{\partial x} = x^2, \qquad \mathrm{Y}_1 = \frac{\partial\psi_1}{\partial x} = 2(1+\sigma)\bar{x}y - 2\sigma xy. \quad (14)$$

These relations will be required to determine the constants of integration.

5. *Integration of* Ω_3.

If (3) is used we have

$$\mathrm{X}_1 + i\mathrm{Y}_1 + \tfrac{1}{2}\mathrm{E}z^2 + \mathrm{F}z + \mathrm{G} = \frac{(1-2\sigma)\sqrt{3}}{4\pi}\iint\left[\log\sqrt{\wp^3(z)} + \frac{0{\cdot}3131}{\sqrt{\wp^3(z)}}\right]dz^2. \quad (15)$$

It is not very easy to evaluate the double integral in (15). Let us put

$$\mathrm{I}_1 = \log\wp(z);$$

then

$$\frac{d\mathrm{I}_1}{dz} = \frac{\wp'(z)}{\wp(z)} = \zeta(z-v) + \zeta(z+v) - 2\zeta(z),$$

where $\wp(v) = 0$. But in the usual notation

$$\zeta(z) = \frac{\eta_1 z}{\omega_1} + \frac{\pi}{2\omega_1}\cot\frac{\pi z}{2\omega_1} + \frac{2\pi}{\omega_1}\sum_{r=1}^{\infty}\frac{q^{2r}}{1-q^{2r}}\sin\frac{r\pi z}{\omega_1},$$

$$q = \exp(i\pi\omega_2/\omega_1),$$

and hence $\iint\log\wp(z)dz^2$ can be tackled.

Again,

$$\int \frac{dz}{\wp^{3/2}(z)} = \int \frac{dh}{h^{3/2}(4h^3+1)^{1/2}} = -2\sqrt[3]{4} \int \frac{l\,dl}{(4l^3+1)^{1/2}},$$

where

$$l = \frac{1}{2\sqrt[3]{2}\,\wp(z)} = \wp(u, 0, -1) \quad \text{(say)}.$$

Therefore

$$\int \frac{dz}{\wp^{3/2}(z)} = -2\sqrt[3]{4}\,\zeta(u).$$

In like manner we find

$$\iint \frac{dz^2}{\wp^{3/2}(z)} = 2\sqrt[3]{2} \int \frac{\zeta(u)}{\wp^{1/2}(u)}\,du,$$

which cannot be easily integrated. To get any definite results we must therefore take to numerical integration of Ω_3. For this purpose we should use (4) and not (3).

6. *Determination of Stress.*

Since the section is symmetrical about Ox, it is sufficient to determine the values of $\widehat{xz}$ and $\widehat{yz}$ for one-half of the section bounded by the x-axis. The value of $\widehat{xz}$ remains unchanged as we pass from the lower to the upper half, while that of $\widehat{yz}$ only changes sign.

(a) Stress at a point on the boundary.

(i.) For the side OA we have from (9) and (13)

$$X_3 = -\frac{(1-2\sigma)\sqrt{3}}{4\pi}\left[\log\frac{t(t-2)}{t-1} + 0{\cdot}3131\,\frac{t(t-2)}{t-1}\right] - E, \quad (16.1)$$

$$Y_3 = \tfrac{1}{4}(1-2\sigma)\sqrt{3}, \quad . \quad . \quad . \quad . \quad . \quad . \quad . \quad . \quad . \quad . \quad (16.2)$$

and hence

$$\frac{\partial^3\chi_1}{\partial s^3} = X_3 \cos 3\alpha_p - Y_3 \sin 3\alpha_p = -X_3 = f'''(s) \quad \text{(say)}, \quad (17)$$

where dashes denote differentiations with respect to s.

Corresponding values of s, t, and $\partial^3\chi/\partial s^3$ can be tabulated with the help of (4) and (16.1). Two successive numerical integrations of (17) with respect to s give the value of $\partial\chi_1/\partial s$. To determine the three constants of integration

we have the values of X_1 and Y_1 at O and A given by (14), and of X_2 and Y_2 at O given by

$$X_2=(1+\sigma)\bar{x}, \quad Y_2=0,$$

which can be obtained by differentiating (8) once with respect to s. Thus the value of $X_1 \cos \alpha_p - Y_1 \sin \alpha_p$ is known, which, combined with that of $X_1 \sin \alpha_p + Y_1 \cos \alpha_p$, given by (8), determines the values of X_1 and Y_1, and hence those of $\widehat{xz}$ and $\widehat{yz}$.

(ii.) For AB we have

$$X_3 = -\frac{(1-2\sigma)\sqrt{3}}{4\pi}\left[\log \frac{t(2-t)}{t-1} - 0{\cdot}3131 \frac{t(2-t)}{t-1}\right] - E,$$

$$Y_3 = 0,$$

and hence

$$\frac{\partial^3 \chi_1}{\partial s^3} = \frac{\partial^3 \chi_1}{\partial x^3} = X_3.$$

Tabulating the corresponding values of x, t, and X_3, and proceeding as in (i.), we get X_1, and hence $\widehat{xz}$. $\widehat{yz}$, of course, vanishes in this case.

In section 7 we have obtained numerical values for $\widehat{xz}$ by taking $\sigma=\frac{1}{4}$.

(iii.) For BC we proceed exactly as in (i.).

(*b*) Stress at a point inside the section.

Let us draw straight lines parallel to the x-axis, and let one of them meet the boundary in L and M. We can get the corresponding values of x, t, X_3, and Y_3 with the help of (4) and (13). y is constant over LM, and hence we can write

$$X_3=f_1''(x), \quad Y_3=f_2''(x).$$

Two successive integrations will give the values of X_1 and Y_1, the constants of integration having been determined by the known values of X_1, X_2, Y_1, Y_2 at the boundary points L and M. Thus $\widehat{xz}$ and $\widehat{yz}$ can be obtained at any point of the section.

In section 8 we have calculated the value of $\widehat{xz}$ for the axis of symmetry over which $\widehat{yz}$ also vanishes.

7. *Value of* $\widehat{xz}$ *over* AB.

In this case we have $z=x-iK'$. The corresponding values of x and t, given in Table I. below, have been calculated at equal intervals of $\frac{1}{24}$ K.

Putting $\sigma=\frac{1}{4}$ in (13), we get

$$\frac{\partial^3\chi_1}{\partial x^3}+\mathrm{E}=\frac{\sqrt{3}}{8\pi}[\tfrac{3}{2}\log h+0{\cdot}3131h^{-3/2}], \quad . \quad . \quad (18)$$

where $$h^{3/2}=\frac{t-1}{t(2-t)}.$$

The corresponding values of x, $\frac{3}{2}\log h$, $0{\cdot}3131\,h^{-3/2}$, and their first and second integrals with respect to x are given in Table II. For numerical integration the

TABLE I.

$z=x-i\mathrm{K}'$.	$\zeta^2=t$.	$z=x-i\mathrm{K}'$.	$\zeta^2=t$.
x/K.	t.	x/K.	t.
$\frac{1}{3}$	1	$\frac{2}{3}$	1·7072
$\frac{3}{8}$	1·0367	$\frac{17}{24}$	1·7934
$\frac{5}{12}$	1·1040	$\frac{3}{4}$	1·8646
$\frac{11}{24}$	1·1918	$\frac{19}{24}$	1·9193
$\frac{1}{2}$	1·2873	$\frac{5}{6}$	1·9578
$\frac{13}{24}$	1·3896	$\frac{7}{8}$	1·9820
$\frac{7}{12}$	1·5026	$\frac{11}{12}$	1·9946
$\frac{5}{8}$	1·6090	$\frac{23}{24}$	1·9993
		1	2

Newton-Cotes formula * with five ordinates has been used. In each case the integral at the point $x=\mathrm{K}$ has been taken to be equal to zero.

Two successive integrations of (18) with respect to x give

$$\frac{\partial\chi_1}{\partial x}+\tfrac{1}{2}\mathrm{E}x^2+\mathrm{F}x+\mathrm{G}=\frac{\sqrt{3}}{8\pi}\int\int[\tfrac{3}{2}\log h+0{\cdot}3131h^{-3/2}]\,dx^2. \quad . \quad . \quad . \quad (19)$$

* *Cf.* Whittaker and Robinson, 'The Calculus of Observations,' p. 155 (1932).

TABLE II.

$z=x-iK'$. x/K.	$-\frac{3}{2}\log h$.	$-\int\frac{3}{2}\log h\,dx$.	$\iint\frac{3}{2}\log h\,dx^2$.	$0{\cdot}3131\,h^{-3/2}=H$.	$-\int H\,dx$.	$\iint H\,dx^2$.
$\frac{1}{3}$	$+\infty$	1·778	4·799	$+\infty$	$+\infty$	0·738
$\frac{3}{8}$	3·305	2·332	4·559	8·529	1·207	0·286
$\frac{5}{12}$	2·257	2·649	4·271	2·993	0·681	0·182
$\frac{11}{24}$	1·614	2·869	3·952	1·573	0·435	0·118
$\frac{1}{2}$	1·161	3·028	3·613	1	0·289	0·077
$\frac{13}{24}$	0·778	3·138	3·259	0·682	0·193	0·049
$\frac{7}{12}$	0·397	3·206	2·893	0·466	0·128	0·031
$\frac{5}{8}$	0·032	3·231	2·523	0·324	0·083	0·019
$\frac{2}{3}$	$-{\cdot}347$	3·214	2·153	0·221	0·052	0·011
$\frac{17}{24}$	$-{\cdot}761$	3·152	1·786	0·146	·032	0·006
$\frac{3}{4}$	$-1{\cdot}231$	3·037	1·429	0·091	·018	0·003
$\frac{19}{24}$	$-1{\cdot}781$	2·864	1·090	0·053	·010	0·002
$\frac{5}{6}$	$-2{\cdot}449$	2·621	0·775	0·027	·005	0·001
$\frac{7}{8}$	$-3{\cdot}315$	2·291	0·492	0·011	·003	0
$\frac{11}{12}$	$-4{\cdot}532$	1·844	0·252	0·003	·002	0
$\frac{23}{24}$	$-6{\cdot}611$	1·214	0·074	0	0	0
1	$-\infty$	0	0	0	0	0

To determine the constants E, F, G we have the conditions

$$\frac{\partial\chi_1}{\partial x}=K^2,\quad \frac{\partial^2\chi_1}{\partial x^2}=\tfrac{2}{3}K,\qquad \text{at } =z-K-iK',$$

and $\dfrac{\partial \chi_1}{\partial x} = \frac{1}{3}\mathrm{K}^2 \quad$ at $z = \frac{1}{3}\mathrm{K} - i\mathrm{K}'$.

Putting these values in (19) and in the first integral of (18), we get

$$\mathrm{E} = 0{\cdot}849,\ \mathrm{F} = -5{\cdot}465,\ \mathrm{G} = 4{\cdot}212.$$

The value of $\widehat{xz}$ is now given by

$$\frac{\mathrm{EI}_y}{\mu \mathrm{W}}\widehat{xz} = \frac{\partial \chi_1}{\partial x} - x^2$$

$$= \frac{\sqrt{3}}{8\pi}\int\int [\tfrac{3}{2}\log h + 0{\cdot}3131\, h^{-3/2}]\, dx^2$$

$$-10{\cdot}916\left(\frac{x}{\mathrm{K}}\right)^2 + 15{\cdot}128\left(\frac{x}{\mathrm{K}}\right) - 4{\cdot}212. \quad (20)$$

With the help of Table II. the following table for $\widehat{xz}$ has been constructed :—

TABLE III.

x/K.	$\frac{\mathrm{EI}_y}{\mu \mathrm{W}}\widehat{xz}$.	x/K.	$\frac{\mathrm{EI}_y}{\mu \mathrm{W}}\widehat{xz}$.
$\frac{1}{3}$	0	$\frac{2}{3}$	1·171
$\frac{3}{8}$	0·260	$\frac{17}{24}$	1·151
$\frac{5}{12}$	0·504	$\frac{3}{4}$	1·092
$\frac{11}{24}$	0·710	$\frac{19}{24}$	0·999
$\frac{1}{2}$	0·878	$\frac{5}{6}$	0·868
$\frac{13}{24}$	1·008	$\frac{7}{8}$	0·701
$\frac{7}{12}$	1·100	$\frac{11}{12}$	0·501
$\frac{5}{8}$	1·154	$\frac{23}{24}$	0·266
		1	0

From Table III. it appears that the maximum value of stress over AB occurs near its mid-point. In fig. 2 below we have plotted $\widehat{xz}$ against x.

8. *Value of $\widehat{xz}$ over the Axis of Symmetry.*

In this case $y=0$, and the corresponding values of x and t are given in Table IV.

Fig. 2.

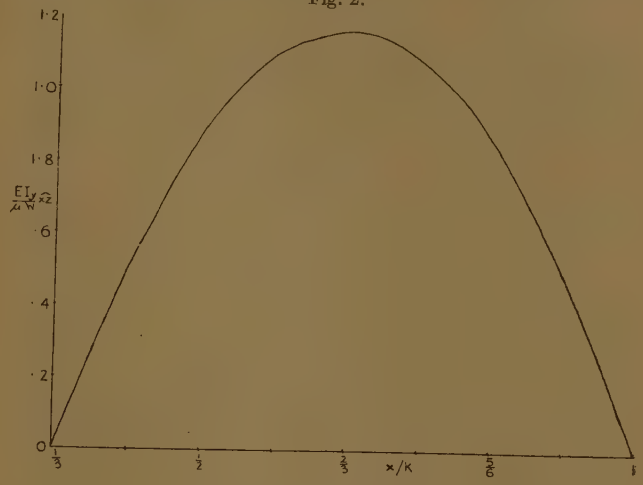

TABLE IV.

x/K.	$-t$.	x/K.	$-t$.
0	0	$\frac{3}{8}$	0·6420
$\frac{1}{24}$	0·0007	$\frac{5}{12}$	0·9895
$\frac{1}{12}$	0·0054	$\frac{11}{24}$	1·5669
$\frac{1}{8}$	0·0184	$\frac{1}{2}$	2·4809
$\frac{1}{6}$	0·0440	$\frac{13}{24}$	4·2139
$\frac{5}{24}$	0·0812	$\frac{7}{12}$	8·6628
$\frac{1}{4}$	0·1567	$\frac{15}{24}$	26·2750
$\frac{7}{24}$	0·2604	$\frac{2}{3}$	$+\infty$
$\frac{1}{3}$	0·4141		

Proceeding as in section 7, we find that $\widehat{xz}$ is given by

$$\frac{EI_y}{\mu W}\widehat{xz} = \frac{\sqrt{3}}{8\pi}\int\int [\tfrac{3}{2}\log h + 0{\cdot}3131\,h^{-3\cdot2}]\,dx^2$$

$$-8{\cdot}043\left(\frac{x}{K}\right)^2 + 4{\cdot}789\left(\frac{x}{K}\right), \quad (21)$$

from which the following table for $\widehat{xz}$ has been obtained :—

TABLE V.

x/K.	$\frac{EI_y}{\mu W}\widehat{xz}$.	x/K.	$\frac{EI_y}{\mu W}\widehat{xz}$.
0	0	$\frac{3}{8}$	0·841
$\frac{1}{24}$	0·191	$\frac{5}{12}$	0·801
$\frac{1}{12}$	0·361	$\frac{11}{24}$	0·734
$\frac{1}{8}$	0·507	$\frac{1}{2}$	0·638
$\frac{1}{6}$	0·628	$\frac{13}{24}$	0·514
$\frac{5}{24}$	0·724	$\frac{7}{12}$	0·365
$\frac{1}{4}$	0·793	$\frac{5}{8}$	0·186
$\frac{7}{24}$	0·836	$\frac{2}{3}$	0
$\frac{1}{3}$	0·852		

In this case, too, the maximum stress occurs near the mid-point of the axis of symmetry. From fig. 3 we can obtain the value of $\widehat{xz}$ for any given value of x on the x-axis.

By drawing straight lines parallel to the x-axis, and proceeding in the manner explained in section 6 (*b*), we can determine the stress at any point within the section;

Fig. 3.

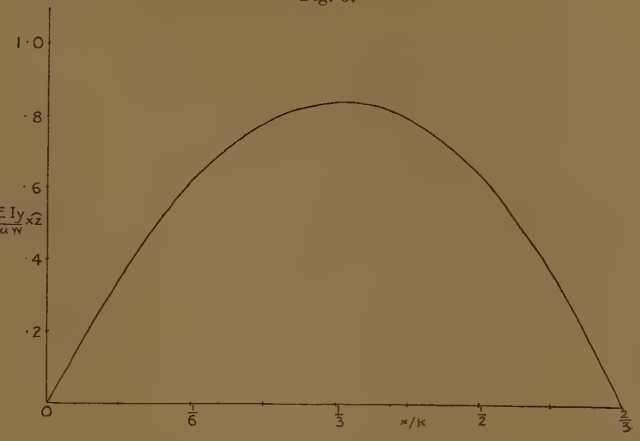

but the arithmetic involved in such cases is too heavy to allow us to discuss them in the present paper.

Hindu College,
Delhi, India.

LXXVI. *Notes on Two-Dimensional Potential Theory.*—II. *Hydrodynamical Problems on the Motion of Cylinders.* *By* Rosa M. Morris, *B.Sc.**

1. IN certain two-dimensional problems in hydrodynamics, it has been the custom for some time to use the complex potential function involving the velocity potential and stream function together. This has been done more especially in cases relating to the streaming of liquid past fixed obstacles which have become of interest in aerodynamical theory. The possibilities of the more general use of the complex function in all two-dimensional potential problems hardly seems to have been realized, and much of the work is still reproduced, either in terms of the potential function or stream function separately. For example, when dealing with cylinders moving in otherwise stationary

* Communicated by Prof. G. H. Livens.

fluids, as the boundary conditions involve only the stream function, most of the solutions are arrived at by employing methods involving the separate evaluation of that function by itself.

In this particular type of problem, of course, the boundaries are not equi-potential surfaces or stream-lines, and the formulation of solutions is not always a simple matter, and, apart from the usual text-book solutions for the elliptical cases and one or two rather artificial problems *, very few examples seem to have been worked out in any detail. Recently, however, Dr. D. M. Wrinch † has worked out the case for the translational and rotational motion of a cylinder in a fluid, when the curve of cross-section of the cylinder is a member of the comprehensive series of curves given by the parametric equations

$$x = a\cos u + \tfrac{1}{2}b\cos 2u,$$
$$y = b\sin u - \tfrac{1}{2}b\sin 2u.$$

Dr. Wrinch introduces the complex potential a good deal in this paper, but does not use it consistently throughout.

A still more general result was given at a much earlier date by J. R. Wilton ‡ in a paper on certain problems in two-dimensional physics, where he has taken the general case of the motion of a cylinder of any form, whose cross-section is defined unicursally, in a fluid at rest at infinity. Here, again, the results are given only in terms of the real velocity and stream functions. This general solution given by Wilton, amongst a series of general solutions of other types of problem, appears, however, to have been entirely overlooked by Dr. Wrinch and subsequent writers.

The object of the present note is to show how much Wilton's general result is simplified by the adoption of the consistent use of the complex potential throughout the discussion, and to show that it includes the solutions of most of the known problems and some others which may be of interest.

* References to the solved cases are given by A. S. Ramsay in his Treatise on Hydromechanics,' pt. ii. chap. iv.

† "Some Problems of Two-dimensional Hydrodynamics," Phil. Mag. vol. xlviii. p. 1089 (1924).

‡ "On the Solution of certain Problems of Two-Dimensional Physics," Phil. Mag. vol. xxx. p. 761 (Dec. 1915).

2. Modifying Wilton's notation somewhat, let us suppose the curve of cross-section of the cylinder is of the form

$$x=x(\xi)\,; \quad y=y(\xi), \quad . \quad . \quad . \quad . \quad . \quad (1)$$

then the transformation

$$x+iy=x(\zeta)+iy(\zeta)$$

or

$$z=z(\zeta),$$

in which $\zeta=\xi+i\eta$ and $x(\zeta)$ and $y(\zeta)$ are real when ζ is real, makes the real axis in the ζ-plane correspond to the curve (1) in the z-plane.

We may therefore take the equation of any analytical boundary in the form

$$z=z(\zeta), \quad \eta=0,$$

or if $\bar{\zeta}=\xi-i\eta$, we have

$$\bar{\zeta}=\zeta$$

on the boundary, which is Wilton's way of expressing the curve.

Let the cylinder be moving with a velocity V in a direction making an angle θ with the x-axis, and let it be rotating with an angular velocity w. Then on the cylinder the stream-function ψ must satisfy the usual condition, viz. :

$$\psi=\mathrm{V}y\cos\theta-\mathrm{V}x\sin\theta-\tfrac{1}{2}w(x^2+y^2),$$

when $\bar{\zeta}=\zeta$.

Now consider the complex potential

$$\Omega=\phi+i\psi=\mathrm{V}e^{-i\theta}z(\zeta)-\tfrac{1}{2}iwz(\zeta)\bar{z}(\zeta)+\mathrm{F}(\zeta),$$

where, for reasons which will appear later, $\mathrm{F}(\zeta)$ is a real function of ζ and is determined from the fact that Ω is nowhere infinite and vanishes at infinity.

With this form for Ω the conjugate potential is

$$\bar{\Omega}=\phi-i\psi=\mathrm{V}e^{+i\theta}z(\bar{\zeta})+\tfrac{1}{2}iwz(\bar{\zeta})\dot{z}(\bar{\zeta})+\mathrm{F}(\bar{\zeta}),$$

assuming F is a real function. By subtraction then we have

$$2i\psi=\mathrm{V}e^{-i\theta}z(\zeta)-\mathrm{V}e^{+i\theta}\bar{z}(\bar{\zeta})$$
$$-\tfrac{1}{2}iw\{z(\zeta)\bar{z}(\zeta)+z(\bar{\zeta})\dot{z}(\bar{\zeta})\}+\mathrm{F}(\zeta)-\mathrm{F}(\bar{\zeta}),$$

which is the equivalent of the form deduced directly by Wilton for the ψ-function. We now see the necessity

for the reality of the function F. The part of ψ depending on it must vanish when $\zeta=\bar{\zeta}$.

Thus on the boundary, when $\zeta=\bar{\zeta}=\xi$ and $z=x+iy$ as defined above,

$$2i\psi=\mathrm{V}e^{-i\theta}(x+iy)-\mathrm{V}e^{+i\theta}(x-iy)-iw(x+iy)(x-iy),$$

$$\psi=\mathrm{V}(y\cos\theta-x\sin\theta)-\tfrac{1}{2}w(x^2+y^2).$$

Thus our general and simple form for Ω satisfies all the conditions, and is, therefore, with the restrictions laid down for F, a solution for the complex potential of the fluid motion round the cylinder.

3. To illustrate the application of our analysis we may consider the case when the cross-section of the cylinder is defined by

$$z=nae^{i\zeta}+be^{-ni\zeta}\;;\quad \eta=0,$$

where $\eta=+\infty$ is infinity in the surrounding liquid and which, when $n=2$, is similar to the case taken by Dr. Wrinch.

With this the formula for Ω contains in the first place the terms

$$na\mathrm{V}e^{-i\theta+i\zeta}+b\mathrm{V}e^{-i\theta-ni\zeta}.$$

The second term contains $e^{+\eta}$ and tends to infinity with η; this term must therefore be removed by taking at least as part of F

$$-b\mathrm{V}e^{-i\theta-ni\zeta}.$$

This, however, is not a real function of ζ, and will not suffice for F—to make it so we add the conjugate of this function, so that then F is

$$-b\mathrm{V}\{e^{-i\theta-ni\zeta}+e^{+i\theta+ni\zeta}\},$$

the additional term securing the reality but reducing to zero at $\eta=\infty$.

The corresponding part of Ω is then

$$na\mathrm{V}e^{-i\theta+i\zeta}-b\mathrm{V}e^{+i\theta+ni\zeta}.$$

Now take the next term in Ω,

$$-\tfrac{1}{2}iwz(\zeta)\bar{z}(\zeta)$$

$$=-\tfrac{1}{2}iw\{nae^{i\zeta}+be^{-ni\zeta}\}\{nae^{-i\zeta}+be^{+ni\zeta}\}$$

$$=-\tfrac{1}{2}iw\{n^2a^2+b^2\}-iwnab\{e^{(n+1)i\zeta}+e^{-(n+1)i\zeta}\}.$$

The last term tends to infinity with η, and we must therefore take at least as part of F

$$iwnabe^{-(n+1)i\zeta},$$

but, as before, this is not a real function of ζ and will not suffice for F—to make it so we add its conjugate and then F is

$$iwnab\{e^{-(n+1)i\zeta}-e^{(n+1)i\zeta}\},$$

the extra term reducing to zero at $\eta=+\infty$.

The corresponding part of Ω, neglecting the constant part, is then

$$-2iwnabe^{(n+1)i\zeta}.$$

Thus, finally,

$$\Omega=naVe^{-i\theta+i\zeta}-bVe^{+i\zeta+ni\zeta}-2iwabe^{(n+1)i\zeta},$$

which is similar to the form obtained by Dr. Wrinch in her solutions.

4. As another general case of probably some practical importance, we can take the cylinder with the thin aerofoil cross-section, defined by

$$z/2a=\cos\zeta+i\epsilon\sin\zeta(1+\cos\zeta)\ ;\quad \eta=0,$$

$\eta=+\infty$ being infinity in the surrounding liquid, and ϵ is small so that we can neglect its square.

With this, the formula for Ω contains, in the first place, the terms

$$2aVe^{-i\theta}\{\cos\zeta+i\epsilon\sin\zeta(1+\cos\zeta)\}$$
$$=aV\{(1+\epsilon)e^{-i\theta+i\zeta}+(1-\epsilon)e^{-i\theta-i\zeta}+\tfrac{1}{2}\epsilon(e^{-i\theta+2i\zeta}-e^{-i\theta-2i\zeta})\}.$$

The second and fourth terms tend to infinity with η, and we must therefore take as F

$$-aV\{(1-\epsilon)e^{-i\theta-i\zeta}-\tfrac{1}{2}\epsilon e^{-i\theta-2i\zeta}+(1-\epsilon)e^{i\theta+i\zeta}-\tfrac{1}{2}\epsilon e^{i\theta+2i\zeta}\},$$

and the corresponding part of Ω is

$$aV\{(1+\epsilon)e^{-i\theta+i\zeta}-(1-\epsilon)e^{i\theta+i\zeta}+\tfrac{1}{2}\epsilon(e^{-i\theta+2i\zeta}+e^{+i\theta+2i\zeta})\}$$
$$=2aV\{e^{i\zeta}(\epsilon\cos\theta-i\sin\theta)+\tfrac{1}{2}\epsilon e^{2i\zeta}\cos\theta\}.$$

The next part of Ω is

$$-\tfrac{1}{2}iwz(\zeta)\bar{z}(\zeta)$$
$$=-2a^2iw\{\cos\zeta+i\epsilon\sin\zeta(1+\cos\zeta)\}$$
$$\times\{\cos\zeta-i\epsilon\sin\zeta(1+\cos\zeta)\},$$

and, neglecting the square of ϵ, this is

$$-a^2iw(1+\cos 2\zeta) = -\tfrac{1}{2}a^2iw(2+e^{2i\zeta}+e^{-2i\zeta}).$$

The third term tends to infinity with η, and so F for this part will be

$$\tfrac{1}{2}a^2iw\{e^{-2i\zeta}-e^{+2i\zeta}\},$$

and the corresponding part of Ω is

$$-a^2iwe^{2i\zeta}.$$

Thus, finally, we have the expression

$$\Omega = 2aV\{e^{i\zeta}(\epsilon\cos\theta - i\sin\theta)+\tfrac{1}{2}\epsilon e^{2i\xi}\cos\theta\}-a^2iwe^{2i\zeta}$$

for the complex potential of the aerofoil in a general motion.

The discussion of the incidence of this formula on general aerodynamic theory will be reserved for a future communication.

Cardiff.
Dec. 1st, 1936.

LXXVII. *Contour Integral Expressions for Bessel Functions.* *By* N. W. McLachlan, *D.Sc.*, *and* A. L. Meyers, *B.Sc.*, *A.M.I.E.E.**

1. *Functions of the Second Kind.*

THE contour integrals

$$J_\nu(t) = \frac{(\frac{1}{2}t)^\nu}{2\pi i}\int_{-\infty}^{(0+)} e^{z-t^2/4z}\frac{dz}{z^{\nu+1}}, \quad . \quad . \quad . \quad (1)$$

and

$$I_\nu(t) = \frac{(\frac{1}{2}t)^\nu}{2\pi i}\int_{-\infty}^{(0+)} e^{z+t^2/4z}\frac{dz}{z^{\nu+1}}, \quad . \quad . \quad . \quad (2)$$

in which no restriction is imposed on either t or ν, are well known†. The contour, which we shall denote by L′, is a loop round the negative side of the real axis considered as a barrier, as shown in fig. 1. The above integrals

* Communicated by the Authors.

† Gray, Mathews, and MacRobert, ' Treatise on Bessel Functions, p. 53 (1922).

are still valid if the barrier, with the contour round it, occupies any angular position in the range $(\frac{1}{2}\pi+\alpha)$ to $(\frac{3}{2}\pi-\beta)$, where $\alpha, \beta>0$. In general, a contour passing to the right of all the singularities of the integrand, cutting

Fig. 1.

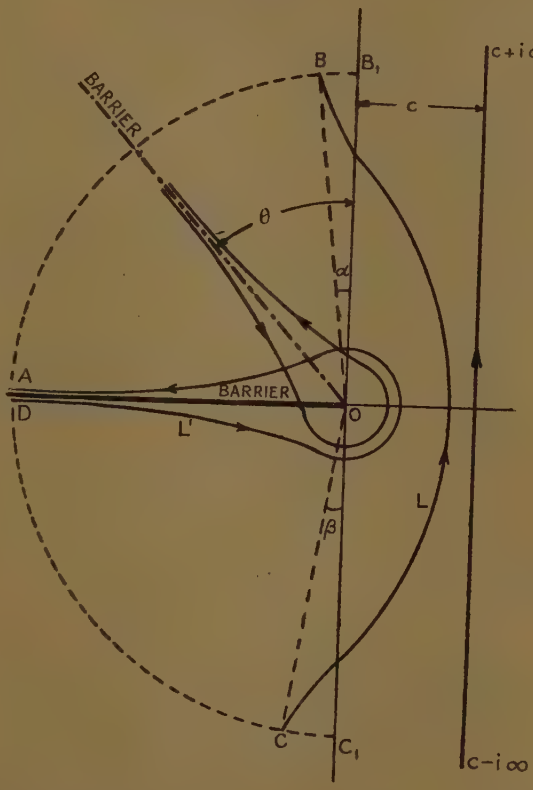

the imaginary axis and extending to infinity in the second and third quadrants, the angles α, β being >0, will be regarded as an L-type contour * (see fig. 1). If the path round the barrier encloses all the singularities of the integrand, and if the integrals along the infinite

* H. Jeffreys, 'Operational Methods in Mathematical Physics,' 2nd ed. p. 29 (1931).

arcs AB, CD vanish, then the L and L′ paths are equivalent. The necessary restrictions on t are treated in the Appendix : ν is restricted to be non-integral, n being used to signify integers.

Weber's Bessel function of the second kind is defined to be

$$\mathrm{Y}_\nu(t) = \frac{1}{\sin \nu\pi}[\cos \nu\pi \mathrm{J}_\nu(t) - \mathrm{J}_{-\nu}(t)] \quad . \quad . \quad . \quad (3)$$

if ν is non-integral, and as the limit of (3) when $\nu \to n$. Substituting from (1) in (3), we obtain

$$\mathrm{Y}_\nu(t) = \frac{1}{\sin \nu\pi} \cdot \frac{1}{2\pi i} \int_{\mathrm{L}} e^{z - t^2/4z}[\cos \nu\pi (2z/t)^{-\nu} - (2z/t)^{\nu}] \frac{dz}{z}, \quad (4)$$

where L signifies either the L′ or L contours throughout the paper. If $\nu = n$, (4) degenerates to the indeterminate form 0/0, so differentiating with respect to ν and proceeding to the limit $\nu \to n$, we get

$$\mathrm{Y}_n(t) = \frac{-1/\pi}{2\pi i} \int_{\mathrm{L}} e^{z - t^2/4z}[(2z/t)^{-n} + (-1)^n (2z/t)^n] \log (2z/t) \frac{dz}{z} .$$

$$. \quad . \quad . \quad (5)$$

In particular, we have

$$\mathrm{Y}_0(t) = \frac{-2/\pi}{2\pi i} \int_{\mathrm{L}} e^{z - t^2/4z} \log (2z/t) \frac{dz}{z} . \quad . \quad . \quad (6)$$

The modified Bessel function of the second kind is defined to be

$$\mathrm{K}_\nu(t) = \frac{\pi/2}{\sin \nu\pi}[\mathrm{I}_{-\nu}(t) - \mathrm{I}_\nu(t)], \quad . \quad . \quad . \quad (7)$$

if ν is non-integral, and as the limit of (7) when $\nu \to n$. Proceeding in the manner indicated above, we find that

$$\mathrm{K}_\nu(t) = \frac{\pi/2}{\sin \nu\pi} \cdot \frac{1}{2\pi i} \int_{\mathrm{L}} e^{z + t^2/4z}[(2z/t)^{\nu} - (2z/t)^{-\nu}] \frac{dz}{z}, \quad . \quad (8)$$

$$\mathrm{K}_n(t) = \frac{(-1)^n/2}{2\pi i} \int_{\mathrm{L}} e^{z + t^2/4z}[(2z/t)^n + (2z/t)^{-n}] \log (2z/t) \frac{dz}{z},$$

$$. \quad . \quad . \quad (9)$$

$$\mathrm{K}_0(t) = \frac{1}{2\pi i} \int_{\mathrm{L}} e^{z + t^2/4z} \log (2z/t) \frac{dz}{z} \quad . \quad . \quad . \quad . \quad . \quad . \quad . \quad (10)$$

Differentiating (10) with respect to t gives

$$-\mathrm{K}_0'(t) = \mathrm{K}_1(t) = -\frac{1}{2\pi i}\int_{\mathrm{L}} e^{z+t^2/4z}[(t/2z)\log(2z/t) - 1/t]\frac{dz}{z}, \quad \ldots \quad (10a)$$

From (9), by substituting $n=1$, we get

$$\mathrm{K}_1(t) = \frac{-1/2}{2\pi i}\int_{\mathrm{L}} e^{z+t^2/4z}[(2z/t)+(t/2z)]\log(2z/t)\frac{dz}{z}, \quad (10b)$$

so that (10a) and (10b) are identical *. The Y-function can be treated in like manner, using (5) and (6). The variable t is unrestricted in (4) to (6) and (8) to (12) inclusive.

If we replace z in the above integrals by $\frac{1}{2}tz$, then on L′, which has the negative half of the real axis as a barrier, the real part of t must be positive, whilst on the L-path, t must be real and positive. This is explained in detail in the Appendix. We obtain the following results :

$$\mathrm{Y}_\nu(t) = \frac{1}{\sin\nu\pi}\cdot\frac{1}{2\pi i}\int_{\mathrm{L}} e^{t(z-1/z)/2}[z^{-\nu}\cos\nu\pi - z^{\nu}]\frac{dz}{z}, \quad (11)$$

$$\mathrm{Y}_n(t) = \frac{-1/\pi}{2\pi i}\int_{\mathrm{L}} e^{t(z-1/z)/2}[z^{-n}+(-1)^n z^n]\log z\frac{dz}{z}, \quad (12)$$

and

$$\mathrm{Y}_0(t) = \frac{-2/\pi}{2\pi i}\int_{\mathrm{L}} e^{t(z-1/z)/2}\log z\frac{dz}{z}. \quad \ldots \quad (13)$$

Also

$$\mathrm{K}_\nu(t) = \frac{(\pi/2\sin\nu\pi)}{2\pi i}\int_{\mathrm{L}} e^{t(z+1/z)/2}[z^{\nu}-z^{-\nu}]\frac{dz}{z}, \quad \ldots \quad (14)$$

$$\mathrm{K}_n(t) = \frac{(-1)^n/2}{2\pi i}\int_{\mathrm{L}} e^{t(z+1/z)/2}[z^n+z^{-n}]\log z\frac{dz}{z}, \quad \ldots \quad (15)$$

and

$$\mathrm{K}_0(t) = \frac{1}{2\pi i}\int_{\mathrm{L}} e^{t(z+1/z)/2}\log z\frac{dz}{z}. \quad \ldots \quad (16)$$

From (1) [putting $\nu=0$ and writing $\frac{1}{2}tz$ for z] and (13),

* Proved in § 3.

we get integrals for the Hankel functions of zero order, namely,

$$H_0^{(1)}(t) = \frac{1}{2\pi i}\int_L e^{t(z-1/z)/2}\left(1-\frac{2i}{\pi}\log z\right)\frac{dz}{z}, \quad . \quad (17^*)$$

and

$$H_0^{(2)}(t) = \frac{1}{2\pi i}\int_L e^{t(z-1/z)/2}\left(1+\frac{2i}{\pi}\log z\right)\frac{dz}{z}, \quad . \quad (18^*)$$

t being restricted as at (11).

To write some of the foregoing integrals in a different form, which we shall need in order to obtain results in another paper, to be published later, we transform them to the ζ-plane by the substitution

$$z = t[\zeta + \sqrt{\zeta^2+a^2}]/2 = t\psi/2,$$

in integrals (4) to (6), and by

$$z = t[\zeta + \sqrt{\zeta^2-a^2}]/2 = t\chi/2,$$

in integrals (8) to (10), a being an unrestricted constant. The conditions pertaining to these substitutions are considered in the Appendix. Using these transformations and replacing ζ by z thereafter, we obtain the following integrals :

$$Y_\nu(at) = \frac{1}{\sin\nu\pi}\cdot\frac{1}{2\pi i}\int_L e^{zt}[(\psi/a)^{-\nu}\cos\nu\pi - (\psi/a)^\nu]\,dz/\sqrt{z^2+a^2}, \quad . \quad . \quad . \quad (19)$$

$$Y_n(at) = \frac{-1/\pi}{2\pi i}\int_L e^{zt}[(\psi/a)^{-n} + (-1)^n(\psi/a)^n]\log(\psi/a)\,dz/\sqrt{z^2+a^2}, \quad (20)$$

$$Y_0(at) = \frac{-2/\pi}{2\pi i}\int_L e^{zt}\log(\psi/a)\,dz/\sqrt{z^2+a^2}, \quad . \quad . \quad . \quad . \quad (21)$$

Also

$$K_\nu(at) = \frac{\pi/2\sin\nu\pi}{2\pi i}\int_L e^{zt}[(\chi/a)^\nu - (\chi/a)^{-\nu}]\,dz/\sqrt{z^2-a^2}, \quad . \quad (22)$$

$$K_n(at) = \frac{(-1)^n/2}{2\pi i}\int_L e^{zt}[(\chi/a)^n + (\chi/a)^{-n}]\log(\chi/a)\,dz/\sqrt{z^2-a^2}, \quad . \quad . \quad . \quad (23)$$

* For unrestricted t,

$$H_0^{(1)(2)}(t) = \frac{1}{2\pi i}\cdot\int_L e^{z-t^2/4z}\left[1\mp\frac{2i}{\pi}\log\left(\frac{2z}{t}\right)\right]\frac{dz}{z},$$

from (1) and (6).

and

$$K_0(at) = \frac{1}{2\pi i}\int_L e^{zt}\log(\chi/a)\,dz/\sqrt{z^2-a^2}. \quad . \quad . \quad . \quad . \quad . \quad (24)$$

In integrals (19) to (24) inclusive $R(t)>0$ on L′ and t must be real and positive on L.

2. *Ber, Bei, Ker, and Kei Functions.*

Writing $ti^{3/2}$ for t in (1), we get

$$J_\nu(ti^{3/2}) = \mathrm{ber}_\nu t + i\,\mathrm{bei}_\nu t = \frac{(t/2)^\nu}{2\pi i}\int_L e^{z+\frac{it^2}{4z}+3\nu\pi i/4}\,dz/z^{\nu+1}.$$

$$. \quad . \quad . \quad (25)$$

Equating real and imaginary parts, we find that

$$\mathrm{ber}_\nu t = \frac{(t/2)^\nu}{2\pi i}\int_L e^z\cos[(t^2/4z)+(3\nu\pi/4)]\,dz/z^{\nu+1}, \quad (26)$$

and

$$\mathrm{bei}_\nu t = \frac{(t/2)^\nu}{2\pi i}\int_L e^z\sin[(t^2/4z)+(3\nu\pi/4)]\,dz/z^{\nu+1}, \quad (27)$$

there being no restrictions on t. Writing $\frac{1}{2}zt$ for z in (26), (27), $R(t)>0$ on the L′ contour, t being real and positive on the L contour, we obtain

$$\mathrm{ber}_\nu t = \frac{1}{2\pi i}\int_L e^{zt/2}\cos[(t/2z)+(3\nu\pi/4)]\,dz/z^{\nu+1}, \quad (28)$$

$$= \frac{(t/2)^{-\nu}}{2\pi i}\int_L e^{zt^2/4}\cos[(1/z)+(3\nu\pi/4)]\,dz/z^{\nu+1}, \quad (29)$$

and

$$\mathrm{bei}_\nu t = \frac{1}{2\pi i}\int_L e^{zt/2}\sin[(t/2z)+(3\nu\pi/4)]\,dz/z^{\nu+1}, \quad . \quad (30)$$

$$= \frac{(t/2)^{-\nu}}{2\pi i}\int_L e^{zt^2/4}\sin[(1/z)+(3\nu\pi/4)]\,dz/z^{\nu+1}. \quad (31)$$

Integrals (29) and (31) are obtained by writing $zt/2$ for z in (28) and (30), so the restrictions are $R(t^2)>0$ on L′ and t^2 real and positive on L.

If in (1) we write $z=t\psi/2$ with $a=i^{3/2}$, then

$$J_\nu(ti^{3/2}) = \mathrm{ber}_\nu t + i\,\mathrm{bei}_\nu t = \frac{i^{3\nu/2}}{2\pi i}\int_L e^{zt}\,dz/\xi^\nu\sqrt{z^2-i}, \quad (32)$$

$$\text{where } \xi = z+\sqrt{z^2-i},$$

with restrictions on t as at (24); and in particular,

$$\text{ber } t+i \text{ bei } t = \frac{1}{2\pi i}\int_L e^{zt}\, dz/\sqrt{z^2-i}. \quad . \quad . \quad (33)$$

Writing $2(ti^3)^{1/2}$ for t in (1), yields

$$J_\nu(2t^{1/2}i^{3/2}) = \frac{(ti^3)^{\nu/2}}{2\pi i}\int_L e^{z+it/z}\, dz/z^{\nu+1}, \quad . \quad . \quad (34)$$

there being no restriction on t.

Substituting zt for z in (34), where $R(t)>0$ for L′ and t is real and positive for L,

$$J_\nu(2t^{1/2}i^{3/2}) = \frac{(i^3/t)^{\nu/2}}{2\pi i}\int_L e^{zt+i/z}\, dz/z^{\nu+1}, \quad . \quad . \quad (35)$$

giving

$$t^{\nu/2}\,\text{ber}_\nu\,(2t^{1/2}) = \frac{1}{2\pi i}\int_L e^{zt}\cos\,[(1/z)+(3\nu\pi/4)]\, dz/z^{\nu+1}, \quad (36)$$

and

$$t^{\nu/2}\,\text{ber}_\nu\,(2t^{1/2}) = \frac{1}{2\pi i}\int_L e^{zt}\sin\,[(1/z)+(3\nu\pi/4)]\, dz/z^{\nu+1}. \quad (37)$$

Integrating

$$f(t) = \frac{1}{2\pi i}\int_L e^{zt}\sum_{r=0}^{\infty}\frac{(t/4z)^{\nu+2r}}{r\,!\,\Gamma(\nu+r+1)}\cdot\frac{dz}{z}, \quad . \quad . \quad (38)$$

term by term, yields

$$f(t) = \sum_{r=0}^{\infty}(t/2)^{2\nu+2r}/[r\,!\,\Gamma(\nu+r+1)\Gamma(\nu+2r+1)], \quad (39)$$

$$= \text{ber}_\nu^2\, t+\text{bei}_\nu^2\, t,$$

so

$$\text{ber}_\nu^2\, t+\text{bei}_\nu^2\, t = \frac{1}{2\pi i}\int_L e^{zt}I_\nu(t/2z)\, dz/z. \quad . \quad . \quad (40)$$

If in (38) we commence with $(1/4z)$ instead of $(t/4z)$, we get

$$\text{ber}_\nu^2\, t^{1/2}+\text{bei}_\nu^2\, t^{1/2} = \frac{1}{2\pi i}\int_L e^{zt}I_\nu(1/2z)\, dz/z. \quad . \quad (41)$$

Writing $a=i^{1/2}$ in (22) yields, for $R(t)>0$ on L′ and t real and positive on L,

$$i^{-\nu}K_\nu(ti^{1/2}) = \text{ker}_\nu\, t+i\,\text{kei}_\nu\, t, \quad . \quad . \quad . \quad . \quad . \quad . \quad . \quad . \quad (42)$$

$$= \frac{(\pi i^{-3\nu/2}/2\sin\nu\pi)}{2\pi i}\int_L e^{zt}[\xi^\nu - i^\nu\xi^{-\nu}]\, dz/\sqrt{z^2-i}.$$

$$. \quad . \quad . \quad (43)$$

Proceeding to the limit $\nu \to n$, we find that

$$i^{-n}\mathrm{K}_n(ti^{1/2}) = \ker_n t + i\,\mathrm{kei}_n t,$$

$$= \frac{(i^{n/2}/2)}{2\pi i}\int_{\mathrm{L}} e^{zt}[\xi^n + i^n\xi^{-n}]\log(\xi/i^{1/2})\,dz/\sqrt{z^2-i}, \quad . \; . \; . \quad (44)$$

and in particular, when $n=0$,

$$\mathrm{K}_0(ti^{1/2}) = \ker t + i\,\mathrm{kei}\,t = \frac{1}{2\pi i}\int_{\mathrm{L}} e^{zt}\log(\xi/i^{1/2})\,dz/\sqrt{z^2-i}, \quad . \; . \; . \quad (45)$$

the restrictions being $\mathrm{R}(t)>0$ on L′, t being real and positive on L.

3. *Integrals of the Type $f(t)/t$.*

From a recurrence formula, we have

$$\nu \mathrm{J}_\nu(at)/at = [\mathrm{J}_{\nu-1}(at) + \mathrm{J}_{\nu+1}(at)]/2. \quad . \; . \quad (46)$$

Using (1) and the substitution

$$z = t[\zeta + \sqrt{\zeta^2+a^2}]/2 = t\psi/2,$$

and replacing ζ by z thereafter, (46) can be written

$$\nu \mathrm{J}_\nu(at)/t = \frac{a^\nu}{2\pi i}\int_{\mathrm{L}} e^{zt}\,dz/\psi^\nu, \quad . \; . \; . \; . \quad (47)$$

the restrictions being as at (24) above. Formula (47) can also be obtained by partial integration in the following way :—

Using the preceding substitution in (1), we get

$$\mathrm{J}_\nu(at) = \frac{a^\nu}{2\pi i}\int_{\mathrm{L}} e^{zt}\,dz/\psi^\nu\sqrt{z^2+a^2} = \frac{a^\nu}{2\pi i}\int_{\mathrm{L}} e^{zt}\,d\psi/\psi^{\nu+1}, \quad (48)$$

$$= 0 - \frac{a^\nu}{2\pi i}\int_{\mathrm{L}} \frac{e^{zt}}{\psi^\nu}[t - (\nu+1)/\sqrt{z^2+a^2}]\,dz, \quad . \; . \quad (49)$$

$$= -\frac{a^\nu t}{2\pi i}\int_{\mathrm{L}} e^{zt}\,dz/\psi^\nu + (\nu+1)\mathrm{J}_\nu(at), \; . \; . \; . \; . \quad (50)$$

from which formula (47) follows immediately.

Rewriting (47) as

$$\mathrm{J}_\nu(at)/ta^\nu = \frac{1/\nu}{2\pi i}\int_{\mathrm{L}} e^{zt}dz/\psi^\nu, \quad . \; . \; . \; . \quad (51)$$

this takes the indeterminate form 0/0 when $\nu=0$. Differentiating with respect to ν, and proceeding to the limit $\nu\to 0$, we find that

$$J_0(at)/t = -\frac{1}{2\pi i}\int_L e^{zt}\log\psi\, dz, \qquad t>0. \quad (52)$$

Writing $a\sqrt{t^2-c^2}$ for t in (1), yields

$$J_\nu(a\sqrt{t^2-c^2}) = (a/2)^\nu(t^2-c^2)^{\nu/2}\cdot\frac{1}{2\pi i}\int_L e^{z-a^2(t^2-c^2)/4z}\, dz/z^{\nu+1}. \quad . \quad . \quad . \quad (53)$$

In (53), substitute

$$z=(t-c)[\zeta+\sqrt{\zeta^2+a^2}]/2,$$

t and c both being real and positive for the L contour ($t>c$), and $R(t-c)>0$ for L′, then

$$[(t-c)/(t+c)]^{\nu/2}J_\nu(a\sqrt{t^2-c^2}) = \frac{a^\nu}{2\pi i}\int_L e^{zt-c\sqrt{z^2+a^2}}\, dz/\psi^\nu\sqrt{z^2+a^2}. \quad (54)$$

Formula (54) can also be derived by partial integration, as exemplified in (48)–(50).

For the modified Bessel function of the first kind, we have

$$\nu I_\nu(at)/t = \frac{a^\nu}{2\pi i}\int_L e^{zt}\, dz/\chi^\nu, \quad . \quad . \quad . \quad . \quad (55)$$

$$I_0(at)/t = \frac{-1}{2\pi i}\int_L e^{zt}\log\chi\, dz, \quad . \quad . \quad . \quad (56)$$

with restrictions as at (24) above, and

$$[(t-c)/(t+c)]^{\nu/2}I_\nu(a\sqrt{t^2-c^2}) = \frac{a^\nu}{2\pi i}\int_L e^{zt-c\sqrt{z^2-a^2}}\, dz/\chi^\nu\sqrt{z^2-a^2}, \quad (57)$$

the restrictions at (54) being applicable.

We shall now confirm that (10 *a*) and (10 *b*) are identical. To do this we have to show that

$$\frac{1}{2\pi i}\int_L e^{z+t^2/4z}\{[(t/2z)-(2z/t)]\log(2z/t)-2/t\}\, dz/z = 0, \quad (58)$$

or that

$$\frac{1}{2\pi i}\int_L e^{z+tz/4z}[(t/2z)-(2z/t)]\log(2z/t)\,dz/z$$

$$= \frac{2/t}{2\pi i}\int_L e^{z+tz/4z}\,dz/z \quad (59)$$

$$= 2I_0(t)/t, \quad . \quad . \quad . \quad (60)$$

from (2) above. Substituting $z=t[\zeta+\sqrt{\zeta^2-1}]/2$ in the first integral in (59), and writing z for ζ thereafter, we get

$$\frac{-2}{2\pi i}\int_L e^{zt}\log(z+\sqrt{z^2-1})\,dz, \quad . \quad . \quad . \quad (61)$$

and from (56), when $a=1$, this is seen to be equal to (60), so the identity of (10 *a*) and (10 *b*) has been confirmed.

It is found from (3) and (47) that

$$\nu Y_\nu(at)/t = \frac{1}{\sin\nu\pi}\cdot\frac{1}{2\pi i}\int_L e^{zt}[(\psi/a)^\nu+\cos\nu\pi(\psi/a)^{-\nu}]\,dz, \quad (62)$$

$$Y_n(at)/t = \frac{1/n\pi}{2\pi i}\int_L e^{zt}[(-1)^n(\psi/a)^n-(\psi/a)^{-n}]\log(\psi/a)\,dz,$$

$$. \quad . \quad . \quad (63)$$

and

$$Y_0(at)/t = \frac{1/\pi}{2\pi i}\int_L e^{zt}[\{\log(\psi/a)\}^2-\tfrac{1}{2}\pi^2]\,dz, \quad . \quad . \quad . \quad . \quad (64)$$

$$= \frac{1/\pi}{2\pi i}\int_L e^{zt}\{\log(\psi/a)\}^2\,dz, \quad . \quad . \quad . \quad . \quad . \quad . \quad (65)$$

From (7) and (55), we get

$$\nu K_\nu(at)/t = \frac{-\pi/2}{\sin\nu\pi}\cdot\frac{1}{2\pi i}\int_L e^{zt}[(\chi/a)^\nu+(\chi/a)^{-\nu}]\,dz, \quad . \quad . \quad (66)$$

$$K_n(at)/t = \frac{(-1)^{n+1}/2n}{2\pi i}\int_L e^{zt}[(\chi/a)^n-(\chi/a)^{-n}]\log(\chi/a)\,dz,$$

$$. \quad . \quad . \quad (67)$$

and

$$K_0(at)/t = \frac{-1/2}{2\pi i}\int_L e^{zt}\{\log(\chi/a)\}^2\,dz, \quad . \quad . \quad . \quad . \quad . \quad (68)$$

the restrictions on t in (62)–(68) inclusive being the same as at (24). Using (54) and (57) integrals of like type can be found for the Y_ν and K_ν functions.

Substituting $a=i^{3/2}$ in (47), gives

$$\nu(\mathrm{ber}_\nu t+i\ \mathrm{bei}_\nu t)/t=\frac{i^{3\nu/2}}{2\pi i}\int_{\mathrm{L}} e^{zt}\,dz/\xi^\nu, \quad . \quad . \quad (69)$$

with restrictions on t as at (24).

Proceeding to the limit $\nu\to 0$, or from (52),

$$(\mathrm{ber}\ t+i\ \mathrm{bei}\ t)/t=\frac{-1}{2\pi i}\int_{\mathrm{L}} e^{zt}\log\left[\xi i^{-3/2}\right]dz \quad . \quad (70)$$

$$=\frac{-1}{2\pi i}\int e^{zt}\log\xi\,dz, \quad . \quad . \quad . \quad (71)$$

the restrictions being those given below (24).

Substituting $a=i^{1/2}$ in (66), gives

$$\nu\,(\mathrm{ker}_\nu t+i\ \mathrm{kei}_\nu t)/t=-\frac{\pi i^{-3\nu/2}/2\sin\nu\pi}{2\pi i}\int_{\mathrm{L}} e^{zt}\left[\xi^\nu+i^\nu\xi^{-\nu}\right]dz,$$

$$. \quad . \quad . \quad (72)$$

$$n(\mathrm{ker}_n t+i\ \mathrm{kei}_n t)/t$$

$$=\frac{-(i^{n/2}/2)}{2\pi i}\int_{\mathrm{L}} e^{zt}\left[\xi^n-i^n\xi^{-n}\right]\log\left(\xi i^{-1/2}\right)dz, \quad (73)$$

and

$$(\mathrm{ker}\ t+i\ \mathrm{kei}\ t)/t=\frac{-1/2}{2\pi i}\int_{\mathrm{L}} e^{zt}\left\{\log\left(\xi i^{-1/2}\right)\right\}^2 dz, \quad . \quad (74)$$

the restrictions being $\mathrm{R}(t)>0$ on L′ and t real positive on L. Integrals for the ber, bei, ker, and kei functions can also be obtained from (54) and (57).

Appendix.

1. *The Contour $c-i\infty$ to $c+i\infty$.*

This has not been used in this paper owing to restrictions imposed upon some integrals, whilst others are not valid on the contour. The restrictions for those which hold on this contour are as follows :

$\mathrm{J}_\nu(t)$, $\mathrm{I}_\nu(t)$, $\mathrm{ber}_\nu(t)$, $\mathrm{bei}_\nu(t)$, $\mathrm{R}(\nu)>-1$;

$\mathrm{Y}_\nu(t)$, $\mathrm{K}_\nu(t)$, $\mathrm{ker}_\nu(t)$, $\mathrm{kei}_\nu(t)$, $1>\mathrm{R}(\nu)>-1$;

$\mathrm{J}_\nu(t)/t$, $\mathrm{I}_\nu(t)/t$, $(\mathrm{ber}_\nu t+i\ \mathrm{bei}_\nu t)/t$, $\mathrm{R}(\nu)>0$.

2. *Transformation of Contours.*

The various transformations will be considered with respect to integral (1) in the paper, upon which the other integrals are based.

(*a*) The transformation

$$z = t\zeta, \quad . \quad . \quad . \quad . \quad . \quad . \quad . \quad . \quad (1)$$

where it is desired to find the restrictions to be imposed on t considered as a complex constant. This transformation applied to the integral in question gives, using the argument at for greater generality,

$$J_\nu(at) = \frac{(a/2)^\nu}{2\pi i} \int_L e^{t(\zeta - a^2/4\zeta)} \zeta^{-\nu-1} \, d\zeta. \quad . \quad . \quad . \quad (2)$$

We have to determine the restrictions on t so that: (i.) the integral (2) vanishes along the infinite arcs AB, CD of fig. 1, thereby making the L and L′ paths equivalent; (ii.) an L′ type contour in the z-plane transforms into a similar contour in the ζ-plane. Condition (i.) is not needed for the L′ path *alone*. For this condition to hold, ζt must be negative, so its phase angle must lie between $(\pi/2)+\alpha$ and $(3\pi/2)-\beta$, α, $\beta>0$. Since on the infinite arcs the phase angle of ζ lies within these limits, it follows that t must be real and positive on the L-path. This being so, it is obvious that the second condition is fulfilled also. Since the barrier in fig. 1 can occupy any angular position within the preceding angle range of ζ, the restriction upon t for the L′ path is that $R(t)>0$.

(*b*) The transformation

$$\left.\begin{aligned} z &= t[\zeta + \sqrt{\zeta^2 + a^2}]/2, \\ \text{or} \quad \zeta t &= z - a^2 t^2/4z, \end{aligned}\right\} \quad . \quad . \quad . \quad . \quad . \quad (3)$$

where a is an unrestricted complex constant. When applied to the integral (1), we get

$$J_\nu(at) = \frac{a^\nu}{2\pi i} \int_L e^{\zeta t} \, d\zeta / (\zeta + \sqrt{\zeta^2 + a^2})^\nu \sqrt{\zeta^2 + a^2}, \quad . \quad (4)$$

and it is desired to find the restriction on t for the above conditions to be satisfied. When $|z|$ and, therefore, $|\zeta|$ is large, the first formula in (3) can be written

$$z \sim \zeta t, \quad . \quad . \quad . \quad . \quad . \quad . \quad . \quad . \quad (5)$$

and since all the contours can be drawn to satisfy (5), this case reduces to that already considered. Hence, on the L′ contour $R(t)>0$, whilst on the L contour t must be real and positive, there being no restrictions on a in either case.

(*c*) The transformation

$$\left.\begin{aligned} z &= t[\zeta+\sqrt{\zeta^2-a^2}]/2, \\ \zeta t &= z+a^2t^2/4z, \end{aligned}\right\} \quad \ldots\ldots \quad (6)$$

is obviously a modification of (*b*), in which a is replaced by ia, so the restrictions on t are the same in both cases.

Owing to the type of L contour used herein, there is no restriction on ν in any of the formulæ, except that it is non-integral. If, however, the more usual L contour, namely, $c-i\infty$ to $c+i\infty$ $(c>0)$ were used, then the restrictions on ν mentioned above are needed to make the contributions to the integrals vanish on those parts of the infinite arcs at each side of the imaginary axis, which subtend small angles at the origin, *i. e.*, BB_1, CC_1, and the corresponding parts on the positive side.

LXXVIII. *The Motions of Electrons in a Gas in the Presence of Variable Electric Fields and a Constant Magnetic Field.* *By* V. A. Bailey, *M.A., D.Phil.(Oxon), F.Inst.P., Professor of Experimental Physics, University of Sydney**.

1. *Introduction.*

In a number of different branches of Physics it is often necessary to determine theoretically the motions of electrons in a gas under the influence of electric and magnetic forces, separate or combined; for example, in the study of high-frequency discharges through gases, the propagation and interaction of radio-waves, and the effects of electric storms on the atmosphere.

It is therefore desirable to have available a general theory of such motions from which the different particular cases may be immediately derived with relatively little labour.

The electric and magnetic fields considered are uniform in space, but in certain circumstances the results are applicable with very little error to the fields which constitute electric waves.

In this communication the general theory is followed by particular examples of its application which illustrate

* Communicated by the Author.

it, and allow its correctness to be tested by comparison with previously known results.

2. *The Mean Work w done on an Electron per Collision.*

The total electric field considered here is of a very general character, and is taken to be the resultant of any number of components having different amplitudes, directions, frequencies *, and damping.

Thus by Fourier's theorem the theory given here also includes alternating fields of non-sinoidal type.

The principal symbols † used are defined in the following table :

Notation.

e=electric charge of an electron in e.s.u. $=-4{\cdot}8\times10^{-10}$.

m=mass of an electron in grams.

$\sigma=-e/m=5{\cdot}3\times10^{17}$,

$\tau=e^2/m=2{\cdot}54\times10^{8}$.

$\mathrm{H}\breve{h}$=constant magnetic field vector, where $\breve{h}$ is a unit vector.

$\Omega=\mathrm{H}\sigma/c$, $\breve{\Omega}=\Omega\breve{h}$.

$\mathrm{E}_n\breve{n}$=amplitude of a component of the electric field $\breve{\mathrm{E}}$, where $\breve{n}$ is a unit vector.

$\breve{\mathrm{E}}=\sum_n \mathrm{E}_n\breve{n}\mathrm{T}_n$, where T_n is a function of the time t.

$\mathrm{Z}_n=\mathrm{E}_n/\sqrt{2}$.

ω_n=angular frequency of T_n.

ϕ_n=phase angle of T_n.

ν_n=damping coefficient of T_n.

$\breve{u}$=mean velocity of a group of electrons.

ν=collision frequency of an electron.

w=mean work done on an electron per collision, at the time t.

$\bar{w}$=average value of w taken over the longest period.

$\partial=\mathrm{D}+\nu$, where $\mathrm{D}=d/dt$.

$$\mathrm{S}=\frac{1}{\partial-i\breve{\Omega}},\quad \mathrm{S}'=\frac{1}{\partial+i\breve{\Omega}}.$$

$c_{mn}=\breve{m}\breve{n}$, $s_{mn}=\mathrm{V}\breve{m}\breve{n}$, where $\breve{m}$ and $\breve{n}$ are unit vectors.

* These may include the frequency zero to correspond to a constant electric field.

† Vectors are represented by letters with curly bars over them, and vector products are indicated by an immediately preceding letter V.

We define a collision between an electron and a molecule as an event in which, on the average, the electron loses all its momentum in any specified direction. Thus the mean loss of momentum per second by an electron is $\nu m\breve{u}$.

The equation of mean motion of an electron is therefore

$$\partial\breve{u} = -\sigma\breve{E} + V\breve{\Omega}\breve{u}. \quad . \quad . \quad . \quad . \quad . \quad (1)$$

On multiplying this by $\breve{\Omega}$ vectorially and scalarly we get respectively

$$\partial V\breve{\Omega}\breve{u} = -\sigma V\breve{\Omega}\breve{E} - \Omega^2\breve{u} + (\breve{\Omega}\breve{u})\breve{\Omega}$$

and

$$\partial(\breve{\Omega}\breve{u}) = -\sigma\breve{\Omega}\breve{E},$$

from which it follows that

$$\partial^2 V\breve{\Omega}\breve{u} = -\partial\sigma V\breve{\Omega}\breve{E} - \partial\Omega^2\breve{u} - \sigma(\breve{\Omega}\breve{E})\breve{\Omega}.$$

Operating on (1) with ∂^2, and using this last result, (1) becomes

$$\partial^3\breve{u} = -\partial^2\sigma\breve{E} - \partial\sigma V\breve{\Omega}\breve{E} - \partial\Omega^2\breve{u} - \sigma(\breve{\Omega}\breve{E})\breve{\Omega},$$

i.e.,

$$-\partial(\partial^2+\Omega^2)\breve{u}/\sigma = \partial^2\breve{E} + \partial\Omega V\breve{h}\breve{E} + \Omega^2\breve{h}(\breve{h}\breve{E}). \quad . \quad (2)$$

The Particular Integral of (2) is $\breve{U}$, where

$$-\breve{U}/\sigma = P\breve{E} + QV\breve{h}\breve{E} + R\breve{h}(\breve{h}\breve{E}), \quad . \quad . \quad . \quad (3)$$

where

$$\left.\begin{aligned} 2P &= \frac{2\partial}{\partial^2+\Omega^2} = S + S', \\ 2Q &= \frac{2\Omega}{\partial^2+\Omega^2} = -i(S - S'), \\ 2R &= \frac{2\Omega^2\partial^{-1}}{\partial^2+\Omega^2} = \frac{2}{\nu - D} - 2P. \end{aligned}\right\} \quad . \quad . \quad . \quad . \quad (4)$$

The Complementary Function is $\breve{V}$, where

$$-\breve{V}/\sigma = e^{-\nu t}(\breve{a}_1 + \breve{a}_2\cos\Omega t + \breve{a}_3\sin\Omega t)$$

and $\breve{a}_1$, $\breve{a}_2$, $\breve{a}_3$ are constant vectors such that $\breve{V}$ satisfies (1) when $\breve{E}=0$. This leads to the result:

$$\breve{a}_1 = \breve{a}\breve{h}, \quad \breve{a}_2 = b\breve{h}_1, \quad \breve{a}_3 = b\breve{h}_2,$$

where $\breve{h}_1$ and $\breve{h}_2$ are unit vectors perpendicular to $\breve{h}$ and to each other and a, b are arbitrary constants. Hence

$$-\breve{\mathrm{V}}/\sigma=e^{-\nu t}(a\breve{h}+b\breve{h}_1\cos\Omega t+b\breve{h}_2\sin\Omega t). \quad . \quad . \quad (5)$$

At the time t the mean work done per second on an electron is $e\breve{\mathrm{E}}\breve{u}$, and in one second ν collisions occur. Therefore

$$w\nu/\tau=-\breve{\mathrm{E}}\breve{u}/\sigma=-\breve{\mathrm{E}}\breve{\mathrm{U}}/\sigma-\breve{\mathrm{E}}\breve{\mathrm{V}}/\sigma. \quad . \quad . \quad (6)$$

Now from (3) it follows that

$$-\breve{\mathrm{E}}\breve{\mathrm{U}}/\sigma=\breve{\mathrm{E}}\mathrm{P}\breve{\mathrm{E}}-\breve{h}\mathrm{V}\breve{\mathrm{E}}\mathrm{Q}\breve{\mathrm{E}}+(\breve{h}\breve{\mathrm{E}})\mathrm{R}(\breve{h}\breve{\mathrm{E}}) \quad . \quad . \quad (7)$$

Also

$$\breve{\mathrm{E}}\mathrm{P}\breve{\mathrm{E}}=\sum_{m,n}\mathrm{E}_m\mathrm{E}_n(\breve{m}\breve{n})\mathrm{T}_m\mathrm{P}\mathrm{T}_n,$$

$$\breve{h}\mathrm{V}\breve{\mathrm{E}}\mathrm{Q}\breve{\mathrm{E}}=\sum_{m,n}\mathrm{E}_m\mathrm{E}_n(\breve{h}\mathrm{V}\breve{m}\breve{n})\mathrm{T}_m\mathrm{Q}\mathrm{T}_n,$$

$$(\breve{h}\breve{\mathrm{E}})\mathrm{R}(\breve{h}\breve{\mathrm{E}})=\sum_{m\ n}\mathrm{E}_m\mathrm{E}_n(\breve{h}\breve{m})(\breve{h}\breve{n})\mathrm{T}_m\mathrm{R}\mathrm{T}_n.$$

Hence

$$-\breve{\mathrm{E}}\breve{\mathrm{U}}/\sigma=\sum_{m,n}\mathrm{E}_m\mathrm{E}_n\mathrm{T}_m\mathrm{O}_{mn}\mathrm{T}_n, \quad . \quad . \quad . \quad . \quad (8)$$

where

$$\mathrm{O}_{mn}=(\breve{m}\breve{n})\mathrm{P}-(\breve{h}\mathrm{V}\breve{m}\breve{n})\mathrm{Q}+(\breve{h}\breve{m})(\breve{h}\breve{n})\mathrm{R}.$$

By a standard theorem in spherical trigonometry, or in vector analysis, we have

$$\breve{m}\breve{n}=(\breve{h}\breve{m})(\breve{h}\breve{n})+(\mathrm{V}\breve{h}\breve{m})(\mathrm{V}\breve{h}\breve{n}),$$

and so

$$\mathrm{O}_{mn}=\mathrm{U}_{mn}\mathrm{P}-\mathrm{V}_{mn}\mathrm{Q}+\mathrm{W}_{mn}\partial^{-1}, \quad . \quad . \quad . \quad (9)$$

where

$$\left.\begin{aligned}\mathrm{U}_{mn}&=(\mathrm{V}\breve{h}\breve{m})(\mathrm{V}\breve{h}\breve{n}),\\ \mathrm{V}_{mn}&=\breve{h}\mathrm{V}\breve{m}\breve{n},\\ \mathrm{W}_{mn}&=(\breve{h}\breve{m})(\breve{h}\breve{n}).\end{aligned}\right\} \quad . \quad . \quad . \quad . \quad . \quad (10)$$

Also from (5) it follows that

$$-\breve{\mathrm{E}}\breve{\mathrm{V}}/\sigma=e^{-\nu t}\sum_n\mathrm{E}_n\mathrm{T}_n[a(\breve{h}\breve{n})$$

$$+b(\breve{h}_1\breve{n})\cos\Omega t+b(\breve{h}_2\breve{n})\sin\Omega t]. \quad (11)$$

Thus

wv/τ=right-hand side of (8)+right-hand side of (11), (12)

and so

$$w=(\tau/v)\sum_{m,\,n} \mathrm{E}_m\mathrm{E}_n\mathrm{T}_m\mathrm{O}_{mn}\mathrm{T}_n+w_0, \quad . \quad . \quad . \quad (13)$$

where $w_0=(\tau/v)\times$right-hand side of (11).

In general we may set

$$\mathrm{T}_n=e^{-\nu_n t}\cos(\omega_n t+\phi_n)=\mathscr{R}(e^{\alpha_n t+i\phi_n}), \quad . \quad . \quad (14)$$

where $\mathscr{R}(y)$ denotes the real part of y,

$$\alpha_n=-\nu_n+i\omega_n, \quad \text{and} \quad \nu_n,\ \omega_n,\ \phi_n \text{ are real.}$$

Since $f(\mathrm{D})$ and $\mathscr{R}$ are commutative operations on any function of t, we find by means of (4) and (9) that

$$2\mathrm{O}_{mn}\mathrm{T}_n=\mathscr{R}(2\mathrm{S}_{mn}e^{\alpha_n t+i\phi_n}),$$

where

$$\left.\begin{aligned} &2\mathrm{S}_{mn}=(\mathrm{U}_{mn}+i\mathrm{V}_{mn})\mathrm{S}_n+(\mathrm{U}_{mn}-i\mathrm{V}_{mn})\mathrm{S}'_n+2\mathrm{W}_{mn}\partial_n^{-1},\\ &\mathrm{S}_n=\frac{1}{\mu_n+i\sigma_n}, \quad \mathrm{S}'_n=\frac{1}{\mu_n+i\sigma'_n}, \quad \partial_n^{-1}=\frac{1}{\mu_n+i\omega_n},\\ &\mu_n=\nu-\nu_n, \qquad \sigma_n=\omega_n-\Omega, \qquad \sigma'_n=\omega_n+\Omega, \end{aligned}\right\} \quad (15)$$

that is

$$2\mathrm{S}_{mn}=\mathrm{A}_{mn}+i\mathrm{B}_{mn},$$

where

$$\left.\begin{aligned} \mathrm{A}_{mn}=&|\mathrm{S}_n|^2(\mu_n\mathrm{U}_{mn}+\sigma_n\mathrm{V}_{mn})+|\mathrm{S}'_n|^2(\mu_n\mathrm{U}_{mn})-\sigma'_n\mathrm{V}_{mn})\\ &+2|\partial_n^{-1}|^2\mu_n\mathrm{W}_{mn},\\ \mathrm{B}_{mn}=&|\mathrm{S}_n|^2(\mu_n\mathrm{V}_{mn}-\sigma'_n\mathrm{U}_{mn})-|\mathrm{S}'_n|^2(\mu_n\mathrm{V}_{mn}+\sigma'_n\mathrm{U}_{mn},\\ &-2|\partial_n^{-1}|^2\omega_n\mathrm{W}_{mn}. \end{aligned}\right\} \quad (16)$$

Therefore

$$\begin{aligned} \mathrm{T}_m\mathrm{O}_{mn}\mathrm{T}_n=&\tfrac{1}{2}e^{-\nu'_{mn}t}\cos(\omega_m t+\phi_m)[\mathrm{A}_{mn}\cos(\omega_n t+\phi_n)\\ &-\mathrm{B}_{mn}\sin(\omega_n t+\phi_n)]\\ =&\tfrac{1}{4}e^{-\nu'_{mn}t}[\mathrm{A}_{mn}\{\cos(\omega'_{mn}t+\phi'_{mn})+\cos(\omega_{mn}t+\phi_n)\}\\ &-\mathrm{B}_{mn}\{\sin(\omega'_{mn}t+\phi'_{mn})-\sin(\omega_{mn}t+\phi_{mn})\}], \end{aligned}$$

where

$$\left.\begin{aligned} &\omega_{mn}=\omega_m-\omega_n, \quad \omega'_{mn}=\omega_m+\omega_n,\\ &\phi_{mn}=\phi_m-\phi_n, \quad \phi'_{mn}=\phi_m+\phi_n\\ &\qquad\qquad \nu'_{mn}=\nu_m+\nu_n. \end{aligned}\right\} \quad . \quad . \quad (17)$$

Hence from (13) it follows that

$$w=\frac{\tau}{4\nu}\sum_{m,n}\mathrm{E}_m\mathrm{E}_n e^{-\nu'_{mn}t}[\mathrm{A}_{mn}\{\cos(\omega_{mn}t+\phi_{mn})+\cos(\omega'_{mn}t+\phi'_{mn})\}$$
$$+\mathrm{B}_{mn}\{\sin(\omega_{mn}t+\phi_{mn})-\sin(\omega'_{mn}t+\phi'_{mn})\}]$$
$$+w_0. \quad . \quad (18)$$

When all the components of the electric force are undamped it may also be necessary to know $\bar{w}$, the average value of w during the longest period.

On setting all the quantities ν_n equal to zero, and averaging over the longest period involved, we obtain the following :

$$\bar{w}=\frac{\tau}{4\nu}\sum_n \mathrm{E}_n^2\mathrm{A}_{nn}+\bar{w}_c+\bar{w}_0, \quad . \quad . \quad . \quad (19)$$

for the averages of all terms involving $m\neq n$ vanish, except the " cross-terms " of elliptically polarized fields, whose averages are collected together under $\bar{w}_c$.

On setting $m=n$ in (16) we have

$$\mathrm{U}_{nn}=s_{hn}^2, \quad \mathrm{V}_{nn}=0, \quad \mathrm{W}_{nn}=c_{hn}^2, \quad \mu_n=\nu,$$

and so

$$\mathrm{A}_{nn}=\nu[(|\mathrm{S}_n|^2+|\mathrm{S}'_n|^2)s_{hn}^2+2|\partial_n^{-1}|^2c_{hn}^2].$$

To determine w_c it is sufficient to calculate the contribution of the cross-terms of one elliptic wave alone. So we proceed to consider the cross-terms due to the following field :

$$\breve{\mathrm{E}}=\mathrm{E}_1\breve{a}\cos\omega t+\mathrm{E}_2\breve{b}\sin\omega t=\mathscr{R}(\mathrm{E}_1\breve{a}-i\mathrm{E}_2\breve{b})e^{i\omega t}.$$

In (17) we now have

$$\nu_1=\nu_2=0, \quad \omega_1=\omega_2=\omega, \quad \phi_1=0, \quad \phi_2=-\frac{\pi}{2}.$$

Therefore

$$\nu_{12}=0, \quad \omega_{12}=0, \quad \omega'_{12}=2\omega, \quad \phi_{12}=\frac{\pi}{2}, \quad \phi'_{12}=-\frac{\pi}{2},$$

$$\nu_{21}=0, \quad \omega_{21}=0, \quad \omega'_{21}=2\omega, \quad \phi_{21}=-\frac{\pi}{2}, \quad \phi'_{21}=-\frac{\pi}{2}.$$

Then from (18) we obtain

$$w_c=\frac{\tau}{4\nu}\mathrm{E}_1\mathrm{E}_2\Big[\mathrm{A}_{12}\cos\Big(2\omega t-\frac{\pi}{2}\Big)$$
$$+\mathrm{B}_{12}\Big\{\sin\frac{\pi}{2}-\sin\Big(2\omega t-\frac{\pi}{2}\Big)\Big\}$$

$$+A_{21}\cos\left(2\omega t-\frac{\pi}{2}\right)$$

$$+B_{21}\left\{\sin\left(-\frac{\pi}{2}\right)-\sin\left(2\omega t-\frac{\pi}{2}\right)\right\}\Big],$$

and so

$$w_c=\frac{\tau}{4\nu}E_1E_2(B_{12}-B_{21}).$$

But from (10) and (15) we have

$$U_{12}=U_{21},\quad V_{12}=-V_{21}=\breve{h}V\breve{a}\breve{b},\quad W_{12}=W_{21},$$
$$\mu_1=\mu_2=\nu,\quad \sigma_1=\sigma_2=\omega-\Omega,\qquad \sigma_1'=\sigma_2'=\omega+\Omega,$$
$$S_1=S_2,\qquad S_1'=S_2',\qquad \partial_1^{-1}=\partial_2^{-1}.$$

So from (16) it follows that

$$B_{12}-B_{21}=\nu[|S|^2(V_{12}-V_{21})-|S'|^2(V_{12}-V_{21})]$$
$$=2\nu(|S|^2-|S'|^2)\breve{h}V\breve{a}\breve{b},$$

and consequently that

$$\bar{w}_c=\tau Z_1Z_2\left(\frac{1}{\nu^2+(\omega-\Omega)^2}-\frac{1}{\nu^2+(\omega+\Omega)^2}\right)\breve{h}V\breve{a}\breve{b}. \quad (20)$$

So from (19) and (20) we have

$$\bar{w}=\tau\sum_n Z_n^2\left[\left(\frac{1}{\nu^2+(\omega_n-\Omega)^2}+\frac{1}{\nu^2+(\omega_n+\Omega)^2}\right)\frac{s^2_{hn}}{2}+\frac{c^2_{hn}}{\nu^2+\omega_n^2}\right]$$
$$+\tau\sum_n Z_{n1}Z_{n2}\left[\left(\frac{1}{\nu^2+(\omega_n-\Omega)^2}-\frac{1}{\nu^2+(\omega_n+\Omega)^2}\right)\breve{h}V\breve{n}_1\breve{n}_2\right]$$
$$+\bar{w}_0. \quad (21)$$

This result may be written in the form

$$\bar{w}=\sum_n \bar{w}_n+\bar{w}_0,$$

where w_n is the average work done by the nth component of the field. Hence we have the following theorem:

The total average energetic effect of the forces of different frequencies is equal to the sum of the separate average effects.

This includes elliptically polarized fields.

3. *Determination of the Collision Frequency ν.*

In the small interval of time dt the number of collisions made by an electron is $\nu\,dt$, so in this interval we have :

The work done by the field on the electron$=w\nu\,dt$;

the energy lost by the electron in collisions$=\eta\nu\,dt$; and

the increase in the kinetic energy of an electron$=d(\frac{1}{2}mu^2)$,

where η is the energy lost at a collision made by an electron with a velocity u.

Therefore

$$d(\tfrac{1}{2}mu^2)+\eta\nu\,dt=w\nu\,dt.$$

But $u=lv$, where l is the mean free path ; hence we must have

$$ml\mathrm{D}u+\eta=w. \quad . \quad . \quad . \quad . \quad . \quad . \quad (22)$$

In most instances no great error ensues when l is taken to be independent of u, and so, except where it is otherwise stated, we shall usually assume l to be constant *.

Thus from (22) we have

$$a\mathrm{D}\nu+\eta=w, \quad . \quad . \quad . \quad . \quad . \quad . \quad (23)$$

where

$$a=ml^2,$$

and a is constant.

The value of ν is given by a solution of this differential equation which satisfies the initial conditions, and so a knowledge is required of the dependence of η on ν.

Even with the simplest types of collisions the relation between η and ν does not make it easy to obtain a general solution of (23), so in different applications of this equation we may need different methods of solution, and often may have to adopt approximate and graphical processes.

Nevertheless the following discussion is useful in a large number of practical situations.

We adopt for brevity the following notation :

When in (23) w is replaced by w the corresponding values of ν and η will be denoted by ν and $\bar{\eta}$ respectively.

* It is not difficult to discuss the problem when the variation of l and u is taken into account, but this may with advantage be left to another occasion.

Thus

$$a\mathrm{D}\bar{\nu}+\bar{\eta}=\bar{w}. \quad . \quad . \quad . \quad . \quad . \quad . \quad . \quad (24)$$

The Steady State is defined as that corresponding to the condition $\mathrm{D}\nu=0$, and the corresponding values of ν, η, and $\bar{w}$ will be denoted respectively by ν_0, η_0, and w_0. Thus

$$\eta_0=w_0. \quad . \quad . \quad . \quad . \quad . \quad . \quad . \quad . \quad (25)$$

Also we define $\bar{\mathrm{R}}$ and R_0 as follows:

$$\bar{\mathrm{R}}=\frac{1}{a}\frac{d\bar{\eta}}{d\bar{\nu}}, \quad \mathrm{R}_0=\frac{1}{a}\frac{d\eta_0}{d\nu_0}. \quad . \quad . \quad . \quad . \quad . \quad (26)$$

The value of $\bar{\nu}$ is found by inverting the following integral derived from (24):

$$t=a\int\frac{d\bar{\nu}}{\bar{w}-\bar{\eta}}, \quad . \quad . \quad . \quad . \quad . \quad . \quad . \quad (27)$$

This process can be carried out graphically merely by plotting t against $\bar{\nu}$, or else by means of the graphical method described below.

When

$$w=\bar{w}+v \quad \text{and} \quad |v| << \bar{w} \quad . \quad . \quad . \quad (28)$$

we have, by Taylor's theorem,

$$\left.\begin{aligned} \nu &\doteq \bar{\nu}+n \\ \text{and} \quad \eta &\doteq \eta+y \end{aligned}\right\}, \quad . \quad . \quad . \quad . \quad . \quad . \quad (29)$$

where $|n| << \bar{\nu}$

and $$y=a\bar{\mathrm{R}}n. \quad . \quad . \quad . \quad . \quad . \quad . \quad . \quad (30)$$

On subtracting (24) from (23) and dividing throughout by a we obtain

$$\left.\begin{aligned} \mathrm{D}n+\bar{\mathrm{R}}n &= a^{-1}v, \\ \text{and so} \quad n &= a^{-1}e^{-\int\bar{\mathrm{R}}\,dt}\int e^{\int\bar{\mathrm{R}}\,dt}v\,dt \end{aligned}\right\}. \quad . \quad . \quad . \quad . \quad (31)$$

Thus from (27), (29), and (31) we can obtain the value of ν.

After a sufficient lapse of time the quantities $\bar{\nu}$, η, and $\bar{w}$ approximate to their steady values ν_0, η_0, and w_0, which values are determined by means of (25).

The relations (28), (29), and (31) then become

$$w=w_0+v \quad \text{and} \quad |v| \ll w_0, \qquad (28.1)$$

$$\left.\begin{aligned} &\nu=\nu_0+n, \quad \eta=\eta_0+a\mathrm{R}_0 n, \\ \text{where} \quad &a\mathrm{R}_0=\frac{d\eta_0}{d\nu_0}, \end{aligned}\right\}, \qquad (29.1)$$

$$n=a^{-1}e^{-\mathrm{R}_0 t}\int e^{\mathrm{R}_0 t}v\,dt. \qquad (31.1)$$

When v is periodic we may then regard n as the periodic variation of ν around its steady value.

With collisions involving a constant coefficient of restitution and a constant mean free path the relation between η and ν is as follows :

$$\eta=\mathrm{C}(\nu^2-\nu_1^2), \qquad (32)^*$$

where C and ν_1 are constants.

We then have

$$\left.\begin{aligned} &\mathrm{R}_0=\mathrm{G}\nu_0, \\ \text{where} \quad &\mathrm{G}=2\mathrm{C}/a. \end{aligned}\right\} \qquad (33)$$

In those situations where w and $\bar{w}$ are not appreciably dependent on the variation of ν we can easily determine, as follows, the mode of approach of $\bar{\nu}$ to the steady value ν_0.

Here we have $w_0=\bar{w}$; so by (25) and (32)

$$\mathrm{C}(\nu_0^2-\nu_1^2)=\bar{w}.$$

Then

$$\bar{w}-\bar{\eta}=\mathrm{C}(\nu_0-\bar{\nu}^2),$$

and so by (27) we have

$$t=\frac{a}{\mathrm{C}}\int_{\nu_1}^{\nu_2}\frac{d\bar{\nu}}{\nu_0^2-\nu^2}=\mathrm{R}_0^{-1}\left[\log\left(\frac{\nu_0+\bar{\nu}}{\nu_0-\bar{\nu}}\right)\right]_{\nu_1}^{\nu_2},$$

where ν_1 and ν_2 are the initial and final values of ν.

Therefore

$$\left.\begin{aligned} &\frac{\nu_2}{\nu_0}=\frac{1-be^{-\mathrm{R}_0 t}}{1+be^{-\mathrm{R}_0 t}}, \\ \text{where} \quad &b=\frac{(\nu_0-\nu_1)}{(\nu_0+\nu_1)}. \end{aligned}\right\} \qquad (34)$$

Similarly the time of decay t' of the value of ν from ν_1' to ν_2' is given by

$$t'=\mathrm{R}_0^{-1}\left[\log\left(\frac{\nu+\nu_1}{\nu-\nu_1}\right)\right]_{\nu_1'}^{\nu_2'}.$$

* This is essentially the same as the formula (14) given by V. A. Bailey and D. F. Martyn in Phil. Mag. xviii. p. 369 (August 1934).

When w is due to several undamped waves of different frequencies then v is expressible in the form (18) with $\nu'_{mn}=0$, *i. e.*,

$$v=\sum_s V_s \cos(\omega_s t+\phi_s),$$

and so

$$n=a^{-1}\sum_s \frac{V_s}{\sqrt{\omega_s^2+R_0^2}}\cos(\omega_s t+\phi_s-\beta_s), \quad . \quad . \quad (35)$$

where $$\tan\beta_s=\omega_s/R_0.$$

Thus the variation of the collision frequency ν contains combination tones.

In some situations the quantities w and w may depend notably on the value of ν; each such problem will then need to be treated by appropriate modifications of the methods given.

The following is a useful example of such a modification: Let

$$w=\frac{z}{\bar{\nu}^2+r^2}, \quad \overline{w}=\frac{\bar{z}}{\nu^2+r^2},$$

where z and $\bar{z}$ are independent of ν, and $\dot{z}$ and r are constants.

Then from (24), (25), and (32) we have

$$a(\bar{\nu}^2+r^2)D\bar{\nu}+C(\bar{\nu}^2+r^2)(\bar{\nu}^2-\nu_1^2)=\bar{z}$$

and

$$C(\nu_0^2+r^2)(\nu_0^2-\nu_1^2)=\bar{z}. \quad . \quad . \quad . \quad . \quad (36)$$

On eliminating $\bar{z}$ we have

$$a(\bar{\nu}^2+r^2)D\bar{\nu}=-C(\bar{\nu}^2-\nu_0^2)(\bar{\nu}^2+\beta^2),$$

where $$\beta^2=\nu_0^2-\nu_1^2+r^2.$$

Therefore

$$a^{-1}Ct=-\int_{\nu_1}^{\nu_2}\frac{(\bar{\nu}^2+r^2).d\bar{\nu}}{(\bar{\nu}^2-\nu_0^2)(\bar{\nu}^2+\beta^2)}$$

$$=-\frac{1}{\nu_0^2+\beta^2}\int_{\nu_1}^{\nu_2}\left(\frac{\nu_0^2+r^2}{\bar{\nu}^2-\nu_0^2}+\frac{\nu_0^2-\nu_1^2}{\bar{\nu}^2+\beta^2}\right)d\bar{\nu}$$

$$=\frac{1}{\nu_0^2+\beta^2}\left[\frac{\nu_0^2+r^2}{2\nu_0}\log\left(\frac{\bar{\nu}+\nu_0}{\bar{\nu}-\nu_0}\right)-\frac{\nu_0^2-\nu_1^2}{\beta}\tan^{-1}\left(\frac{\nu}{\beta}\right)\right]_{\nu_1}^{\nu_2}.$$

Therefore

$$t=\left[\frac{1}{R'}\log\left(\frac{\bar{\nu}+\nu_0}{\bar{\nu}-\nu_0}\right)-\frac{aC^{-1}(\nu_0^2-\nu_1^2)}{\beta(\nu_0^2+\beta^2)}\tan^{-1}\left(\frac{\nu}{\beta}\right)\right]_{\nu_1}^{\nu_2}, \quad (37)$$

where

$$R'=R_0\left(\frac{\nu_0^2+\beta^2}{\nu_0^2+r^2}\right). \quad . \quad . \quad . \quad . \quad . \quad . \quad (38)$$

After a sufficient lapse of time the quantities ν, $\bar{\eta}$, and $\bar{w}$ approximate to their steady values ν_0, η_0, and w_0, which are given by (36).

So in (28) we have

$$v=\frac{z}{\nu^2+r^2}-\frac{\bar{z}}{\nu_0^2+r^2};$$

$$\doteq -\bar{z}\frac{2\nu_0 n}{(\nu_0^2+r^2)^2}+\zeta\frac{1}{\nu_0^2+r^2},$$

where

$$\zeta=z-\bar{z}. \quad . \quad . \quad . \quad . \quad . \quad . \quad . \quad (39)$$

Therefore from (31) we find that

$$Dn+R'n=\frac{a^{-1}\zeta}{\nu_0^2+r^2}, \quad . \quad . \quad . \quad . \quad (40)$$

where R′ is given by (38).

When the relation between η and ν is given by means of an experimentally determined curve of complicated form it may be necessary to have recourse to some form of graphical integration such as that now to be described.

The curves (ν, η) and (t, w) being given, it is required to derive from them the curve (t, ν).

The equation (23) may be written in the form

$$\xi\frac{d\eta}{dt}+\eta=w, \quad . \quad . \quad . \quad . \quad . \quad . \quad (41)$$

where

$$\xi=a\frac{d\nu}{d\eta}.$$

From the given curve (ν, η) we first derive the curve (ξ, η) shown on the left-hand side of fig. 1.

On the right-hand side we have the curve (t, w), the quantities η and w having the same vertical scale.

Let P and Q be simultaneous points on the curves (t, w) and (t, η), N and R their projections on the vertical axis, and S the intersection of QR and the curve (ξ, η).

Then we have

$$\tan\theta=\frac{NR}{RS}=\frac{w-\eta}{\xi}=\frac{d\eta}{dt}$$

in virtue of (41).

Thus the tangent at Q is parallel to SN.

This property offers the possibility of determining a succession of points Q by suitable manipulation of a sheet of transparent squared paper on which the curve (ξ, η) is drawn, this sheet being moved about on a sheet of similar but opaque squared paper on which the curve (t, w) is drawn (to the same vertical scale as η) *.

In discussing one such method with Mr. J. M. Somerville he proposed the following elegant alternative, which is based on the same property :—

In fig. 2 let Q_0 be a known point on the curve (t, η). The transparent sheet is set so that its ξ-axis coincides with the t-axis and its vertical η-axis passes through Q_0.

Fig. 1.

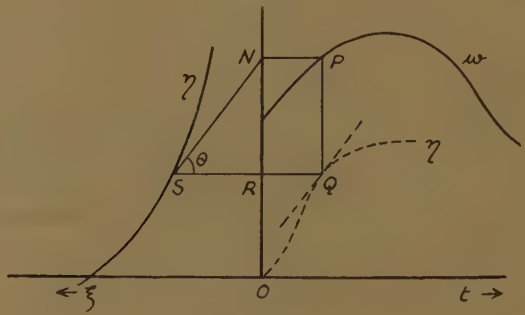

Where the η-axis cuts the curve (t, w) a point p_0 is marked on the transparent sheet. This sheet is then moved again until the curve (ξ, η) passes through the point Q_0, and we prick through p_0 to mark a point q_0 on the opaque sheet. The line Q_0q_0 is then the tangent at Q_0, and so any near point Q_1 on this line may be taken as the point succeeding Q. In this simple way a whole succession of points on the curve (t, η) may be obtained. In many problems the initial value of η is 0, and so the initial point Q_0 is at the origin.

If w varies notably with ν a similar procedure may be followed provided that the points on the curve (t, w) are plotted concurrently with those on the curve (t, η).

* Or by an obvious analogous graphical process with a single sheet of squared paper containing both curves.

Thus if P_0 and Q_0 are the points representing w and η when $t=0$, the above construction gives Q_1 first; from this and the curve (ν, η) we obtain ν, and so the point P_1 may be determined. The next operation gives Q_2 and P_2 in succession, and so on.

The variation of the mean free path l with the velocity u can also be taken into account in this method simply by putting (22) in the form given in (41), but with

$$\xi = ml\frac{du}{d\eta}.$$

Fig. 2.

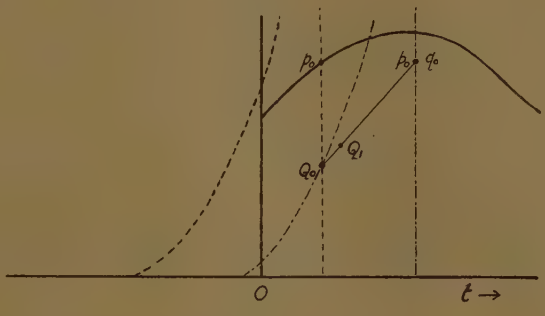

4. *Two Examples.*

The simplest illustration of the use of our formulæ is offered by the study of the effects caused by a sinoidal electric field.

This is accomplished by setting $m=1$, $n=1$, $\nu_n=0$, $\phi_n=0$ in all the formulæ where they occur.

Thus we obtain the following results:

$$U=s^2, \quad V=0, \quad W=c^2, \quad . \quad . \quad . \quad (10.1)$$

where $s=\sin\theta$, $c=\cos\theta$, and θ is the angle between $\breve{E}$ and $\breve{H}$.

$$\mu=\nu, \quad \sigma=\omega-\Omega, \quad \sigma'=\omega+\Omega\,; \quad . \quad . \quad (15.1)$$

$$\left.\begin{aligned} A &= \left(\frac{\nu}{\nu^2+(\omega-\Omega)^2}+\frac{\nu}{\nu^2+(\omega+\Omega)^2}\right)s^2+\frac{2\nu}{\nu^2+\omega^2}c^2, \\ B &= -\left(\frac{\omega-\Omega}{\nu^2+(\omega-\Omega)^2}+\frac{\omega+\Omega}{\nu^2+(\omega+\omega)^2}\right)s^2-\frac{2\omega}{\nu^2+\omega^2}c^2; \end{aligned}\right\}$$

$$. \quad . \quad . \quad (16.1)$$

$$\left.\begin{aligned} \omega_{11}=0, \qquad & \omega'_{11}=2\omega, \\ \phi_{11}=0, \qquad & \phi'_{11}=0, \\ & \nu'_{11}=0\ ; \end{aligned}\right\} \quad . \ . \ . \quad (17.1)$$

$$w=\frac{\tau}{2\nu}\mathrm{Z}^2\left[\mathrm{A}(1+\cos 2\omega t)-\mathrm{B}\sin 2\omega t\right]; \quad (18.1)$$

$$\overline{w}=\tfrac{1}{2}\tau\mathrm{Z}^2\left[\left(\frac{1}{\nu^2+(\omega-\Omega)^2}+\frac{1}{\nu^2+(\omega+\Omega)^2}\right)s^2+\frac{2}{\nu^2+\omega^2}c^2\right]. \quad . \ . \ . \quad (21.1)$$

When $\breve{\mathrm{E}}$ is perpendicular to $\breve{\mathrm{H}}$ the formula for $\overline{w}$ becomes identical with that given in a former publication *, and there supposed to hold true for any angle between $\breve{\mathrm{E}}$ and $\breve{\mathrm{H}}$. This supposition is now seen to be incorrect, and it will also be seen that the error is due to the incorrect assumption that the component of $\breve{\mathrm{H}}$ in the direction of $\breve{\mathrm{E}}$ has no influence on the work done by $\breve{\mathrm{E}}$ on an electron. The consequent changes in the theoretical conclusions on the interaction of radio-waves will be considered elsewhere.

When $\omega=0$, the formula for $\overline{w}$ becomes that corresponding to a constant electric field, namely,

$$\overline{w}=\tau\mathrm{Z}^2\cdot\frac{1}{\nu^2+\Omega^2}.$$

From this result we can deduce a formula, due to J. S. Townsend †, for the drift-velocity W of electrons in a magnetic field which is perpendicular to the electric field. For in the steady state the drift-velocity W enables the field to do work on an electron at the rate of ZeW ergs/sec. Hence

$$Ze\,\mathrm{W}=\nu\overline{w}.$$

Therefore

$$\mathrm{W}=\frac{Ze}{m}\cdot\frac{\nu}{\nu^2+\Omega^2}$$

$$=\frac{Ze}{m}\cdot\frac{\mathrm{T}}{1+\Omega^2\mathrm{T}^2},$$

* V. A. Bailey and D. F. Martyn, Phil. Mag. vol. xviii. p. 372 (Aug. 1934).

† J. S. Townsend, 'Electricity in Gases' (Clarendon Press, 1915), p. 101.

where T is the mean free time between successive collisions of an electron with molecules.

This is essentially Townsend's result.

Our next example is that of an electric field having two undamped components, of different frequencies, which are parallel to each other and perpendicular to the magnetic field, and each has its phase-angle equal to zero.

With this each of the suffixes m and n runs through the values 1 and 2, $\nu=0$, and the essential formulæ simplify to the following :

$$\left.\begin{aligned} &U_{mn}=1, \quad V_{mn}=0, \quad W_{mn}=0\,; \\ &A_{mn}=\nu(|S_n|^2+|S'_n|^2), \\ &B_{mn}=-|S_n|^2\sigma_n-|S'_n|^2\sigma'_n\,; \end{aligned}\right\} \quad . \quad . \quad (16.2)$$

$$\left.\begin{aligned} &\omega_{mn}=\begin{matrix} & \xrightarrow{\qquad n} \\ \downarrow m & \end{matrix}\begin{vmatrix} 0, & \omega_1-\omega_2, \\ \omega_2-\omega_1, & 0, \end{vmatrix} \qquad \omega'_{mn}=\begin{matrix} & \xrightarrow{\qquad n} \\ \downarrow m & \end{matrix}\begin{vmatrix} 2\omega_1, & \omega_1+\omega_2, \\ \omega_1+\omega_2 & 2\omega_2, \end{vmatrix} \\ &\phi_{mn}=0, \quad \phi'_{mn}=0, \quad \nu'_{mn}=0\,; \end{aligned}\right\}$$

$$. \quad . \quad . \quad (17.2)$$

$$\begin{aligned} w=\frac{\tau}{2\nu}\big[&Z_1^2\{A_{11}(1+\cos 2\omega_1 t)-B_{11}\sin 2\omega_1 t\} \\ &+Z_1Z_2\{\overline{A_{12}+A_{21}}\,.\,(\cos\overline{\omega_1-\omega_2}t+\cos\overline{\omega_1+\omega_2}t) \\ &+\overline{B_{12}-B_{21}}\,.\,\sin\overline{\omega_1-\omega_2}t-\overline{B_{12}+B_{21}}\,.\,\sin\overline{\omega_1+\omega_2}t\} \\ &+Z_2^2\{A_{22}(1+\cos 2\omega_2 t)-B_{22}\sin 2\omega_2 t\}\big]\,; \end{aligned}$$

$$. \quad . \quad . \quad (18.2)$$

$$\begin{aligned} \overline{w}=\tfrac{1}{2}\tau\Big[&Z_1^2\Big(\frac{1}{\nu^2+(\omega_1-\Omega)^2}+\frac{1}{\nu^2+(\omega_1+\Omega)^2}\Big) \\ &+Z_2^2\Big(\frac{1}{\nu^2+(\omega_2-\Omega)^2}+\frac{1}{\nu^2+(\omega_2+\Omega)^2}\Big)\Big]. \end{aligned}$$

$$. \quad . \quad . \quad (21.2)$$

On setting $\omega_2=0$ we have the results corresponding

to an electric field composed of an alternating part and a constant part, namely :

$$w = \frac{\tau}{2\nu}\,[Z_1^2\{A_{11}(1+\cos 2\omega_1 t) - B_{11}\sin 2\omega_1 t\} + 2Z_1Z_2\{\overline{A_{12}+A_{21}}\,.\cos\omega_1 t - B_{21}\sin 2\omega_1 t\} + 2Z_2^2 A_{22}], \quad . \; . \; . \quad (18.3)$$

and

$$\overline{w} = \tfrac{1}{2}\tau\left[Z_1^2\left(\frac{1}{\nu^2+(\omega_1-\Omega)^2} + \frac{1}{\nu^2+(\omega_1-\Omega)^2}\right) + Z_2^2\left(\frac{2}{\nu^2+\Omega^2}\right)\right]. \quad . \; . \; . \quad (21.3)$$

The expressions (21.2) and (21.3) for $\overline{w}$ also hold when the two components of electric force are not parallel to each other, provided that they are both perpendicular to the magnetic force.

The same formula (21.3) has also been derived in an investigation of the situation just mentioned by means of methods similar to those used in the former publication *.

The detailed application of the results presented here to the study of the interaction of radio-waves and to related topics will be given in other communications in the near future.

It may, however, be stated here that these results indicate the existence of two interesting phenomena which have not hitherto been recognized. Thus the formulæ (18) and (35) lead to the conclusion that two waves whose frequencies differ only by an audible frequency may cause variations in ν of an audible kind, and so may produce an audible background in the reception of a third wave whose frequency differs considerably from the frequencies of the other two †. Similarly the formulæ (21) and (40) lead to the conclusion that a kind of resonance may occur in the well-known radio-interaction of two waves when the frequency of one of them passes through the value of the local gyro-frequency ‡.

* V. A. Bailey and D. F. Martyn, *loc. cit.*

† Some recent observations of W. L. Hafekost may be explained by means of (18) and (35). ('Wireless Engineer,' xiii. p. 298 (June 1936).

‡ *v.* V. A. Bailey, 'Nature,' cxxxix. p. 68 (Jan. 9, 1937).

In conclusion I would like to acknowledge the valuable assistance rendered by Mr. J. M. Somerville, who has checked all the calculations and made useful suggestions. The assistance of Mr. Somerville has been made possible through research grants made to the University of Sydney by the Carnegie Corporation and by the Commonwealth of Australia.

LXXIX. *The Magneto-Optical Dispersion of Organic Liquids in the Ultra-Violet Region of the Spectrum.*—Part X. *The Magneto-Optical Dispersion of Iso-Amyl Acetate, Methyl Iso-Valerate, and Acetone.* *By* BERYL P. M. WALTERS, *Ph.D.*, *and* Prof. E. J. EVANS, *D.Sc.*, *Physics Department, University College of Swansea* *.

ACCORDING to Larmor's theory [1] the value of Verdet's constant of a substance for wave-length λ is given by the expression.

$$= \frac{e}{2mC^2} \cdot \lambda \cdot \frac{dn}{d\lambda}, \quad . \quad . \quad . \quad . \quad . \quad (1)$$

where n is the refractive index, e/m is the ratio of the charge to the mass of the resonators, and c is the velocity of light. In the above expression the charge e is measured in electrostatic units and the magnetic field in electromagnetic units.

If the ordinary dispersion of each liquid is represented by an equation of the type

$$n^2-1=b_0+\frac{b_1}{\lambda^2-\lambda_1^2}+ \quad . \quad . \quad . \quad . \quad . \quad (2)$$

and the magneto-optical dispersion over the range of spectrum investigated is controlled by only one absorption band in the Schumann-Lyman region of the spectrum it can be shown that

$$\phi = n\delta\lambda^2 = K\left(\frac{\lambda^2}{\lambda^2-\lambda_1^2}\right)^2, \quad . \quad . \quad . \quad . \quad (3)$$

where K is a constant and λ_1 the wave-length of the absorption band.

* Communicated by Prof. E. J. Evans.

Further, it can be deduced from the three equations given above that

$$\frac{e}{m} = \frac{2K C^2}{b_1} \cdot \quad . \quad . \quad . \quad . \quad . \quad . \quad . \quad (4)$$

In the present investigation the values of Verdet's constant and the refractive index of iso-amyl acetate, methyl iso-valerate, and acetone have been determined in the violet and the near ultra-violet regions of the spectrum, and the experimental results examined in relation to Larmor's theory.

The experimental methods employed in the determination of the magneto-optical rotations and the refractive indices have been described [2] in detail previously, and in this paper only the results and their relation to the theory will be considered.

Each of the three liquids was subjected to a process of fractional distillation, and the fraction which distilled over in the neighbourhood of the accepted boiling-point was employed in the determinations of the magneto-optical rotations and refractive indices.

The refractive indices given in Table I. (B) were determined at temperatures in the neighbourhood of 20° C., and the values were corrected to the temperatures at which the magneto-optical rotations were measured by means of the known values of the temperature coefficients of the three liquids. It was found that the refractive indices of iso-amyl acetate, methyl iso-valerate, and acetone diminished by about $\cdot 0005_0$, $\cdot 0004_2$, and $\cdot 0004$ respectively per degree C. rise of temperature.

The refractive indices of the three liquids are given in Tables I. (A) and I. (B), and are plotted in fig. 1.

Magneto-Optical Dispersion.

Iso-Amyl Acetate.

The sample of iso-amyl acetate distilled over at 142·2° C. at a pressure of 760·5 mm. of mercury, the correct boiling-point [3] being 142° C. at 756·5 mm. The specimen employed in the present investigation was found to be optically active, and the natural rotation of the liquid at various wave-lengths was first determined. It was found that for a column of liquid of length 30·5 cm. the natural rotation was 2° 45′ at ·4226 μ and 4° 45′ at

Experimental Results.

Ordinary Dispersion.

Table I. (A).

Visual Determinations.

Wave-length in microns.	Refractive indices.		
	Iso-amyl acetate at 14·9° C.	Methyl iso-valerate at 10·5° C.	Acetone at 8·4° C.
·6678	$1{\cdot}4008_0$	$1{\cdot}3953_5$	$1{\cdot}3611_1$
·5893	$1{\cdot}4033_4$	$1{\cdot}3974_2$	$1{\cdot}3634_2$
·5876	$1{\cdot}4033_6$	$1{\cdot}3974_4$	$1{\cdot}3634_4$
·5016	$1{\cdot}4071_3$	$1{\cdot}4013_3$	$1{\cdot}3673_0$
·4922	$1{\cdot}4077_2$	$1{\cdot}4020_0$	$1{\cdot}3678_6$
·4713	$1{\cdot}4091_8$	$1{\cdot}4032_8$	$1{\cdot}3692_4$
·4472	$1{\cdot}4110_3$	$1{\cdot}4050_9$	$1{\cdot}3711_0$

Fig. 1.

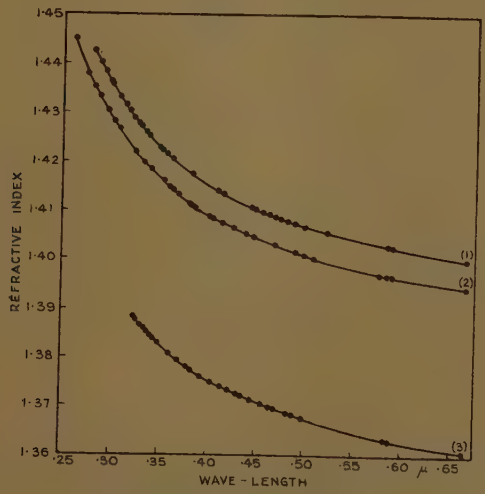

(1) Iso-amyl acetate at 14·9° C.
(2) Methyl iso-valerate at 10·5° C.
(3) Acetone at 8·4° C.

·3510 μ. The sum of the magnetic and natural rotation at each wave-length was next measured, and by sub-

TABLE I. (B).

Photographic Determinations.

Iso-amyl acetate at 14·9° C.		Methyl iso-valerate at 10·5° C.		Acetone at 8·4° C.	
Wave-length in microns.	Refractive index.	Wave-length in microns.	Refractive index.	Wave-length in microns.	Refractive index.
·5218	$1{\cdot}4062_0$	·5782	$1{\cdot}3976_2$	·4698	$1{\cdot}3693_6$
·4836	$1{\cdot}4083_2$	·5106	$1{\cdot}4009_0$	·4675	$1{\cdot}3694_9$
·4767	$1{\cdot}4088_8$	·4481	$1{\cdot}4050_6$	·4587	$1{\cdot}3701_6$
·4651	$1{\cdot}4096_0$	·4416	$1{\cdot}4055_8$	·4481	$1{\cdot}3710_2$
·4587	$1{\cdot}4102_2$	·4275	$1{\cdot}4069_7$	·4378	$1{\cdot}3717_8$
·4485	$1{\cdot}4109_2$	·4173	$1{\cdot}4079_0$	·4242	$1{\cdot}3730_4$
·4173	$1{\cdot}4137_2$	·4063	$1{\cdot}4090_0$	·4178	$1{\cdot}3736_9$
·4123	$1{\cdot}4142_5$	·4023	$1{\cdot}4094_3$	·4070	$1{\cdot}3748_6$
·3861	$1{\cdot}4176_6$	·3925	$1{\cdot}4106_8$	·3976	$1{\cdot}3759_5$
·3656	$1{\cdot}4207_5$	·3881	$1{\cdot}4112_2$	·3867	$1{\cdot}3773_6$
·3610	$1{\cdot}4216_0$	·3861	$1{\cdot}4114_9$	·3840	$1{\cdot}3777_2$
·3545	$1{\cdot}4227_0$	·3689	$1{\cdot}4137_9$	·3745	$1{\cdot}3792_5$
·3512	$1{\cdot}4233_5$	·3625	$1{\cdot}4148_9$	·3654	$1{\cdot}3805_4$
·3413	$1{\cdot}4255_1$	·3600	$1{\cdot}4153_8$	·3524	$1{\cdot}3828_1$
·3365	$1{\cdot}4263_7$	·3545	$1{\cdot}4163_8$	·3476	$1{\cdot}3838_0$
·3308	$1{\cdot}4275_3$	·3422	$1{\cdot}4186_7$	·3455	$1{\cdot}3841_7$
·3291	$1{\cdot}4280_0$	·3338	$1{\cdot}4205_9$	·3413	$1{\cdot}3850_5$
·3250	$1{\cdot}4290_8$	·3274	$1{\cdot}4220_9$	·3382	$1{\cdot}3856_0$
·3190	$1{\cdot}4306_0$	·3094	$1{\cdot}4266_8$	·3354	$1{\cdot}3863_4$
·3142	$1{\cdot}4318_2$	·3036	$1{\cdot}4284_1$	·3338	$1{\cdot}3865_2$
·3090	$1{\cdot}4333_1$	·2961	$1{\cdot}4306_4$	·3290	$1{\cdot}3875_8$
·3010	$1{\cdot}4358_0$	·2883	$1{\cdot}4334_9$	·3274	$1{\cdot}3880_2$
·2997	$1{\cdot}4363_0$	·2825	$1{\cdot}4356_4$		
·2932	$1{\cdot}4385_5$	·2767	$1{\cdot}4380_8$		
·2883	$1{\cdot}4402_5$				

tracting the natural rotation at a particular wave-length it was possible to obtain the magneto-optical rotation of iso-amyl acetate at that wave-length. The experimental results are given in Table II. (A) and fig. 2.

TABLE II. (A).

Verdet's Constants of Iso-Amyl Acetate at various Wave-lengths.

Temperature = 14·9° C.

Wave-length in microns.	Verdet's constant in min./cm. gauss.	Wave-length in microns.	Verdet's constant in min./cm. gauss.
·4438	$·0225_2$	·3804	$·0320_3$
·4325	$·0237_2$	·3750	$·0331_8$
·4235	$·0249_0$	·3693	$·0343_9$
·4151	$·0260_5$	·3639	$·0355_9$
·4078	$·0272_6$	·3592	$·0367_5$
·4007	$·0284_5$	·3540	$·0379_5$
·3936	$·0296_2$	·3490	$·0391_5$
·3870	$·0308_1$		

Fig. 2.

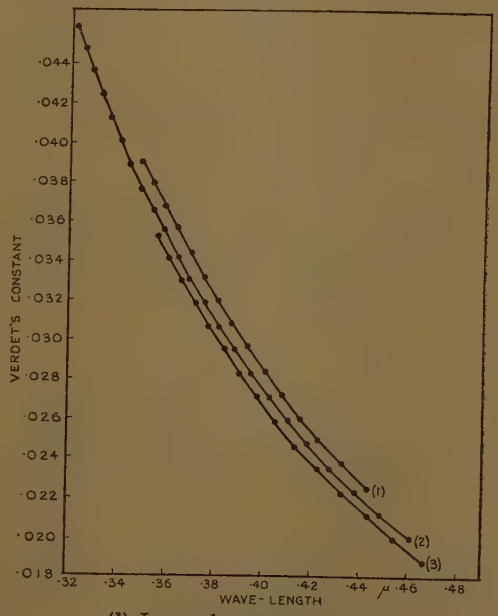

(1) Iso-amyl acetate at 14·9° C.
(2) Methyl iso-valerate at 10·5° C.
(3) Acetone at 8·4° C.

Table II. (B) gives a series of values, obtained from fig. 1 and Table II. (A), of the refractive index n and Verdet's constant δ for the given wave-lengths. It was found that the experimental results could be represented by a formula of the type

$$\phi = n\delta\lambda^2 = K\left(\frac{\lambda^2}{\lambda^2 - \lambda_1^2}\right)^2,$$

and from pairs of values obtained from Table II. (B) λ_1 and K were calculated.

Substitution in the above equation gave the following results :—

From (A) and (B) $\lambda_1 = \cdot1089\,\mu$ and $K = 5\cdot548_3 \times 10^{-3}$.
,, (B) ,, (C) $\lambda_1 = \cdot1088\,\mu$,, $K = 5\cdot548_5 \times 10^{-3}$.
,, (A) ,, (C) $\lambda_1 = \cdot1088\,\mu$,, $K = 5\cdot548_6 \times 10^{-3}$.

TABLE II. (B).

	λ in microns.	δ in min./cm. gauss.	n.
(A).....	·4007	$\cdot0284_5$	$1\cdot4156_1$
(B).....	·3870	$\cdot0308_1$	$1\cdot4175_9$
(C)	·3540	$\cdot0379_5$	$1\cdot4227_8$

The mean values of λ_1 and K are $\cdot1088\,\mu$ and $5\cdot54_8 \times 10^{-3}$ respectively, and the equation representing the magneto-optical dispersion of active iso-amyl acetate over the range of spectrum investigated at a temperature of 14·9° C. is

$$n\delta = 5\cdot54_8 \times 10^{-3} \frac{\lambda^2}{\{\lambda^2 - (\cdot1088)^2\}^2}.$$

The above equation was used to calculate the values of Verdet's constant for wave-lengths at which experimental results had already been obtained, and a comparison between the observed and calculated values is given in Table II. (C).

The value of δ calculated from the above equation for sodium light is $\cdot0122_1$, and assuming $\cdot0131_0$ as the value of Verdet's constant for water at $\cdot5893\,\mu$, the specific rotation of active iso-amyl acetate at 14·9° C. is therefore ·932.

TABLE II. (C).

λ (microns).	δ (observed).	δ (calculated).
·4438	$·0225_2$	$·0225_9$
·4235	$·0249_0$	$·0250_0$
·4078	$·0272_6$	$·0273_2$
·3936	$·0296_2$	$·0296_3$
·3804	$·0320_3$	$·0320_6$
·3750	$·0331_8$	$·0331_4$
·3693	$·0343_9$	$·0343_9$
·3639	$·0355_9$	$·0355_9$
·3490	$·0391_5$	$·0392_3$

Methyl Iso-Valerate.

The methyl iso-valerate distilled over between 116·7° C. and 116·8° C. at a pressure of 762 mm., its true boiling-point being 116·7° C. at 760 mm.

The experimental results are given in Table III. (A) and fig. 2.

TABLE III. (A).

Verdet's Constants of Methyl Iso-Valerate at various Wave-lengths.

Temperature = 10·5° C.

Wave-length in microns.	Verdet's constant in min./cm. gauss.	Wave-length in microns.	Verdet's constant in min./cm. gauss.
·4612	$·0200_3$	·3643	$·0341_7$
·4491	$·0212_1$	·3590	$·0353_5$
·4384	$·0224_0$	·3541	$·0365_3$
·4284	$·0235_8$	·3492	$·0377_1$
·4190	$·0247_5$	·3446	$·0389_0$
·4106	$·0259_3$	·3404	$·0400_8$
·4026	$·0271_0$	·3365	$·0412_6$
·3954	$·0282_7$	·3324	$·0424_4$
·3884	$·0294_6$	·3286	$·0436_2$
·3818	$·0306_4$	·3251	$·0447_9$
·3754	$·0318_2$	·3215	$·0459_6$
·3697	$·0329_9$		

In Table III. (B) values of Verdet's constant and the refractive index corresponding to certain wave-lengths are given, and these values were used to calculate the constants of the dispersion equation for methyl iso-valerate.

Using these values we obtain :—

From (A) and (B) $\lambda_1 = \cdot1070\ \mu$ and $K = 5\cdot346_2 \times 10^{-3}$.
,, (B) ,, (C) $\lambda_1 = \cdot1079\ \mu$,, $K = 5\cdot332_4 \times 10^{-3}$.
,, (A) ,, (C) $\lambda_1 = \cdot1076\ \mu$,, $K = 5\cdot340_0 \times 10^{-3}$.

The mean values of λ_1 and K are $\cdot1075\ \mu$ and $5\cdot33_9 \times 10^{-3}$ respectively, and the equation representing the magneto-optical dispersion of methyl iso-valerate over the region of the spectrum investigated is

$$n\delta = 5\cdot33_9 \times 10^{-3} \frac{\lambda^2}{\{\lambda^2 - (\cdot1075)^2\}^2}.$$

TABLE III. (B).

	λ (microns).	δ (min./cm. gauss).	*n*.
(A)	·4491	$\cdot0212_1$	$1\cdot4050_2$
(B)	·3754	$\cdot0318_2$	$1\cdot4129_0$
(C)	·3251	$\cdot0447_9$	$1\cdot4226_0$

This equation was used to calculate δ for several wave-lengths at which experimental determinations had been carried out, and a comparison of the observed and calculated values is given in Table III. (C).

The value of δ, calculated from the above equation for sodium light, is $\cdot0117_7$ at 10·5° C., and assuming $\cdot0131_0$ as the value of Verdet's constant for water at $\cdot5893\ \mu$, the specific rotation of methyl iso-valerate at 10·5° C. is therefore ·898.

Acetone.

The specimen of acetone employed in the measurements of the magneto-optical rotations distilled over between 56·2° C. and 56·4° C., when the pressure was 765·4 mm. of mercury, the correct boiling point [5] being 56·1° C.

at 760 mm. The values of Verdet's constant for different wave-lengths are given in Table IV. (A) and fig. 2.

TABLE III. (C).

λ (microns).	δ (observed).	δ (calculated).
·4612	$·0200_3$	$·0199_9$
·4384	$·0224_0$	$·0223_7$
·4284	$·0235_8$	$·0235_6$
·4190	$·0247_5$	$·0247_5$
·4026	$·0271_0$	$·0271_0$
·3954	$·0282_7$	$·0282_4$
·3818	$·0306_4$	$·0306_0$
·3643	$·0341_7$	$·0341_2$
·3541	$·0365_3$	$·0365_7$
·3492	$·0377_1$	$·0377_1$
·3446	$·0389_0$	$·0389_2$
·3404	$·0400_8$	$·0400_7$
·3324	$·0424_4$	$·0424_4$
·3286	$·0436_2$	$·0436_1$
·3215	$·0459_6$	$·0460_0$

TABLE IV. (A).

Verdet's Constant of Acetone at various Wave-lengths.

Temperature=8·4° C.

Wave-length in microns.	Verdet's constant in min./cm. gauss.	Wave-length in microns.	Verdet's constant in min./cm. gauss.
·4671	$·0188_3$	·3906	$·0282_6$
·4543	$·0200_2$	·3839	$·0294_4$
·4433	$·0211_8$	·3775	$·0306_2$
·4325	$·0223_4$	·3714	$·0318_0$
·4229	$·0235_4$	·3658	$·0329_6$
·4138	$·0247_0$	·3603	$·0341_6$
·4051	$·0259_0$	·3554	$·0353_5$
·3977	$·0270_8$		

In Table IV. (B) values of Verdet's constant and the refractive index corresponding to certain wave-lengths are given. These were employed to calculate the constants of the magneto-optical dispersion equation of acetone.

Using these values, it was found that :—

From (A) and (B) $\lambda_1 = \cdot 1120\ \mu$ and $K = 4 \cdot 994_0 \times 10^{-3}$.
,, (B) ,, (C) $\lambda_1 = \cdot 1130\ \mu$,, $K = 4 \cdot 980_0 \times 10^{-3}$.
,, (A) ,, (C) $\lambda_1 = \cdot 1122\ \mu$,, $K = 4 \cdot 989_7 \times 10^{-3}$.

The mean values of λ_1 and K are $\cdot 1124\ \mu$ and $4 \cdot 98_8 \times 10^{-3}$ respectively, and the equation representing the magneto-

TABLE IV. (B).

	λ in microns.	δ in min./cm. gauss.	n.
(A).....	·4543	$\cdot 0200_2$	$1 \cdot 3705_6$
(B).....	·3977	$\cdot 0270_8$	$1 \cdot 3759_5$
(C)	·3603	$\cdot 0341_6$	$1 \cdot 3814_6$

optical dispersion of acetone at 8·4° C. over the range of wave-lengths investigated is

$$n\delta = 4 \cdot 98_8 \times 10^{-3} \frac{\lambda^2}{\{\lambda^2 - (\cdot 1124)^2\}^2}.$$

The accuracy of the representation of the results by this equation is shown in Table IV. (C), where a comparison is made of the values of Verdet's constant obtained experimentally and the values calculated from the equation.

The specific rotation of acetone is ·8687 at 15·2° C. according to Perkin [6] and ·855 at 20° C. according to Lowry [7]. Correcting for the relative density of the liquid which diminishes by about 1·24 per cent. for 10° C. rise of temperature, Lowry's value of the specific rotation becomes ·867 at 8·4° C.

The value of Verdet's constant of acetone at 8·4° C. for sodium light was also calculated from the magneto-optical dispersion equation, and was found to be $\cdot 0113_4$. Assuming the value of Verdet's constant for water to

be ·0131 at ·5893 μ, the specific rotation of acetone at 8·4° C. is ·866, which is in good agreement with the value obtained by Lowry.

The values of the magnetic rotary power relative to that at ·5893 μ have been calculated from the previous equation and compared with the values obtained by Lowry [8]. The comparison is given in Table IV. (D).

TABLE IV. (C).

λ (microns).	δ (observed).	δ (calculated).
·4671	$·0188_3$	$·0188_1$
·4433	$·0211_8$	$·0211_4$
·4325	$·0223_4$	$·0223_5$
·4229	$·0235_4$	$·0235_2$
·4138	$·0247_0$	$·0247_1$
·4051	$·0259_0$	$·0259_5$
·3906	$·0282_8$	$·0282_5$
·3839	$·0294_4$	$·0294_2$
·3775	$·0306_2$	$·0306_0$
·3714	$·0318_0$	$·0318_0$
·3658	$·0329_6$	$·0329_6$
·3554	$·0353_5$	$·0352_8$

TABLE IV. (D).

λ (microns).	Magnetic rotary power relative to that at ·5893 μ.	
	Lowry.	Present results.
·5461	1·181	1·178
·4359	1·942	1·938

The Dispersion Equations.

The experimental results have shown that the magneto-optical dispersion of each of the liquids investigated can be explained by the presence of a single absorption band. If the assumption is now made that the same absorption band is responsible for the ordinary dispersion

of the liquids over the same range of wave-length, then the ordinary dispersion of each of the liquids can be represented by the equation

$$n^2-1 = b_0+\frac{b_1}{\lambda^2-\lambda_1^2}.$$

The constants of the equation can be calculated from two values of the refractive index, corresponding to two known wave-lengths.

Iso-Amyl Acetate.

The pairs of values employed in calculating the constants b_0 and b_1 for acetone are given below :—

λ (microns).	n.	$b_1\times10^2$.	b_0.
·6678	$1{\cdot}4008_0$	$\cdot953_8$	$\cdot9402_7$
·3861	$1{\cdot}4176_6$		
·4713	$1{\cdot}4091_8$	$\cdot953_0$	$\cdot9404_3$
·3512	$1{\cdot}4233_5$		
·4472	$1{\cdot}4110_3$	$\cdot954_6$	$\cdot9401_3$
·3365	$1{\cdot}4263_7$		

TABLE V.

λ (microns).	n (observed).	n (calculated).
·4922	$1{\cdot}4077_2$	$1{\cdot}4077_3$
·4836	$1{\cdot}4083_2$	$1{\cdot}4082_9$
·4651	$1{\cdot}4096_0$	$1{\cdot}4096_0$
·4485	$1{\cdot}4109_2$	$1{\cdot}4108_8$
·4123	$1{\cdot}4142_5$	$1{\cdot}4142_0$
·3545	$1{\cdot}4227_0$	$1{\cdot}4227_3$
·3308	$1{\cdot}4275_3$	$1{\cdot}4275_9$
·3142	$1{\cdot}4318_2$	$1{\cdot}4318_2$
·3090	$1{\cdot}4333_1$	$1{\cdot}4333_2$
·2883	$1{\cdot}4402_5$	$1{\cdot}4402_0$

The mean values of the constants b_1 and b_0 are $\cdot953_8\times10^{-2}$ and $\cdot9402_8$ respectively, and the ordinary dispersion equation of iso-amylacetate at 8·4° C. is

$$n^2 = 1{\cdot}9402_8+\frac{\cdot954\times10^{-2}}{\lambda^2-(\cdot1088)^2}.$$

This equation was used to calculate n for some wavelengths at which experimental values had been obtained. Table V. contains a comparison of the calculated and experimental values.

Methyl Iso-Valerate.

The following pairs of values of λ and n were used in calculating the constants of the dispersion equation of methyl iso-valerate :—

λ (microns).	n.	$b_1 \times 10^2$.	b_0.
·6678	$1{\cdot}3953_5$		
·4275	$1{\cdot}4069_7$	$\cdot 920_0$	$\cdot 9258_2$
·5876	$1{\cdot}3974_4$		
·3881	$1{\cdot}4112_2$	$\cdot 922_7$	$\cdot 9251_9$
·5016	$1{\cdot}4013_3$		
·3422	$1{\cdot}4186_7$	$\cdot 920_1$	$\cdot 9252_8$
·4713	$1{\cdot}4032_8$		
·2961	$1{\cdot}4306_4$	$\cdot 924_3$	$\cdot 9252_9$

TABLE VI.

λ (microns).	n (observed).	n (calculated).
·4922	$1{\cdot}4020_0$	$1{\cdot}4019_1$
·4481	$1{\cdot}4050_6$	$1{\cdot}4050_3$
·4173	$1{\cdot}4079_0$	$1{\cdot}4078_8$
·4063	$1{\cdot}4090_0$	$1{\cdot}4090_6$
·3925	$1{\cdot}4106_8$	$1{\cdot}4107_1$
·3861	$1{\cdot}4114_9$	$1{\cdot}4115_3$
·3625	$1{\cdot}4148_9$	$1{\cdot}4150_2$
·3338	$1{\cdot}4205_0$	$1{\cdot}4204_8$
·3274	$1{\cdot}4220_0$	$1{\cdot}4219_2$
·3094	$1{\cdot}4266_8$	$1{\cdot}4265_2$
·2883	$1{\cdot}4334_0$	$1{\cdot}4332_8$
·2767	$1{\cdot}4380_8$	$1{\cdot}4378_0$

The mean values of b_1 and b_0 are $\cdot 921_8 \times 10^{-2}$ and $\cdot 9253_9$ respectively. Thus the ordinary dispersion equation of methyl iso-valerate at 10·5° C. is

$$n^2 = 1 \cdot 9253_9 + \frac{\cdot 922 \times 10^{-2}}{\lambda^2 - (\cdot 1075)^2}.$$

From this equation values of n were calculated for several wave-lengths at which experimental values had been found. A comparison of the two is given in Table VI.

Acetone.

The constants of the dispersion equation of acetone were calculated using the following pairs of values of λ and n:—

λ (microns).	n.	$b_1 \times 10^2$.	b_0.
·6678	$1 \cdot 3611_1$	$\cdot 889_0$	$\cdot 8321_1$
·4242	$1 \cdot 3730_4$		
·5876	$1 \cdot 3634_4$	$\cdot 885_8$	$\cdot 8323_4$
·3976	$1 \cdot 3759_5$		
·5016	$1 \cdot 3673_0$	$\cdot 898_9$	$\cdot 8319_5$
·3745	$1 \cdot 3792_5$		
·4472	$1 \cdot 3711_9$	$\cdot 898_6$	$\cdot 8320_8$
·3354	$1 \cdot 3863_4$		

The mean values of b_1 and b_0 are $\cdot 893 \times 10^{-2}$ and ·8321 respectively. The ordinary dispersion equation of acetone at 8·4° C. is therefore

$$n^2 = 1 \cdot 8321_0 + \frac{\cdot 893 \times 10^{-2}}{\lambda^2 - (\cdot 1124)^2}.$$

Table VII. contains a comparison of the experimental results at certain wave-lengths and the values calculated from this equation.

The Calculation of e/m.

The value of e/m can be calculated from the results of the experiments on the magneto-optical and ordinary dispersion of the three liquids.

It can be shown that when the experimental results are represented by equations involving only one absorption band the value of e/m can be deduced from the simple relation

$$\frac{e}{m} = \frac{2KC^2}{b_1}.$$

TABLE VII.

λ (microns).	n (observed).	n (calculated).
·6563	$1{\cdot}3613_5$	$1{\cdot}3614_2$
·5893	$1{\cdot}3634_2$	$1{\cdot}3633_7$
·4861	$1{\cdot}3682_3$	$1{\cdot}3682_2$
·4698	$1{\cdot}3693_6$	$1{\cdot}3693_4$
·4587	$1{\cdot}3701_6$	$1{\cdot}3701_5$
·4378	$1{\cdot}3717_8$	$1{\cdot}3718_6$
·4178	$1{\cdot}3736_9$	$1{\cdot}3737_9$
·4070	$1{\cdot}3748_6$	$1{\cdot}3749_4$
·3840	$1{\cdot}3777_2$	$1{\cdot}3777_9$
·3654	$1{\cdot}3805_4$	$1{\cdot}3805_7$
·3455	$1{\cdot}3841_7$	$1{\cdot}3841_1$
·3338	$1{\cdot}3865_2$	$1{\cdot}3865_2$
·3274	$1{\cdot}3880_2$	$1{\cdot}3880_0$

The above relation holds when δ is measured in radians per cm. gauss and λ in cm., and the values previously given for K and b_1 must therefore be recalculated.

Substituting these new values in the equation, the following results are obtained for e/m :—

Iso-amyl acetate ... $e/m = 1{\cdot}01_5 \times 10^7$ E.M.U.
Methyl iso-valerate.. $e/m = 1{\cdot}01_1 \times 10^7$,,
Acetone ..... $e/m = {\cdot}97_5 \times 10^7$,,

SUMMARY.

The experimental results show that the magneto-optical dispersion of iso-amyl acetate, methyl-iso-valerate,

and acetone in the violet and near ultra-violet regions of the spectrum can be represented by the equation

$$n\delta = \mathrm{K}\frac{\lambda^2}{(\lambda^2-\lambda_1^2)^2},$$

where δ and n are the values of Verdet's constant and the refractive index of the liquid for a wave-length λ, and λ_1 the wave-length of the absorption band, which is situated in the Schumann-Lyman region of the spectrum. The constant K varies from liquid to liquid.

The refractive indices of the three liquids can also be represented within experimental error by an equation of the type

$$n^2-1 = b_0+\frac{b_1}{\lambda^2-\lambda_1^2},$$

where λ_1 for a given liquid has the same value as that deduced from the magneto-optical experiments and the constants b_0 and b_1 vary from liquid to liquid.

The three liquids examined in this work have different structures, and the value of λ_1 does not vary regularly with increasing molecular weight as in the case of substances belonging to the same homologous series.

The values of e/m for the three liquids are in the neighbourhood of $1{\cdot}0\times10^7$ E.M.U., and are therefore much lower than the accepted value. A value of this magnitude has been found for all the liquids examined in this laboratory, and is in agreement with the work of other observers.

The theory of magneto-optical rotation employed in this investigation satisfactorily accounts for the variation of the rotation with wave-length, but leads to a low value of e/m.

References.

(1) 'Æther and Matter,' Appendix F, p. 352.
(2) Stephens and Evans, Phil. Mag. x. p. 759 (1930)
(3) Bilestein, vol. ii. p. 132.
(4) Int. Crit. Tables, vol. i. p. 203.
(5) Int. Crit. Tables, vol. i. p. 183.
(6) Perkin, J. C. S., vol. i. p. 480 (1884)
(7) Lowry, J. C. S., vol. i. p. 91 (1914).
(8) Lowry, Int. Crit. Tables, vol. vi. p. 433.

Nov. 1936.

LXXX. *A Note on Laguerre Polynomials.*

By W. T. Howell, *M.Sc.**

IN this note a few properties of the Generalized Laguerre or Sonine polynomials are established starting from an integral representation of the confluent hypergeometric function, occurring in the theory of Bessel functions. These functions occur in problems of the reflexion of sound and light waves at a paraboloidal surface.

§ 1. *The Generalized Laguerre Polynomial.*

When $L_n^{\alpha}(x)$ is defined as the coefficient of z^n in the expansion of

$$\exp\left(-\frac{xz}{1-z}\right)\Big/(1-z)^{\alpha+1}$$

in ascending powers of z, it may be shown that

$$L_n^{\alpha}(x)=\frac{(\alpha+1)_n}{n!}\,{}_1F_1(-n,\ \alpha+1,\ x)$$

$$=\frac{e^x x^{-\frac{\alpha}{2}}}{n!}\int_0^{\infty} e^{-t}t^{n+\frac{\alpha}{2}}J_{\alpha}(2\sqrt{tx})\,dt, \quad (1.1)$$

where [1] $R(n+\alpha+1)>0$, $\left|\arg\frac{1}{2\sqrt{x}}\right|<\frac{\pi}{4}$, $R(\alpha)>-1$.

When α takes the special values $\pm\frac{1}{2}$ the functions $L_n^{\alpha}(x^2)$ can be expressed in terms of Hermite's polynomial [2] $U_n(x)$ by the relations

$$L_n^{-\frac{1}{2}}(x^2)=\frac{(-)^n 1}{2^{2n}n!}\,U_{2n}(x), \quad . \quad . \quad . \quad . \quad . \quad (1.2)$$

$$xL_n^{\frac{1}{2}}(x^2)=\frac{(-)^n 1}{2^{2n+1}n}\,U_{2n+1}(x). \quad . \quad . \quad . \quad (1.3)$$

§ 2. *Products of Laguerre Polynomials.*

Using (1.1) we get at once

$$n!\,m!\,(2\sqrt{x})^{2n+2m+2\alpha+2}x^{\alpha+1}e^{-2x}L_n^{\alpha}(x)L_m^{\alpha}(x)$$

$$=\int_0^{\infty} e^{-\frac{u^2}{4x}}u^{2n+\alpha+1}J_{\alpha}(u)\,du\cdot\int_0^{\infty} e^{-\frac{v^2}{4x}}v^{2m+\alpha+1}J_{\alpha}(v)\,dv,$$

* Communicated by Dr. R. H. Pickard, F.R.S.

and writing $u=p\cos\theta$, $v=p\sin\theta$, the product on the right-hand side may be written as

$$\int_0^\infty\int_0^\infty e^{-\frac{p^2}{4x}}p^{2n+2m+2\alpha+3}(\cos\theta)^{2n+\alpha+1}(\sin\theta)^{2m+\alpha+1}$$
$$\mathrm{J}_\alpha(p\cos\theta)\mathrm{J}_\alpha(p\sin\theta)\,dp\,d\theta, \quad (2.1)$$

the process being justified by a reasoning similar to that used in deducing the relation between the Beta and Gamma functions. To evaluate this double integral we note[3]

$$\mathrm{J}_\alpha(p\cos\theta)\mathrm{J}_\alpha(p\sin\theta)$$
$$=\frac{1}{2\pi i}\int_{c-\infty i}^{c+\infty i}\exp\left\{\frac{t}{2}-\frac{p^2}{2t}\right\}\mathrm{I}_\alpha\left(\frac{p^2\cos\theta\sin\theta}{t}\right)\frac{dt}{t},$$

whence, expanding I_α in powers of the argument

$$\frac{p^2\cos\theta\sin\theta}{t}$$

and integrating with respect to θ, we get

$$\int_0^{\frac{\pi}{2}}(\cos\theta)^{2n+\alpha+1}(\sin\theta)^{2m+\alpha+1}\mathrm{J}_\alpha(p\cos\theta)\,\mathrm{J}_\alpha(p\sin\theta)\,d\theta$$
$$=\sum_{s=0}^{\infty}\frac{1}{2\pi i}\int_{c-\infty i}^{c+\infty i}\exp\left\{\frac{t}{2}-\frac{p^2}{2t}\right\}\frac{\mathrm{A}_s}{t}\left(\frac{p^2}{2t}\right)^{\alpha+2s}dt, \quad (2.2)$$

where

$$\mathrm{A}_s=\frac{1}{2}\frac{\Gamma(n+\alpha+s+1)\Gamma(m+\alpha+s+1)}{s!\,\Gamma(\alpha+s+1)\Gamma(n+m+2\alpha+2s+2)}.$$

The right-hand side of (2.2) may be evaluated as follows. Expanding $\exp(-p^2/2t)$ and deforming the contour of integration we have

$$\sum_{s=0}^{\infty}\mathrm{A}_s\frac{1}{2\pi i}\int_{-\infty}^{0+}\exp\frac{t}{2}\cdot\left(\frac{p^2}{2t}\right)^{\alpha+2s}\left[\sum_{l=0}^{\infty}\frac{(-)^l}{l!}\left(\frac{p^2}{2t}\right)^l\right]\frac{dt}{t}$$
$$=\sum_{s=0}^{\infty}\mathrm{A}_s\frac{1}{2\pi i}\int_{-\infty}^{0+}\sum_{l=0}^{\infty}\frac{(-)^l}{l!}\left(\frac{p^2}{2t}\right)^{l+\alpha+2s}\frac{\exp\frac{t}{2}}{\left(\frac{t}{2}\right)^{l+\alpha+2s}}dt$$
$$=\sum_{s=0}^{\infty}\mathrm{A}_s\sum_{l=0}^{\infty}\frac{(-)^l}{l!\,(l+\alpha+2s)!}\left(\frac{p^2}{4}\right)^{l+\alpha+2s}$$
$$=\sum_{s=0}^{\infty}\mathrm{A}_s\mathrm{J}_{\alpha+2s}(p)\cdot\left(\frac{p}{2}\right)^{\alpha+2s}.$$

Thus (2.1) becomes

$$\sum_{s=0}^{\infty} \frac{A_s}{2^{\alpha+2s}} \int_0^{\infty} e^{-\frac{p}{4x}} p^{2n+2m+3\alpha+2s+3} J_{\alpha+2s}(p)\, dp.$$

Evaluating this [4] we find

$$n!\, m!\, e^{-x} L_n^{\alpha}(x) L_m^{\alpha}(x)$$

$$= \sum_{s=0}^{\infty} \frac{\Gamma(n+\alpha+s+1)\Gamma(m+\alpha+s+1)\Gamma(n+m+\alpha+2)}{s!\,(\alpha+s+1)\Gamma(n+m+2\alpha+2s+2)} \cdot x^{\alpha+2s} L_{n+m+\alpha+1}^{\alpha+2s}(x), \quad (2.3)$$

and since, whenever $n+m+\alpha+1$ is a positive integer or zero,

$$x^{\alpha+2s} L_{n+m+\alpha+1}^{\alpha+2s}(x) = (-)^{\alpha+2s} \frac{\Gamma(n+m+2\alpha+2s+2)}{\Gamma(n+m+\alpha+2)} L_{n+m+2\alpha+2s+1}^{-\alpha-2s}(x),$$

we have alternatively

$$n!\, m!\, e^{-x} x^{\alpha} L_n^{\alpha}(x) L_m^{\alpha}(x) = \sum_{s=0}^{\infty} (-)^{\alpha+2s} \frac{\Gamma(n+\alpha+s+1)\Gamma(m+\alpha+s+1)}{s!\,\Gamma(s+\alpha+1)} \cdot L_{n+m+2\alpha+2s+1}^{-\alpha-2s}(x). \quad (2.4)$$

The relations (1.2), (1.3) further enable us to express products of Hermite polynomials as a series of generalized Laguerre polynomials.

§ 3. *Miscellaneous Results.*

Hankel's inversion formula states that if

$$F(x) = \int_0^{\infty} J_m(xt) f(t) t\, dt,$$

then

$$f(t) = \int_0^{\infty} J_m(xt) F(x) x\, dx.$$

Applying this formula to (1.1) we get

$$e^{-x} x^{n+\frac{\alpha}{2}} = n! \int_0^{\infty} e^{-t} t^{\frac{\alpha}{2}} J_{\alpha}(2\sqrt{xt}) L_n^{\alpha}(t)\, dt. \quad (3.1)$$

Now since

$$x^{\alpha}L_n^{\alpha}(x) = \frac{e^x}{n!}\frac{d^n}{dx^n}(e^{-x}x^{n+\alpha}), \quad . \quad . \quad . \quad (3.2)$$

we have from (3.1)

$$e^{-x}x^{\alpha}L_n^{\alpha}(x) = \int_0^{\infty} e^{-t}t^{\frac{\alpha}{2}}L_n^{\alpha}(t)\frac{d^n}{dx^n}\left[x^{\frac{\alpha}{2}}J_{\alpha}(2\sqrt{tx})\right]dt,$$

which reduces to

$$e^{-x}x^{\frac{n+\alpha}{2}}L_n^{\alpha}(x) = \int_0^{\infty} e^{-t}t^{\frac{n+\alpha}{2}}L_n^{\alpha}(t)J_{\alpha-n}(2\sqrt{xt})\,dt, \quad (3.3)$$

which states that

$$e^{-\frac{x^2}{2}}\left(\frac{x^2}{2}\right)^{\frac{n+\alpha}{2}}L_n^{\alpha}\left(\frac{x^2}{2}\right)$$

is symmetrical in a Hankel transform of order $\alpha-n$. This result is of similar character to that given by Wilson [5] and Koshliakov [6].

If we take (1.1) and write τv^2 for t, $\rho^2/4\tau$ for x, we get

$$2^{-\alpha-1}\tau^{-n-\alpha-1}\rho^{\alpha}e^{-\frac{\rho^2}{4\tau}}L_n^{\alpha}\left(\frac{\rho^2}{4\tau}\right) = \int_0^{\infty} e^{-v^2\tau}v^{2n+\alpha+1}J_{\alpha}(\rho v)\,dv.$$

Now multiply both sides by $e^{-\lambda\tau^2}$ and integrate with respect to τ both sides between 0 and ∞ we get

$$\rho^{\alpha}2^{-\alpha-1}\int_0^{\infty} e^{-\lambda^2\tau}\tau^{-n-\alpha-1}e^{-\frac{\rho^2}{4\tau}}L_n^{\alpha}\left(\frac{\rho^2}{4\tau}\right)d\tau$$

$$= -\int_0^{\infty}\frac{v^{2n+\alpha+1}J_{\alpha}(v\rho)}{v^2+\lambda^2}dv. \quad (3.4)$$

According to Bateman [7] the right-hand side reduces to a Bessel function. Watson [8] shows, however, that this is only the case when $n=0$ when it takes the value

$$-\tfrac{1}{2}\lambda^{\alpha}K_{\alpha}(\lambda\rho).$$

In the equation (1.1) write $x+y$ for x and express the Bessel function under the integral sign as an expansion of Lommel's [9] type when we get immediately

$$e^{-y}L_n^{\alpha}(x+y) = \sum_{m=0}^{\infty}\frac{(-)^m}{m!}y^m L_n^{\alpha+m}(x). \quad . \quad . \quad (3.5)$$

Integrals of the type discussed by Van der Pol and Niessen (10) may be evaluated by the use of the known properties of Bessel functions: for example, we find

$$\int_0^x e^{\xi}(x-\xi)^{\alpha} L_n^{\alpha}(x-\xi)\, d\xi$$

$$= x^{\frac{\alpha+1}{2}} e^x \int_0^{\infty} e^{-t} t^{n+\frac{\alpha-1}{2}} I_{\alpha+1}(2\sqrt{tx})\, dt. \quad (3.6)$$

References.

(1) Watson, 'Theory of Bessel Functions,' § 13.3.
(2) Bateman, 'Partial Differential Equations of Mathematical Physics,' p. 454.
(3) Watson, *ibid.* § 13.7 (1).
(4) Watson, *ibid.* § 13.3 (3).
(5) Wilson, Messenger of Maths. vol. liii. p. 159 (1924).
(6) Koshliakov, *ibid.* vol. lv. p. 153 (1926).
(7) Bateman, 'Electrical and Optical Wave Motion,' p. 103 (223)
(8) Watson, 'Theory of Bessel Functions,' § 13.6.
(9) Watson, *ibid.* § 5.22 (1).
(10) Van der Pol and Niessen, Phil. Mag. 7 ser. vol. xiii. p. 575 (1932).

LXXXI. *The Theory of Electrosmotic Circulation in Closed Vessels.* By PAUL WHITE, *M.A., Ph.D., Lecturer in Physics in the University of Reading* *.

WHEN a sol is placed in an electric field the dispersed particles take up velocities which vary according to their position in the liquid. The velocity in any small region is the resultant of that imposed on the particles by electrophoresis and of that possessed by the dispersion fluid in the region. The motion of the dispersion fluid is initiated by electrosmosis at the boundary and communicated to the interior by viscosity. This motion produces a hydrostatic pressure-gradient which causes a return flow in the middle of the vessel. When measuring the electrophoretic and electrosmotic mobilities by means of the ultramicroscope the effect of this return flow must be taken into account.

In 1914 v. Smoluchowski † elaborated the theory of the return flow, and in 1919 Svedberg and Andersson ‡

* Communicated by the Author.

† v. Smoluchowski, M., article in Graetz's *Handbuch der Elektrizität und des Magnetismus*, ii. p. 382 (1921).

‡ Svedberg, T., and Andersson, E., *Koll.-Zeit.* xxiv. p. 156 (1919).

verified it experimentally for chambers of rectangular section. v. Smoluchowski's treatment was, however, founded on certain assumptions. These assumptions were justified in Svedberg and Andersson's experiments, but are frequently overlooked, and may lead to serious errors. It is proposed to show here how two of these sources of error may be eliminated.

In the first place the electrosmotic mobility at one face of the cell containing the colloidal suspension is assumed by v. Smoluchowski to be equal to that at the opposite face. In practice the two mobilities are often found to differ considerably. They will certainly do so if the walls of the cell are of different materials or if they have not been cleaned in the same way, and may even do so when the materials and conditions of the walls appear to be exactly the same. Cells are frequently built with opposite faces of different kinds of glass, and Lane and the author * have found this to be sufficient to cause a marked inequality in mobility. Moreover, the extent of this inequality was found to vary in the course of a protracted experiment, presumably on account of progressive adsorption or dissolution of traces of impurity.

In § 1 we shall elaborate the modification of v. Smoluchowski's theory made necessary by inequality of electrosmosis. We prove that the distribution of velocity which, according to his theory, is represented by a parabola symmetrically situated in the cell remains parabolic but is no longer symmetrically situated. This asymmetry has been observed by many workers. It has been suggested that the displacement of the parabola is due either to convection of the liquid or to sedimentation of the dispersed particles. In §§ 2 and 3 we demonstrate that neither of these hypotheses is tenable.

Secondly, v. Smoluchowski assumed that, for cells of rectangular section, two dimensions of the cell are each much larger than the third, with the result that the electrosmotic drag set up at the more distant walls is negligible compared with that set up at the closest pair. We have been unable to find in the literature any criterion for determining how nearly this condition is satisfied in a cell of given finite size. Where measure-

* Lane, T. B., and White, P., Phil. Mag. xxiii. p. 824 (1937).

ments are to be made by means of a slit ultramicroscope the simple theory is especially open to objection on the grounds that the region of the liquid under observation is usually at comparable distances from three faces, namely, the face through which the illuminating beam enters and the two faces perpendicular to the axis of the microscope. In § 4 we estimate the magnitude of the error introduced by neglecting the electrosmotic drag set up at the first of these faces.

§ 1. *Unequal Electrosmosis at Opposite Faces.*

We consider first the case of a rectangular cell in which the electrosmotic velocity w' at the upper face differs from that w at the lower face and in which the depth $2h$ is small compared with the length $2c$ and breadth $2b$. The effects of the end and side faces on the motion of the liquid can therefore be neglected. The cell is assumed to be staunch, and so there is no net transport of fluid across any section perpendicular to the electric field.

If the electrosmotic velocities w and w' were equal the electrophoretic velocity K could be found by making a single set of measurements of particle-velocity at either of the anelectrosmotic levels of von Smoluchowski, *i. e.*, at a distance $h/\sqrt{3}$ above or below the middle plane of the cell. The observed velocities would then be equal to one another and to the electrophoretic velocity. But, since w and w' are unequal, the velocities at these two levels are also unequal, and we are confronted with the problem of calculating from the observed values the electrophoretic velocity and the two electrosmotic velocities.

To evaluate separately the three unknowns, w, w', and K, it will, of course, be necessary to make three sets of measurements at three different levels. It can, however, be shown that if *two* suitable levels are chosen, measurements at these two levels are sufficient to give *one* of the three unknowns. The other two cannot then be calculated separately. For example, measurements at the two levels indicated by v. Smoluchowski enable us to determine K, although they do not in general provide as accurate an estimate as that given by certain other pairs of levels. Neither set of them taken alone is sufficient to give any of the unknowns explicitly.

We begin by obtaining expressions for the three unknown velocities in terms of three observed velocities v_1, v_2, v_3 at *any* three levels y_1, y_2, y_3 respectively. The origin of coordinates is at the mid-point of the cell, and the x-axis is parallel to the electric field. For convenience in description the y-axis is spoken of as vertical, but the validity of the following analysis is independent of the position of the cell relative to the direction of gravity.

It is proved in § 2 that even when w and w' are unequal the relationship between v and y remains of the parabolic form found by v. Smoluchowski. Let the parabola be

$$y^2 = av + by + c. \quad . \quad . \quad . \quad . \quad . \quad (1)$$

Then we have

$$y_1^2 = av_1 + by_1 + c,$$
$$y_2^2 = av_2 + by_2 + c,$$
$$y_3^2 = av_3 + by_3 + c.$$

Hence

$$a = \frac{1}{\Delta}\begin{vmatrix} y_1^2 & y_1 & 1 \\ y_2^2 & y_2 & 1 \\ y_3^2 & y_3 & 1 \end{vmatrix} = \Delta_a/\Delta, \text{ say} \quad . \quad (2a)$$

$$= -\Delta^{-1}(y_2 - y_3)(y_3 - y_1)(y_1 - y_2);$$

$$b = \frac{1}{\Delta}\begin{vmatrix} v_1 & y_1^2 & 1 \\ v_2 & y_2^2 & 1 \\ v_3 & y_3^2 & 1 \end{vmatrix}; \quad . \quad . \quad . \quad . \quad . \quad (2b)$$

$$c = \frac{1}{\Delta}\begin{vmatrix} v_1 & y_1 & y_1^2 \\ v_2 & y_2 & y_2^2 \\ v_3 & y_3 & y_3^2 \end{vmatrix}; \quad . \quad . \quad . \quad . \quad . \quad (2c)$$

where

$$\Delta = \begin{vmatrix} v_1 & y_1 & 1 \\ v_2 & y_2 & 1 \\ v_3 & y_3 & 1 \end{vmatrix}. \quad . \quad . \quad . \quad . \quad . \quad . \quad . \quad (2d)$$

The velocity v is the actual velocity of a particle at a height y above the middle point of the cell. The liquid

in the neighbourhood of this particle has a velocity u, equal to $v-\mathrm{K}$. K can be evaluated in terms of a, b, and c (and hence in terms of the measured quantities) by equating to zero the aggregate transport of liquid across a section of unit breadth, thus :—

$$\int_{-h}^{+h} u\,dy = \int_{-h}^{+h} (v-\mathrm{K})\,dy = 0,$$

or

$$\int_{-h}^{+h} v\,dy = \int_{-h}^{+h} \mathrm{K}\,dy = 2\mathrm{K}h.$$

Hence, from (1)

$$2\mathrm{K}h = \int_{-h}^{+h} \frac{1}{a}(y^2-by-c)\,dy,$$

and from (2a), (2c)

$$\mathrm{K} = \frac{1}{a}(\tfrac{1}{3}h^2-c) \quad . \quad . \quad . \quad . \quad . \quad . \quad (3)$$

$$= \Delta_a^{-1} \begin{vmatrix} 1 & 0 & \tfrac{1}{3}h^2 & 0 \\ 1 & v_1 & y_1^2 & y_1 \\ 1 & v_2 & y_2^2 & y_2 \\ 1 & v_3 & y_3^2 & y_3 \end{vmatrix} . \quad . \quad . \quad . \quad . \quad (4)$$

We proceed to evaluate the electrosmotic velocities by making use of the fact that the particle-velocity at the lower surface is $(w+\mathrm{K})$ and at the upper surface $(w'+\mathrm{K})$.

From (1)

$$w+\mathrm{K} = \frac{1}{a}(h^2+bh-c),$$

$$w'+\mathrm{K} = \frac{1}{a}(h^2-bh-c).$$

Inserting from (3) we obtain

$$w = \frac{h}{a}(\tfrac{2}{3}h+b),$$

$$w' = \frac{h}{a}(\tfrac{2}{3}h-b).$$

Hence $w=\Delta_a^{-1}\begin{vmatrix} 0 & 0 & \frac{2}{3}h^2 & -h \\ 1 & v_1 & y_1^2 & y_1 \\ 1 & v_2 & y_2^2 & y_2 \\ 1 & v_3 & y_3^2 & y_3 \end{vmatrix}$ and

$$w'=\Delta_a^{-1}\begin{vmatrix} 0 & 0 & \frac{2}{3}h^2 & +h \\ 1 & v_1 & y_1^2 & y_1 \\ 1 & v_2 & y_2^2 & y_2 \\ 1 & v_3 & y_3^2 & y_3 \end{vmatrix} . \quad . \quad (5)$$

From equations (4) and (5) it can be shown that by choosing suitable levels y_2 and y_3 for the measurement of v_2 and v_3 we can dispense with the measurement of v_1 in finding K, though not in finding w and w' separately; for if we make the minor of v_1 in the determinant of (4) zero, this equation for K will be independent of v_1. The corresponding minors in the determinants of (5) can be made zero (and thus w and w' found separately) only by choosing other suitable values of y_2 and y_3.

To determine K from two measurements only we must therefore have

$$\begin{vmatrix} 1 & \frac{1}{3}h^2 & 0 \\ 1 & y_2^2 & y_2 \\ 1 & y_3^2 & y_3 \end{vmatrix} = (y_2-y_3)(y_2y_3+\tfrac{1}{3}h^2)=0. \quad . \quad (6)$$

If y_2 and y_3 are equal Δ_a is zero, and the value obtained for K from (4) is indeterminate. The second factor in (6) must therefore be made zero, and we may say that:

In order to evaluate K from two velocity-measurements only, when the electrosmotic mobilities at the upper and lower faces of the cell are unknown and unequal, the two levels at which the velocities are measured must be on opposite sides of the middle plane of the cell, and the product of their distances from the middle plane must be one-twelfth of the square of the depth of the cell.

When this condition is satisfied the value of K is given by

$$K=\frac{v_3y_2-v_2y_3}{y_3-y_2}.$$

The two levels indicated by v. Smoluchowski ($y=h/\sqrt{3}$) are among the pairs of levels which fulfil this condition. In this case the value of K is the arithmetic mean of the observed velocities.

In order to obtain w explicitly by two measurements only, y_2 and y_3 must be so chosen that

$$y_2+y_3=-\tfrac{2}{3}h, \quad . \quad . \quad . \quad . \quad . \quad . \quad (7)$$

in which case $$w=h\frac{v_2-v_3}{y_3-y_2}.$$

The conditions (6) and (7) for finding K and w explicitly are simultaneously satisfied when y_2 and y_3 are equal to $-h$ and $+\frac{1}{3}h$. The motion at each of these levels is entirely independent of the electrosmosis at the upper face. Similarly measurements at $y=+h$ and $-\frac{1}{3}h$ give K and w' independently of w. It is not possible to obtain w and w' independently of K by two observations only. This is also obvious on physical grounds.

From the results of the foregoing paragraph it is easy to express the equation to the displaced parabola in terms of the electrokinetic velocities, thus

$$v=\mathrm{K}+\frac{w'}{4h^2}(y+h)(3y-h)+\frac{w}{4h^2}(y-h)(3y+h). \quad . \quad (8)$$

§ 2. *Convection Currents.*

The foregoing treatment can easily be extended to take into account the effects of incipient thermal and electrolytic convection currents. In practice care is taken to minimize convection, and no measurements are made until the particles are observed to be (but for Brownian motion) at rest when the field is switched off. This is no guarantee, however, that the motion observed when the field is acting is not disturbed by differences in density due either to temperature or to separation of electrolytic products. It is therefore desirable to have some means of discovering from the measurements themselves whether convection is taking place.

Changes in density due to electrolysis arise only at the electrodes, while those due to heat may arise at any wall of the cell. However, the only thermal effects relevant to the present problem are those occurring

near the electrodes, since no others are capable of setting up convection in the direction in which the component of particle-velocity is measured. We further simplify the conditions by assuming that the heating and electrolysis have not been acting long enough to cause differences in temperature or chemical composition between the various layers of fluid in the middle of the cell where measurements are made.

When the density of the fluid is uniform throughout the cell the vertical pressure-gradient is also uniform, and hence the horizontal pressure-gradient $\partial p/\partial x$ set up along the cell by electrosmosis and viscosity is the same at all levels; on the other hand, when the density is different in the neighbourhood of the two electrodes the horizontal pressure-gradient varies with depth and the constant term (l) must be supplemented by a function of y ($f(y)$, say) in the equation of motion, which then runs

$$\eta \frac{\partial^2 u}{\partial y^2} = \frac{\partial p}{\partial x} = l + f(y),$$

where η is the coefficient of viscosity.

It is out of the question to specify $f(y)$ exactly, but sufficient information about its general form can be gained from the following considerations. The immediate result of electrolysis and of diffused heat supply at the end faces is to generate a layer of liquid of abnormal density and of roughly uniform thickness over the electrodes. The presence of this uniform layer gives rise to a term in $f(y)$ proportional to y. As this layer sinks or floats and is replenished modifications appear which we may represent by higher powers of y, possibly associated with a constant. Thus we can write

$$f(y) = m + qy + ry^2 + \ldots + sy^n + \ldots,$$

where the term qy is always present and is initially the only important term. Moreover, it is clear that the constant can only occur if the higher terms are also present; for otherwise there would be a net force tending to drive the liquid bodily along the cell. Hence we have

$$\eta u = c_1 + c_2 y + \tfrac{1}{2}(l+m)y^2 + \tfrac{1}{6}qy^3 + \ldots + \frac{sy^{(n+2)}}{(n+1)(n+2)} + \ldots,$$

where c_1 and c_2 are constants of integration.

If the relation between u and y is found experimentally to be parabolic the only coefficient in $f(y)$ which can differ from zero is m; but as $f(y)$ cannot consist of m alone without higher terms it must be zero, and no convection can be taking place in the xy-plane. We thus reach the important conclusion that a parabolic velocity-distribution cannot arise from convection; it can only arise from electrosmosis. The parabola may be either symmetrically situated in the cell, as found by v. Smoluchowski, or unsymmetrically situated, as found in our experiments* and others. In each case its occurrence is evidence of the absence of convection. The onset of convection is indicated by a transition from parabolic form—first to cubic, then to a more complicated distribution.

§ 3. *Sedimentation.*

We have hitherto supposed that the effect of gravity on the dispersed particles could be neglected. Let us now assume that each particle has a vertical velocity V, which may be of either sign (buoyancy or sedimentation). Let its motion be subject to a viscous drag equal to k times its velocity relative to the neighbouring liquid. Then, if the velocity of the liquid is given by

$$u=\alpha+\beta y+\gamma y^2,$$

the equation of horizontal motion of the particle is

$$m\dot{v}=k(\alpha+\beta y+\gamma y^2+\mathrm{K}-v)$$

with

$$\dot{y}=\mathrm{V},$$

m being the effective inertia of the particle (mass plus hydrodynamical inertia).

The solution to this equation can easily be shown to be

$$v=v_0\exp\left(-\frac{kt}{m}\right)+\alpha+\frac{m^2\mathrm{V}^2}{k^2}\gamma+\beta\left(y-\frac{m\mathrm{V}}{k}\right)+\gamma\left(y-\frac{m\mathrm{V}}{k}\right)^2+\mathrm{K},$$

where v_0 is a constant of integration determined by the initial conditions. The exponential term in this expression

* Lane and White, *loc. cit.*

diminishes exceedingly rapidly. The remainder represents a parabola of the same size, but not in the same position, as that which would be obtained if V were zero. The effect of the vertical motion is to displace the parabola by a distance $\frac{m\mathrm{V}}{k}$ vertically and $\frac{m^2\mathrm{V}^2\gamma}{k^2}$ horizontally.

To form a numerical estimate of the magnitude of this displacement we take the case of a spherical particle of radius r and density ρ, suspended in a liquid of density ρ'. If Stokes's law holds, k equals $6\pi\eta r$ and V equals

$$\frac{2g}{9\eta}(\rho-\rho')r^2.$$

The vertical displacement of the parabola (δ, say) is given by

$$\delta = \frac{m\mathrm{V}}{k} = \frac{2g}{81\eta^2}(2\rho+\rho')(\rho-\rho')r^4.$$

For a quartz sphere in water :

when $r=1$ micron, δ is about 2×10^{-10} cm.

when $r=10$ microns, δ is about 2×10^{-6} cm.

when $r=100$ microns, δ is about 200 microns.

We may conclude that with particles of less than a fifth of a millimetre in linear dimensions the displacement of the parabola by sedimentation will be quite impossible to detect.

§ 4. *Finite Breadth of Cell.*

We now consider the case in which the electrosmotic velocity w is the same at all the walls, but the breadth ($2b$) of the cell perpendicular to the field, though very small relative to the length, is comparable with the depth ($2h$).

The motion is clearly equivalent to that which would be set up by a suitable pressure-gradient in a pipe of rectangular section moving in the direction of its length with velocity w. The problem of flow through a rectangular pipe at rest has been solved by Cornish *, and the solution can be transferred to meet the present requirements by superimposing a velocity w on the

* Cornish, R. J., Proc. Roy. Soc. A, cxx. p. 697 (1928).

whole system and then assigning to the pressure-gradient such a value that there is no net transport of fluid over the cross-section.

The solution given by Cornish, after transforming to our notation and impressing a velocity w, runs

$$u = w - \frac{1}{2\eta}\frac{\partial p}{\partial x}(h^2 - y^2) + \frac{32}{\pi^3}\frac{h^2}{2\eta}\frac{\partial p}{\partial x}\mathscr{E}(h, b, y, z),$$

where

$$\mathscr{E}(h, b, y, z) = \sum_{r=0}^{\infty}\left[(-1)^r(2r+1)^{-3} \times \frac{\cosh\overline{(2r+1).\pi z/2h)}}{\cosh\overline{(2r+1).\pi b/2h)}}\cos\frac{\overline{2r+1}.\pi y}{2h}\right].$$

Integrating over the whole cross-section we obtain the net volume transported in unit time,

$$Q = 4bhw - \frac{4}{3}\frac{bh^3}{\eta}\frac{\partial p}{\partial x} + \frac{256}{\pi^5}\cdot\frac{h^4}{\eta}\cdot\frac{\partial p}{\partial x}\mathscr{I}(b, h),$$

where

$$\mathscr{I}(b, h) = \sum_{r=0}^{\infty}\left[(2r+1)^{-5}\tanh\frac{\overline{2r+1}.\pi b}{2h}\right].$$

By setting $Q=0$ we can obtain the required expression for $\partial p/\partial x$ in terms of w, and on inserting this expression in the original equation for u we have finally

$$u = w\left[\frac{3y^2}{2h^2} - \frac{1}{2} + \frac{48}{\pi^3}\mathscr{E} - \frac{192}{\pi^5}\frac{h}{b}\mathscr{I}\right] \div \left[1 - \frac{192}{\pi^5}\frac{h}{b}\mathscr{I}\right].$$

For practical purposes what we require to know is the position of points in the cell where the electrosmotic and return currents balance out ($u=0$), since measurements of particle-velocity at these points give the electrophoretic velocity directly. Such points lie on an oval cylinder which, when h is vanishingly small relative to b, opens out into the two planes given by v. Smoluchowski. Two cases of special interest are shown in figs. 1 and 2. Fig 1 illustrates the arrangement frequently used with the slit ultramicroscope, the breadth being large and the working region being close to one of the vertical faces. In fig. 2 the section of the cell

is a square. For the case of fig. 1 the following table gives the fluid-velocity at the level $y=h/\sqrt{3}$ and the depth at which the fluid-velocity is zero.

Fig. 1.

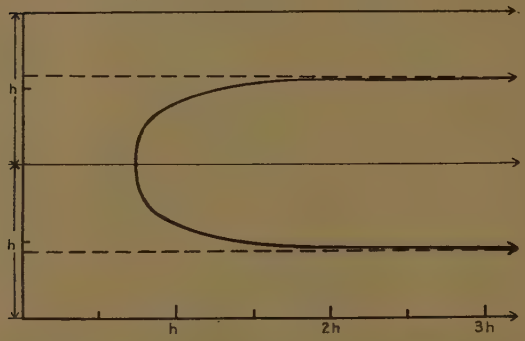

Surface of zero velocity near the side of a long, shallow cell.
— — — —, levels given by v. Smoluchowski.

Fig. 2.

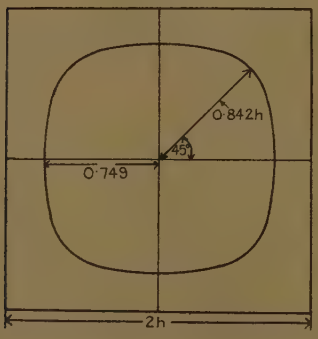

Surface of zero velocity in a long cell of square section.

The error introduced by working at the levels given by v. Smoluchowski, when the electrosmosis is the same at all faces, is thus less than 1 per cent. of the

electrosmotic velocity, provided that the point of observation is more than one and a half times the depth of the cell from the side face.

Distance from vertical wall in terms of depth of cell ($2h$).	Fluid velocity at the level $y=h/\sqrt{3}$.	Distance (from mid plane) of points where $u=0$.
$\frac{1}{2}\times 2h$	$0{\cdot}199w$	$0{\cdot}400h$
$1\times 2h$	$0{\cdot}041w$	$0{\cdot}553h$
$1\frac{1}{2}\times 2h$	$0{\cdot}009w$	$0{\cdot}572h$
Large	nil.	$0{\cdot}577h$

It is a pleasure to have this opportunity of thanking Prof. J. A. Crowther for his stimulating interest in this work and Dr. W. N. Bond for valuable advice in discussion.

Summary.

Two sources of error which may arise in electrophoretic measurements can be eliminated if the observations are interpreted in the light of the following modifications to v. Smoluchowski's theory of electrosmotic circulation.

(1) The parabola representing the distribution of electrosmotic velocity in a closed rectangular cell is not necessarily situated symmetrically in the cell. When it is found to be displaced the electrokinetic velocities can be calculated by the formulæ (8).

The asymmetry arises from inequality of electrosmosis at opposite faces of the cell. It cannot be caused by convection as long as the distribution curve is a true parabola (§ 2), nor can it usually be attributed to buoyancy or sedimentation of the particles (§ 3).

(2) In using a slit ultramicroscope an error may be introduced by working near the face of the chamber through which the illuminating beam enters. This error (which is due to electrosmotic drag at the face in question) is less than 1 per cent. of the electrosmotic velocity when observations are made at a distance from this face greater than one and a half times the depth of the chamber.

LXXXII. *An Improved Method of Measuring Electrophoresis by the Ultramicroscope.*

By T. B. Lane, *B.Sc., a Senior Scholar of the University of Reading, and* Paul White, *M.A., Ph.D., Lecturer in Physics in the University of Reading* *.

IN the course of some experiments on electrophoresis in rectangular cells we have recently obtained results which are in conflict with v. Smoluchowski's theory of electrosmotic circulation. According to this theory † the velocity of the liquid varies with depth in a manner which may be represented by a parabola symmetrically situated in the cell. In our experiments the variation with depth obeyed a parabolic law, but was often markedly unsymmetrical. Since the accepted method of measuring electrophoretic velocities is based on v. Smoluchowski's theory, this asymmetry may lead to serious errors. The discrepancy between the true electrophoretic velocity and that which would have been obtained by the usual method frequently exceeded 30 per cent. and varied irregularly from one set of observations to another. By slightly generalizing the theory and modifying the method of measurement to correspond, the values obtained could be made mutually consistent to within about 5 per cent., even in the most unfavourable cases.

The results of a typical set of observations at different levels in a hydrosol of graphite are shown in the figure. It will be seen that the plotted points fit a parabola to within the limits of experimental error, but that the parabola is displaced downwards from a central position through a distance equal to about 1/20th of the depth of the cell ($d=3$ mm.). According to v. Smoluchowski's theory the velocity of the liquid due to electrosmosis should be zero at the two levels marked by broken lines in the figure ($0{\cdot}211\,d$ from top or bottom face), and the velocity of a particle at either of these levels should be simply its electrophoretic velocity. The values actually obtained by interpolation are, however, 11·4 and $22{\cdot}0\,\mu$/sec. in this case. Since there is no reason

* Communicated by the Authors.

† v. Smoluchowski, M., article in Graetz's *Handbuch der Elektrizität und des Magnetismus,*' ii. p. 382 (1921).

why the electrophoresis should vary systematically from place to place in a well-mixed sol, the circulation of the liquid clearly cannot be that required by theory.

Disturbances of the electrosmotic flow might be ascribed to the action of one or more of the following three agencies: convection, sedimentation, and inequality of electrosmotic mobility at the top and bottom walls of the cell. The effect of each of these factors has been examined theoretically by one of us in the paper immediately preceding this *. It has been shown that the result

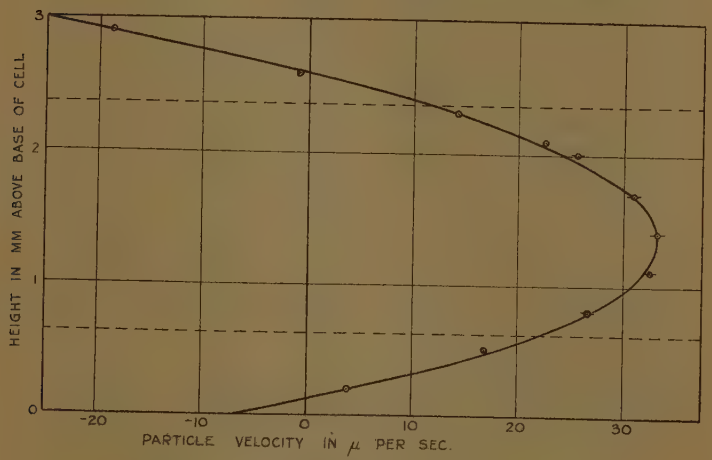

Variation of particle-velocity with depth in cell.

-------- Levels of v. Smoluchowski.
Particle-velocity at v. Smoluchowski's level (upper): 11·4 μ/sec.
" " " (lower): 22·0 μ/sec.
Hence :—Electrophoretic velocity: 16·7 μ/sec.
Particle-velocity at walls (upper): −25·1 μ/sec.
" " (lower): −6·6 μ/sec.
Hence :—Electrosmotic velocity (upper wall): 41·8 μ/sec.
" " (lower wall): 23·3 μ/sec.
The whole length of the stroke through a plotted point represents twice the probable error of the mean. Where no stroke is drawn, the probable error was too small to be shown on this scale.

of incipient convection is to distort the velocity-parabola into a curve of higher order. No arrangement of convection-currents can simulate the effect of viscosity and

* White, P., Phil. Mag. xxiii. p. 811 (1937).

electrosmosis in producing a parabola, whether central or displaced. Sedimentation certainly causes a displacement of the curve, but by an amount which is quite undetectable unless the sedimentation is rapid enough to cause the suspension to settle out completely in a time comparable with the duration of the experiment. Since the observed velocity-distribution is parabolic, and since the sols used were quite stable over a period of several months, both convection and sedimentation can be ruled out in the present case.

When the electrosmotic mobilities at the top and bottom faces of the cell are unequal, it has been shown (*ibid.*) that the velocity-diagram remains parabolic, but is displaced vertically, as found experimentally. The levels given by v. Smoluchowski are now no longer those at which the motion of the particles is due simply to electrophoresis. However, the electrophoretic velocity can be found in this case by observing at *both* these levels and taking the mean of the two values so obtained. No useful information is to be gained by measuring at one of the levels only. In the case shown in the figure the electrophoretic velocity (K) is actually 16·7 μ/sec., and a single set of measurements made at either of the prescribed levels would have been in error by 31·7 per cent. if taken alone as an estimate of K.

It is noteworthy that the agreement between the experimental points and the parabola (in this, as in every case we observed) continues to hold up to the smallest, conveniently-measurable distances from the walls. It seems reasonable to conclude that the asymmetry is evidence of a genuine difference of electrosmosis, and is not immediately caused by any agency operating in the body of the liquid.

Further evidence that the displacement of the parabola is a purely electrosmotic phenomenon and that the electrophoretic motion is in no way affected by it, is provided by the results of a series of observations made at the prescribed levels on different samples of the same material in the same cell. These data, which emphasize the necessity of measuring at both levels, are contained in the following table.

The most striking feature of these results is the close agreement between the electrophoretic velocities obtained by averaging v_1 and v_2 (the velocities at the prescribed

levels) in spite of wide variations of v_1 and v_2 individually. It will be seen that the velocity as deduced from measurements made only at the top level varies from 10·0 to 15·4, and at the bottom level from 14·8 to 20·1 μ/sec. The velocity as determined by averaging v_1 and v_2 (column 4) varies only between the values 14·7 and 15·7 μ/sec. with a probable error for a single entry of only 2·3 per cent.

We have not been able to establish with certainty what mechanism causes this variable difference between the electrosmosis at the top and bottom faces. As,

Age of sol.	Measured velocities. Top, v_1.	Measured velocities. Bottom, v_2.	Electrophoretic velocity $\frac{1}{2}(v_1+v_2)$.	Percentage error. Single level.	Percentage error. Two levels.
<1 hour .	15·4	15·3	15·4	1	1
9 hours.	15·1	15·1	15·1	<1	<1
1 day . .	14·6	14·8	14·7	3–4	3
2 days .	14·1	17·1	15·6	7–13	3
3 days .	14·5	16·7	15·6	5–10	3
6 days .	10·1	19·6	14·8	34, 29	3
7 days .	10·8	20·0	15·4	32, 29	1
8 days .	10·0	19·0	14·5	34, 32	5
9 days .	11·4	20·0	15·7	25, 32	3
10 days .	11·9	18·8	15·3	22, 24	<1
11 days .	11·4	19·6	15·5	25, 29	2
13 days .	10·1	20·1	15·1	34, 33	<1
14 days .	12·3	17·8	15·1	19, 17	<1
15 days .	12·9	17·9	15·4	15, 18	1
16 days .	11·6	18·1	14·8	24, 19	3
Probable error of a single entry	20·4 %		General mean, 15·2$_0$ 2·3 %		

however, the design of the cell necessitated the use of glass cut from different sheets, it seems probable that the extent to which ions were adsorbed on the glass from the sol differed between the faces and varied from one experiment to the next.

Summary.

The usual method of measuring electrophoresis by determining the velocities of suspended particles under the ultramicroscope at one of the levels given by v. Smoluchowski has been found to be in error by

amounts which vary irregularly and may exceed 30 per cent. of the true value. This discrepancy is due to the fact that electrosmosis at the top face of the containing vessel is not, in practice, equal to that at the bottom face, as v. Smoluchowski assumed.

The error can be eliminated by measuring at *both* the prescribed levels. The true electrophoretic velocity is the arithmetical mean of the two values so obtined.

A series of experiments on a graphite sol gave results with a probable error of 20·4 per cent. when treated in the usual way, but of only 2·3 per cent. when averaged in the manner suggested.

It is a pleasure to have this opportunity of thanking Prof. J. A. Crowther for his interest in this work and Dr. H. Liebmann for his advice and assistance.

LXXXIII. *Notices respecting New Books.*

Statistical Mechanics. By R. H. Fowler. Second Edition. [Pp. x+864.] (Cambridge University Press, 1936. Price 50*s*.)

THE former edition (1929) of Fowler's great treatise, quaintly called a monograph, is known to all those who are seriously interested in statistical mechanics and its applications. The new edition is revised and considerably enlarged (from 560 to 856 pages of text), and it will be appropriate to indicate the main changes.

The discussion of Fermi-Dirac and Einstein–Bose statistics, previously given in a final chapter, is now incorporated in the general theoretical treatment early in the book. Most of the chapters, such as those on the specific heats of gases and crystals, are extended by the inclusion of accounts of later theoretical work, the greatest increase being in the former chapters on thermionics and on electric and magnetic susceptibility. The thermionics chapter has grown into a long chapter on the metallic state, and includes a full account of the energy distribution of electrons in metals and semi-conductors, and a general discussion of conductivity and related properties. In the susceptibility chapter certain aspects of ferromagnetism are discussed, a full account being given of the theoretical treatments of the basic problem as approached by the Heisenberg method, and of the theory of the properties of single crystals. There are considerable extensions in the chapter on fluctuations, and an entirely new chapter is included dealing

with co-operative and other phenomena, such as those brought into prominence by recent work on alloys.

A very high standard of logical rigour is consistently maintained, and the book as a whole is an outstanding achievement. It has much of the comprehensiveness of a Handbuch, with the advantages of a work designed and carried out with the unifying outlook of a single author—though, in this connexion, due recognition should be given to Sutherland, Buckingham, Guggenheim, and Chandrasekhar, whose assistance with particular chapters is acknowledged.

The completeness of the book is naturally on the statistical theoretical side, and unless this is borne in mind the reader might gain a misleading impression of the state of development in connexion with some of the topics discussed. The references, moreover, sometimes appear to have been rather casually and arbitrarily chosen.

The main criticism which may be put forward is that although the book, with minor reservations, may be "unassailable in accuracy" it is far from "perfect in form" from the point of view of many of those who might wish to make use of it. The readers contemplated here are those physicists and chemists to whom the applications discussed are of the greatest interest, but who are not primarily mathematicians. The author is so familiar with the intricacies of the mathematical technique of his methods that he is not at any pains to put the statistical results in the simple and illuminating forms which are usually possible and appropriate for molar applications. Statistical mechanics may be complicated, but, at least in application, it need not be as complicated as much of it here appears. Further, although a chapter is devoted to an excellent critical discussion of the relationship of equilibrium theory to classical thermodynamics, little use is made of this relationship elsewhere, although it would often clarify the exposition. These comments are particularly relevant if the book is to be used as a work of reference; it would often be difficult to gain more than the vaguest understanding of the treatment of particular topics later in the book without a fairly detailed grasp of the general mathematical procedure which is expounded in the early chapters. The intending but baffled reader will, however, be well advised to make the additional effort which is required; he will be amply repaid. As the ground covered by the book, and even by individual chapters, is so extensive, it may be suggested that an adequate table of contents would be a most desirable addition. The comments made here are, perhaps, a reflexion on the frailties of readers; for the author's casual mastery of a difficult technique, and for the effortless manner in which he ranges over the whole field of physics, there can be nothing but profound admiration.

It is hardly necessary to add that the book is excellently produced ; the compositors were given a formidable task, and the result of their work may well be taken as a model of its kind.

The Theory of the Properties of Metals and Alloys. By N. F. Mott and H. Jones. [Pp. 326+xiii.] (Published by Humphrey Milford, Oxford University Press. Price 25*s.* net.)

In view of the important advances which have been made in the theory of the metallic state during the last five years the appearance of this book is most opportune. The subject is of great interest to physicists and workers in related fields, and they will welcome a book which gives a very readable account of these new developments. Until a few years ago relatively little progress had been made in explaining the characteristic properties of individual metals and alloys, but this deficiency is now being rapidly made good as a result of the application of quantum-mechanical methods.

Technical and experimental physicists will observe that the book is concerned almost entirely with quantum-mechanical theory, and that aspects of the subject which can be treated by more classical methods, as, for example, the recent work of Bragg and Williams and thermodynamic methods, occupy relatively little space. The mathematical treatment is not unnecessarily difficult, and the reader with an average knowledge of recent physical theory should have no great difficulty in following the argument ; in certain places a simplified treatment is given rather than a rigorous mathematical discussion, but the limitations of the simpler method are indicated. This must not be taken as implying either that the book is elementary or that it evades difficulties by quoting results without indicating how they are obtained. On the contrary, the mathematical theory is very carefully discussed, so that physicists whose knowledge of quantum mechanics is somewhat limited will still be able to appreciate the main stages of the argument ; the authors have obviously taken great care to bring out clearly the essential physical ideas embodied in the theory.

The scope of the book can only be briefly described. The first chapter is mainly classical and deals with thermal vibrations in crystal lattices and thermal equilibrium in alloys. The second and third chapters deal with the motion of electrons in metal crystals, and in particular with the theoretical developments associated with Bloch, Brillouin, and Wigner and Seitz. The fourth chapter treats the question of cohesion in metals and their elastic constants. Chapter V. is specially interesting ; it describes the forms of the Brillouin

zones for different crystal types and the interesting work of Jones on the electron-atom ratios of alloys. The last two chapters, which form almost half the book, discuss respectively the magnetic properties and the electrical resistance of metals and alloys.

The book covers a fairly wide range of topics, but is not exhaustive; aspects of the subject which are less closely connected with the central theme are omitted or are dealt with briefly. The general impression left on the reader is that the subject is still in a state of rapid progress. The general underlying principles appear to be now fairly well established, but much work remains to be done in filling in the details. Physicists who are not familiar with the details of the developments which have so far taken place will therefore be grateful to Professor Mott and Dr. Jones for putting out a book at this stage so that they will be able to catch up and follow more easily the later developments which will doubtless take place in the next few years.

Practical Photo-Micrography. By J. E. Barnard and F. V. Welch. Third Edition. [Pp. xii+352.] (London: Edward Arnold & Co., 1936. Price 21*s.* net.)

To those who are already acquainted with the earlier editions of this book, it is only necessary to say that the present edition retains all the good features of the previous ones and has much useful matter in addition. To new readers the book can be strongly recommended; beginners in the art of photo-micrography will find it a mine of useful information, and more experienced workers will doubtless pick up many useful hints. The value of the book is enhanced by the many excellent diagrams and beautifully reproduced plates.

In the present edition more attention is given to the photo-micrography of metals and opaque objects; the authors wisely refrain from giving any account of the methods of polishing and etching metal surfaces, for this is an extensive subject in itself and cannot be satisfactorily compressed into a few pages. A short section on the use of infra-red radiation has been added, as well as an entirely new and very interesting chapter dealing with work in the ultra-violet region.

The authors' policy in giving relatively few references to original sources is open to criticism. It is true that the book is essentially a practical one, and it is not worth while to attempt to assign every development in an experimental technique to particular individuals. On the other hand, the almost complete absence of references will handicap the reader in following up aspects of the subject in greater detail; a carefully selected list of references at the end of each chapter would add to the value of the book. In this connexion it is

only fair to add that the authors give a very useful guide to firms supplying instruments and materials, without any obvious bias towards particular firms—apart from the fact that English firms are, of course, more generally mentioned.

In conclusion, it may be stated that, apart from the criticism regarding references, the reviewer finds the book excellent in every respect and can strongly recommend it to all workers in this field.

Phenomena in High-Frequency Systems. By AUGUST HUND. [Pp. xv+642.] (McGraw-Hill Book Co.)

THIS book may be said to bring into a form convenient for reference the most advanced results of theoretical and experimental investigation into a variety of phenomena encountered in high-frequency working. Inasmuch as the present volume succeeds the author's earlier work on 'High-Frequency Measurement,' we find that certain aspects of communication technique, as, for instance, resonant circuits and modulation phenomena, are not here dealt with at length. There is, on the other hand, comprehensive treatment of some less familiar parts of the subject.

Thus, in the present volume there are extensive chapters dealing with the piezo-electric effect in quartz and also with high-frequency phenomena in transmission lines. In both of these chapters there is a great deal of hitherto scattered information.

It is natural that amplification should receive full treatment. The chapter on amplifiers justifiably extends in this case to almost one hundred pages and includes some useful notes on regeneration, both incidental and intended. We would remark here, however, that the reciprocal of the valve amplification factor is not well described by the term "through-grip" introduced here, and which is evidently intended as a translation of the "*durchgriff*" employed by many writers.

Other chapters which will be found useful are those on generators and on directive systems. There is also an admirable presentation of the electromagnetic theory and of the action of the ionized layer.

The opening chapter deals adequately with the physics of valves, while in the closing one we find a clear statement of the facts about filters and other recurrent circuits.

References to papers and other articles are profuse throughout the book, which undoubtedly will prove of extreme value to the research worker employing high-frequency currents for whatever purpose.

[*The Editors do not hold themselves responsible for the views expressed by their correspondents.*]